

Characterization of a novel weak cation-exchange
hydrogel membrane through the separation of lysozyme
from egg white

by
Andrew Stephen Yeh

A thesis
presented to the University of Waterloo
in fulfillment of the
thesis requirement for the degree of
Master of Applied Science
in
Chemical Engineering

Waterloo, Ontario, Canada, 2012

© Andrew Stephen Yeh 2012

I hereby declare that I am the sole author of this thesis. This is the true copy of the thesis, including any required final revisions, as accepted by my examiners.

I understand that my thesis may be made electronically available to the public.

Abstract

Membrane chromatography was investigated as an alternative method to packed-bed chromatography for protein recovery. The purification of lysozyme from egg white with Natrix *adsept*TM weak cation-exchange membranes was investigated by conducting static and dynamic binding studies. The weak cation-exchange membrane consisted of a carboxylic acid-based, environmentally-responsive hydrogel layer bonded to a polymer matrix. Lysozyme was chosen to illustrate protein-membrane binding interactions due to its well-characterized nature and common appearance in pharmaceutical and biotechnological applications. Two sources of lysozyme were considered for the pH and sodium chloride (NaCl) static binding study: ethanol soluble egg whites (ESEW) and pure lysozyme. When binding and elution steps were performed at constant pH, increasing pH and NaCl addition decreased protein binding, while increasing total protein and lysozyme activity recovery from the membrane and process recovery for ESEW and pure lysozyme. For binding at pH 4.5 and elution under variable pH the total protein and lysozyme activity recovery from the membrane and process recovery increased with increasing pH while NaCl addition did not produce a significant impact. At pH 4.5 binding and elution and no NaCl addition, maximum total protein binding (82.6 mg lysozyme/ml membrane) was observed; however, poor total protein and lysozyme activity process recovery (4.5 % and 0.4 %, respectively for pure lysozyme; 14.3 % and 4.9 % for ESEW) were achieved due to non-selective binding. At pH 7.5 binding and elution and no NaCl addition, the high total protein and lysozyme activity process recovery was obtained for ESEW (36.9 % and 74.0 %, respectively) and pure lysozyme (85.7 % and 114.4 %, respectively). The process recovery under these conditions was similar to the lysozyme recovery for published cation-exchange membrane materials in a dynamic set-up. Increasing pH and no NaCl addition increased lysozyme selectivity, measured through SDS-PAGE. When binding and elution at pH 4.5 with no NaCl addition, polypeptide bands corresponding to ovomucoid, an egg white protein, were visualized in the elution stream, in addition to lysozyme polypeptide bands. In all other binding conditions, only lysozyme was present.

The binding characteristics of the weak cation-exchange membrane were investigated in a dynamic cross-flow set-up with recycle for binding and elution at pH 7.5 and no NaCl addition during the binding step. Breakthrough conditions were studied for pure

lysozyme at pH 7.5 with no NaCl addition. Pure lysozyme dynamic binding capacity at 10 % breakthrough (167.3 mg/ml membrane for a 0.35 mg/ml total protein feed solution) was independent of feed concentration. The binding capacity of the 0.35 mg/ml pure lysozyme solution at pH 7.5 in the dynamic set-up was 2.2 times the static binding capacity under similar conditions and was significantly higher than previously published data for other types of cation-exchange membrane materials. Regeneration of the membrane material with 0.1 M NaOH did not impact total protein recovery from the membrane over five separation cycles. Four different lysozyme sources were considered for the breakthrough study in a dynamic flow system: aqueous egg white in 50 mM phosphate citrate at pH 7.5 (AEW); aqueous egg white in 50 mM phosphate citrate at pH 7.5 with 100 mM NaCl (ASEW), ethanol soluble egg white (ESEW) and pure lysozyme. Similar total protein recovery from the membrane was obtained for all egg white solutions (approximately 45 %). High lysozyme activity recovery from the membrane was observed for ESEW (75.7 %). Increasing the presence of other egg white proteins in solution decreased lysozyme activity recovery from the membrane, as approximately 40 % of the bound lysozyme was recovered during elution for the two aqueous egg white solutions. Despite low total protein process recovery for AEW (11.7 %) and ASEW (12.7 %), the lysozyme activity process recovery for AEW (57.1 %) was comparable to ESEW (64.1 %). The lysozyme activity recovery through the separation process decreased when NaCl was present in the binding solution (33.4 % for ASEW). Lysozyme purity was analyzed through size-exclusion high-performance liquid chromatography (SE-HPLC), UV detection and peak heights. Following separation of ESEW, lysozyme purity increased to 74.3 %, and was similar to the egg white separation purities obtained for other cation-exchange membrane materials. The lysozyme purity for the two aqueous egg white solutions was significantly lower (28.8 % for AEW and 33.9 % for ASEW) due to increased competitive protein binding to the membrane. Overall, lysozyme separation was determined to be more effective using ESEW as a feed solution in comparison to aqueous egg white due to production of high lysozyme purity, and high lysozyme recovery elution stream. The application of feed-side pressure during dynamic operation was investigated. Lower lysozyme activity recovery from the membrane was obtained for ESEW at 14 kPa (45 %) compared to when no pressure was applied (75.7 %). Total protein process recovery was similar at the two pressures (23.1 % at 0 kPa and 26 % at

14 kPa), while the overall process recovery of lysozyme activity was higher when no pressure was applied (64.1 %) compared to 14 kPa (51.7 %). Lysozyme purity of the elution solution was independent of applied pressure, with a composition of 73.4 % lysozyme. Operation at 14 kPa was shown to be less effective than binding without applied pressure as although processing times were reduced by a factor of 10, protein aggregates formed along the membrane surface, limiting the protein functionality in the elution stream.

The dynamic binding and elution of pure lysozyme was highly effective, with 99.3 % of bound lysozyme activity recovered off the membrane and an overall lysozyme recovery of 88.6 %. Coupled with the high dynamic binding capacity, the potential for a separation with very high lysozyme recovery was demonstrated with the weak cation-exchange membrane material. Although, the dynamic lysozyme activity recovery for the separation of ESEW was lower than other cation-exchange membrane materials reported in literature, an elution stream with high lysozyme purity was recovered.

The lysozyme model may be further expanded to the separation of other, larger target proteins. Binding operation may be manipulated such that the target protein or proteins possess a desirable net positive charge, while other protein impurities are imparted with a net negative charge. Bound target proteins may then be eluted through the addition of NaCl and the application of a pH gradient to separate out several different protein streams.

Acknowledgements

I would like to express my deepest gratitude to my advisor, Christine Moresoli, for accepting me as a graduate student and providing me with the opportunity to conduct interesting and thought-provoking research. The guidance, training, and support provided by Christine over the course of my project have greatly affected my growth both as a researcher and as a person. Her advice throughout my Masters work has been invaluable in the completion of my thesis work.

I would like to acknowledge the National Sciences and Engineering Research Council of Canada and the Ontario Ministry of Training, Colleges, and Universities for their financial assistance. I would also like to thank the Department of Chemical Engineering and the University of Waterloo for their financial support in many ways throughout my graduate studies. I am indebted to Natrix Separations Inc. for graciously supplying their membrane material and providing advice.

Special recognition and appreciation are expressed to Raymond Legge and the members of the Legge-Moresoli research group. Jamie Cousineau, Katharina Hassel, Barbara Guettler, Sarah Meunier, Rachel Campbell, Ramila Peiris, Sahan Ranamukhaarachchi, Nicholas Ignagni, and Nikhil Kumar have greatly enhanced my graduate studies at the University of Waterloo, and have provided a welcoming and enjoyable work environment.

Special thanks to Sarah Meunier for her guidance and training on the HPLC system and to Priscilla Lai and Stephen Wei for their support and technical contributions to my research. Their assistance and ideas were tremendous over the course of my project.

I am thankful to the reviewers of my thesis, Prof. Marc Aucoin and Prof. Xianshe Feng for their time and invaluable feedback.

I would not be where I am today without to constant love, support, and encouragement from my friends and family. My wonderful parents, Larry and Theresa Yeh, have never stopped pushing me to excel and enjoy life to the fullest. Together with my siblings, Jonathan and Stefanie Yeh, they have provided me with an outstanding support system and I am forever in your gratitude. Special thanks also go out to Joyce Yeh, Richard DaSilva, and Teresa DaSilva.

Finally, I express by deepest admiration, appreciation, and dedication to Sarah DaSilva for your love and support, and for making every moment in my life special.

Table of Contents

<i>List of Figures</i>	<i>xiii</i>
<i>List of Tables</i>	<i>xviii</i>
<i>List of Abbreviations</i>	<i>xxi</i>
1. Introduction	1
1.1. Research Motivation	1
1.2. Project Objectives	2
1.2.1. Goals	2
1.2.2. Hypotheses	2
1.2.3. Objectives	3
1.3. Thesis Organization	4
2. Literature Review	6
2.1. Protein Purification	6
2.1.1. Packed-Bed Chromatography	6
2.2. Ion-Exchange Chromatography	7
2.2.1. Membrane Chromatography	10
2.2.1.1. Membrane chromatography review for lysozyme purification	11
2.2.1.2. Cation-Exchange Membrane Chromatography	14
2.2.1.3. Natrix adsept™ Weak Cation-Exchange Membrane Material	15
2.3. Egg White	16
2.3.1. Egg White Proteins	16
2.4. Lysozyme	18
2.4.1. Lysozyme Surface Charge	19
2.4.2. Effect of Salt	20
2.4.3. Effect of Organic Solvents	21
2.4.4. Lysozyme Binding Properties	21
2.5. Protein Precipitation	22
2.5.1. Ethanol Precipitation	22
2.5.2. Separation of Lysozyme from Hen Egg White	23
2.6. Protein Quantitation	24

2.6.1.	UV-vis Absorbance	25
2.6.2.	Bradford Protein Assay	26
2.6.3.	Sodium Dodecyl Sulfate Poly(Acrylamide) Gel Electrophoresis (SDS-PAGE)	27
2.6.4.	Size-Exclusion High-Performance Liquid Chromatography (SE-HPLC)	28
3.	<i>Separation of Lysozyme from Egg White through Incubation with a Novel Weak Cation-Exchange Membrane</i>	29
3.1.	Overview	30
3.2.	Introduction	31
3.3.	Experimental	33
3.3.1.	Materials	33
3.3.2.	Egg white pretreatment with ethanol	34
3.3.3.	Static adsorption experiments	34
3.3.4.	Total protein recovery	36
3.3.5.	Determination of lysozyme activity	36
3.3.6.	Lysozyme activity recovery	37
3.3.7.	Sodium dodecyl sulphate poly(acrylamide) gel electrophoresis (SDS-PAGE)	37
3.3.8.	Statistical analysis	38
3.4.	Results and Discussion	39
3.4.1.	Ethanol precipitation of egg whites	39
3.4.2.	Pure lysozyme and ESEW solution properties	40
3.4.3.	Lysozyme and egg white static binding capacity	42
3.4.4.	Total protein and lysozyme recovery from the membrane	47
3.4.4.1.	Binding and elution at the same pH	47
3.4.4.2.	Binding at pH 4.5 with a variable elution pH	49
3.4.5.	Total protein and lysozyme process recovery	51
3.4.5.1.	Binding and elution at the same pH	51
3.4.5.2.	Binding at pH 4.5 with a variable elution pH	52
3.4.6.	Specific lysozyme activity after elution	53
3.4.7.	Protein binding selectivity (SDS-PAGE)	55
4.	<i>Dynamic Separation of Lysozyme from Egg White Through Weak Cation-Exchange Membrane Chromatography</i>	60
4.1.	Overview	61
4.2.	Introduction	62

4.3.	Experimental	63
4.3.1.	Materials	63
4.3.2.	Egg white solutions	64
4.3.3.	Tangential flow set-up	65
4.3.4.	Breakthrough curves	66
4.3.5.	Membrane regeneration analysis	67
4.3.6.	Dynamic separation of egg white	67
4.3.7.	Total protein recovery	69
4.3.8.	Lysozyme activity	70
4.3.9.	Lysozyme activity recovery	70
4.3.10.	Membrane staining	71
4.3.11.	Sodium dodecyl sulphate poly(acrylamide) gel electrophoresis (SDS-PAGE)	71
4.3.12.	Size-exclusion high-performance liquid chromatography (SE-HPLC)	72
4.3.13.	Statistical analysis	73
4.4.	Results and Discussion	73
4.4.1.	Dynamic Binding Capacity	73
4.4.1.1.	Membrane Regeneration	75
4.4.2.	Lysozyme recovery from egg white	76
4.4.2.1.	Loading step	76
4.4.2.2.	Elution Profiles	78
4.4.3.	Material balance around the dynamic binding process	81
4.4.4.	Membrane Staining	83
4.4.5.	Dynamic separation of lysozyme from ethanol soluble egg white at 0 kPa	84
4.4.5.1.	Membrane staining	84
4.4.5.2.	Lysozyme membrane recovery and process recovery	85
4.4.5.3.	Protein selectivity through SDS-PAGE	87
4.4.5.4.	Lysozyme purity measured by size-exclusion high-performance liquid chromatography (SEC-HPLC)	89
4.4.6.	Dynamic separation of lysozyme from aqueous egg white solutions	90
4.4.6.1.	Membrane staining	91
4.4.6.2.	Lysozyme membrane recovery and process recovery	91
4.4.6.3.	Protein selectivity through SDS-PAGE	92
4.4.6.4.	Lysozyme purity measured by SEC-HPLC	93
4.4.7.	Effect of pressure (Ethanol soluble egg white at 14 kPa)	94
4.4.7.1.	Membrane staining	94
4.4.7.2.	Lysozyme membrane recovery and process recovery	95
4.4.7.3.	Protein selectivity through SDS-PAGE	95

4.4.7.4. Lysozyme purity measured by SEC-HPLC	96
4.5. Conclusion	97
5. Conclusions	100
References	105
Appendix	112
Derivation of Initial Protein Binding Rate	112
UV Absorbance Calibration	112
Lysozyme Activity	113
SDS-PAGE Calibration	116
HPLC Calibration	116
Ethanol Precipitation and the Effect of Storage Temperature	118
Bradford analysis	118
Total solids analysis	118
Ethanol Precipitation Comparison	118
Dynamic lysozyme separation volumes	119
Lysozyme Activity Breakthrough Curves for Egg White Separation	120
Mass and Activity Balances	120
Membrane Regeneration Mass Balances	121
Membrane Regeneration Activity Balances	123
Breakthrough Study Mass Balance	124
Dynamic Separation Mass Balances	125
Dynamic Separation Activity Balance	127
Precipitation Mass Balance	130
Permeate Flow Rates	130
Sample Calculations	133
Static binding capacity estimation	133
Static membrane recovery and process recovery	133
Dynamic binding capacity estimation	134
Dynamic membrane recovery and process recovery	135
Time-Dependent static binding curve data	136

List of Figures

Figure 1. The ion exchange process of a cation exchanger. (a) Blue counter-ions surround the negatively charged surface; (b) Red counter-ions displace blue counter-ions on the exchanger surface.....	8
Figure 2. Comparison of mass transport mechanisms between (a) packed-bed chromatography and (b) membrane chromatography operations. Thick arrows represent bulk convection, thin arrows represent film diffusion, and curly arrows represent pore diffusion	11
Figure 3. Cation-exchange membrane chromatography operation. (a) A mixture of proteins is passed through the membrane with negatively charged pores; (b) positively charged proteins bind to the negatively charged ligands; (c) negatively charged proteins pass through the membrane in solution; (d) positively charge proteins are eluted from the membrane surface and collected.	14
Figure 4. Effect of environmental conditions on protein binding in cation-exchange membrane chromatography. (a) Proteins bound to the membrane in solution; (b) effect of increasing salt concentration; (c) effect of increasing pH	15
Figure 5. Structure of weak cation-exchange membrane: (1) Porous polyolefin support; (2) hydrogel layer affixed to support; (3) membrane pores.....	16
Figure 6. Structure of Coomassie brilliant blue R-250	26
Figure 7. Separation of solutes in SEC-HPLC. (a) A mixture of solutes in injected into the column; (b) solutes are separated according to size, with small solutes diffusing into adsorbent pores; (c) large solute molecules are eluted while smaller solutes continue through the adsorbent material.	28
Figure 8. SDS-PAGE analysis of the ethanol precipitation process on 15 % acrylamide gel, stained with Coomassie brilliant blue. Lane 1: protein ladder (values given on the left); Lanes 2 and 3: crude egg white following storage at room temperature and -20 °C, respectively, diluted with Milli-Q water to concentration of 0.3 mg/ml (2 µg of protein loaded); Lanes 4 and 5: crude egg white diluted 33.3 % (v/v) with 50mM phosphate citrate, pH 4.8, after storage at room temperature and -20 °C, respectively, to concentration of 0.6 mg/ml (4 µg); Lanes 6, 7, and 8: ESEW after storage at room temperature, 4 °C, and -20 °C, respectively (4 µg); Lane 9: 1.0 mg/ml lysozyme (4 µg).....	39

Figure 9. Time dependent total protein static binding capacity for pure lysozyme and ESEW at 0 mM and 300 mM NaCl concentrations for (a) pH 4.5, (b) pH 6.0, and (c) pH 7.5. Error bars represent standard error for $n = 4$. The lines were calculated from experimental data and equation 3-2. 43

Figure 10. SDS-PAGE analysis on 15 % acrylamide gel, stained with Coomassie brilliant blue. (a) 0 mM NaCl binding solutions prior to the static binding process; (b) 300 mM NaCl binding solutions prior to the static binding process; (c) 0 mM NaCl protein binding solutions following 48 hour membrane incubation; (d) 300 mM NaCl protein binding solutions following 48 hour membrane incubation. Lanes 1 and 10: protein ladder; Lane 2: ESEW; Lanes 3, 4, and 5: ESEW aqueous solutions at pH 4.5, 6.0 and 7.5, respectively; Lanes 6, 7, and 8: aqueous lysozyme solutions at pH 4.5, 6.0, and 7.5, respectively; Lane 9: 1.0 mg/ml lysozyme. Approximately 2 μg of protein was loaded into each well..... 55

Figure 11. SDS-PAGE analysis of elution solutions on 15 % acrylamide gel, stained with Coomassie brilliant blue. (a) After binding with 0 mM NaCl when binding and elution are at the same pH; (b) after binding with 300 mM NaCl when binding and elution are at the same pH; (c) after binding at pH 4.5 with 0 mM NaCl and elution at variable pH; (d) after binding at pH 4.5 with 300 mM NaCl and elution with variable pH. Lanes 1 and 10: protein ladder; Lane 2: ESEW; Lanes 3, 4, and 5: ESEW aqueous solutions at pH 4.5, 6.0 and 7.5, respectively; Lanes 6, 7, and 8: aqueous lysozyme solutions at pH 4.5, 6.0, and 7.5, respectively; Lane 9: 1.0 mg/ml lysozyme. Approximately 2 μg of protein was loaded into each well. 56

Figure 12. Schematic diagram of the tangential flow set-up. 65

Figure 13. Breakthrough curves for different initial inlet lysozyme concentrations in 50 mM phosphate citrate buffer at pH 7.5 and no NaCl addition for Natrix Weak C membranes versus the normalized permeate volume. Feed flow rate was 160 ml/min. Total protein concentration (C) measured by UV absorbance at 280 nm was normalized based on the initial inlet total protein concentration (C_0). Volume (V) was normalized based on the final volume of collected permeate (V_{final}), as described in Section 4.3.4..... 74

Figure 14. Effect of regeneration cycles on the total protein and lysozyme activity recovery from the membrane for the dynamic binding of 0.35 mg/ml lysozyme in 50 mM phosphate

citrate at pH 7.5 to Natrix Weak C membranes. Feed flow rate was 160 ml/min. Error bars represent standard error where $n = 3$ for regeneration cycle 1, otherwise $n = 1$ 75

Figure 15. Normalized total protein concentration breakthrough curves for different egg white solution at pH 7.5 for Natrix Weak C membranes. Feed flow rate was 160 ml/min. Total protein concentration (C) measured by UV Absorbance at 280 nm was normalized based on the initial total protein concentration (C_0). Permeate volume (V) was normalized based on the final volume of collected permeate (V_{final}), shown in Table 11, column 3. Error bars represent standard error for $n = 2$ 77

Figure 16. Elution curves for ESEW proteins at pH 7.5 from Natrix Weak C membranes based on total protein concentration following binding at (a) 0 kPa and (b) 14 kPa. Lysozyme activity elution curves are shown for (c) ESEW binding at 0 kPa, and (d) ESEW binding at 14 kPa. . Pure lysozyme elution curves (x). Feed flow rate was 160 ml/min. Permeate volume (V) was normalized based on the final volume of collected permeate (V_{final}), shown in Table 11, column 7. 79

Figure 17. Total protein elution curves for (a) AEW proteins at pH 7.5 and (b) ASEW proteins at pH 7.5 from Natrix Weak C membranes. Lysozyme activity elution curves are shown for (c) AEW proteins and (d) ASEW proteins. Pure lysozyme elution curves (x). Feed flow rate was 160 ml/min. Permeate volume (V) was normalized based on the final volume of collected permeate (V_{final}), shown in Table 11, column 7..... 80

Figure 18. Specific lysozyme activity observed in the permeate and retentate streams collected after the elution step. Error bars represent standard error, where $n = 2$ 81

Figure 19. Stained images of the feed side of weak cation-exchange membrane material (a) new; (b) after regeneration and equilibration; (c) after 15 seconds contact time with 5.00 mg/ml lysozyme solution recirculation in the tangential flow cell; (d) after 30 seconds contact time with 5.00 mg/ml lysozyme solution recirculation in the tangential flow cell; (e) after 5 minutes contact time with 5.00 mg/ml lysozyme solution recirculation in the tangential flow cell..... 84

Figure 20. Stained images of weak cation-exchange membrane material after the elution step. (a) Permeate side; (b) feed side and 1.35 mg/ml lysozyme; (c) feed side and ESEW proteins at 0 kPa; (d) feed side and ESEW proteins at 14 kPa; (e) feed side and AEW; (f) feed side and ASEW. 85

Figure 21. SDS-PAGE analysis on 15 % acrylamide gel, stained with Coomassie brilliant blue. For each gel, Lanes 1 and 10: protein ladder; Lane 2: 1.35 mg/ml total protein crude egg white solution; and Lane 9: 1.00 mg/ml pure lysozyme solution. Each well was loaded with 2.5 µg of protein. (a) Initial egg white solutions and collected retentate after sample loading. Lanes 3, 4, and 5: initial binding solutions of AEW, ASEW, and ESEW, respectively; Lanes 6, 7, and 8: retentate solutions after sample loading of AEW, ASEW, and ESEW, respectively; (b) Collected permeate after sample loading and wash solutions. Lanes 3, 4, and 5: permeate collected after the loading step of AEW, ASEW, and ESEW, respectively; Lanes 6, 7, and 8: wash solutions of AEW, ASEW, and ESEW, respectively; (c) Collected retentate and permeate solutions after the elution step. Lanes 3, 4, and 5: retentate for AEW, ASEW, and ESEW, respectively; Lanes 6, 7, and 8: permeate for AEW, ASEW, and ESEW, respectively; (d) Comparison of initial egg white solutions, wash solutions, and collected permeate solutions after the elution step for ESEW bound at 0 kPa and at 14 kPa. Lanes 3 and 4: initial solutions of ESEW at 0 kPa and 14 kPa, respectively; Lanes 5 and 6: wash solutions of ESEW for loading at 0 kPa and 14 kPa, respectively; Lanes 7 and 8: elution permeate solutions of ESEW for loading at 0 kPa and 14 kPa, respectively. 88

Figure 22. Typical SEC-HPLC chromatograms (a) ESEW feed, and (b) ESEW elution stream for binding at 0 kPa. Flow rate was 1.0 ml/min of a phosphate buffer, pH 7.0, detection by UV absorbance at 280 nm..... 89

Figure 23. Calibration curve for UV absorbance at 280 nm. Lysozyme standards over the range of 0.1 mg/ml to 1.0 mg/ml was used to determine absorbance..... 113

Figure 24. Sample lysozyme calibration curve for the turbidimetric assay showing the change in absorbance at 450 nm over time for the prepared lysozyme standards. 114

Figure 25. Linearization of the lysozyme standard calibration curve presented in Figure 24 demonstrating the change in absorbance at 450 nm over time. 114

Figure 26. Calibration curve relating the activities of the prepared lysozyme standards to the actual lysozyme activity based on the change in absorbance at 450 nm over time. 115

Figure 27. Calibration curve relating the slope for the change in absorbance at 450 nm over time to the corrected lysozyme activity. 115

Figure 28. SDS-PAGE calibration curve relating the molecular weight of a sample and the distance migrated through a 15 % acylamide-bis resolving gel. 116

Figure 29. SEC-HPLC calibration curve relating component retention time to molecular weight for peak identification. BSA, lipase, and lysozyme were used as model proteins. Flow rate = 1.0 ml/min..... 117

Figure 30. Lysozyme calibration curve through the SEC-HPLC system for protein quantitation. Lysozyme concentrations ranging from 0.15 mg/ml to 1.50 mg/ml were tested. 117

Figure 31. Lysozyme activity breakthrough curves for (a) ESEW at two different pressures and (b) aqueous egg white solutions (with and without NaCl) at pH 7.5 using Natrix Weak C membranes. Feed flow rate was 160 ml/min. Lysozyme activity (A) was normalized based on the initial lysozyme activity (A_0). Volume (V) was normalized based on the final permeate volume (V_{final}). Error bars represent standard error for $n = 2$ 120

Figure 32. Rate of permeate collection for each trial of dynamic separation of egg white during the loading step. (a) Comparison of ESEW at 0 kPa and ESEW at 14 kPa; (b) comparison of the aqueous egg whites (AEW and ASEW). All trials were compared to pure lysozyme at 1.35 mg/ml (x). Feed flow rate was 160 ml/min for all trials. Permeate volume (V) is presented as a ration to the total permeate volume (V_{final}). 131

Figure 33. Rate of permeate collection for each trial of dynamic separation of egg white during the elution step. (a) Comparison of ESEW at 0 kPa and ESEW at 14 kPa; (b) comparison of the aqueous egg whites (AEW and ASEW). All trials were compared to pure lysozyme at 1.35 mg/ml (x). Feed flow rate was 160 ml/min for all trials. Permeate volume (V) is presented as a ration to the total permeate volume (V_{final}). 132

List of Tables

Table 1. Comparison of dynamic binding capacity ($Q(\text{DBC})_{10\%}$) and static binding capacity ($Q(\text{SBC})$) for lysozyme separation between cation-exchange membrane chromatography materials.....	12
Table 2. Comparison of lysozyme purity and lysozyme purification factor for the separation of lysozyme from egg white with different cation-exchange chromatography materials.	13
Table 3. Hen Egg White Protein Components [19]	17
Table 4. Comparison of molecular weight estimates of major egg white proteins obtained by SDS-PAGE analysis. Estimates based on crude egg white after storage at room temperature (Lane 2 in Figure 8)	39
Table 5. Total protein concentration and lysozyme activity of pure lysozyme and ESEW solutions, as measured by UV-vis absorbance at 280 nm and a turbidimetric assay at 450 nm, respectively.	41
Table 6. Conductivity of 50 mM phosphate citrate, ESEW, and lysozyme solutions according to pH and NaCl conditions.....	42
Table 7. Maximum protein binding capacities and initial protein binding rates to Weak C membranes according to pH and NaCl conditions after 48 hour incubation.	45
Table 8. Total protein and lysozyme activity recovery from the membrane and process recovery for binding at different pH and NaCl concentrations and elution at 1 M NaCl and the same pH.	48
Table 9. Total protein and lysozyme activity recovery from the membrane and process recovery for binding at pH 4.5 and different NaCl concentrations and elution at 1 M NaCl and variable pH.	50
Table 10. Specific lysozyme activity in the elution solution after membrane incubation according to pH and NaCl concentration for two different binding and elution pH strategies with 1 M NaCl elution.	54
Table 11. Breakdown of the volumes during the dynamic separation of lysozyme from egg white.....	68
Table 12. Effect of pure lysozyme initial inlet concentration on dynamic binding capacity .	74
Table 13. Effect of the sample loading process on egg white solution physical properties ...	78

Table 14. Total protein and lysozyme activity recovery in the wash and elution streams for dynamic separation of lysozyme.....	82
Table 15. Total protein and lysozyme activity recovery from the membrane and process recovery during dynamic binding and elution operation for different egg white protein solutions.....	86
Table 16. Comparison of protein elution times after injection into SEC-HPLC at 1.0 ml/min	116
Table 17. Total solids content, total protein, and lysozyme activity of crude egg white and ESEW.....	119
Table 18. Breakdown of the individual stream volumes during the dynamic separation of lysozyme from egg white.....	119
Table 19. Protein mass balance for experiments testing the effect of membrane regeneration membrane recovery and protein recovery. For all trials, the first digit signifies the membrane sample number and the second show the number of regeneration cycles (X-X). Feed solution was 0.35 mg/ml pure lysozyme at pH 7.5. Feed flow rate was 160 ml/min.....	121
Table 20. Lysozyme activity balance for experiments testing the effect of membrane regeneration membrane recovery and protein recovery. For all trials, the first digit signifies the membrane sample number and the second show the number of regeneration cycles (X-X). Feed solution was 0.35 mg/ml pure lysozyme at pH 7.5. Feed flow rate was 160 ml/min ..	123
Table 21. Protein mass balances for breakthrough curves of different pure lysozyme feed concentrations at pH 7.5. Feed flow rate was 160 ml/min	124
Table 22. Protein mass balances for the dynamic separation of lysozyme for egg white. Feed solution was 1.35 mg/ml at pH 7.5 for all egg white solutions. Feed flow rate was 160 ml/min.....	125
Table 23. Lysozyme activity balances for the dynamic separation of lysozyme for egg white. Feed solution was 1.35 mg/ml at pH 7.5 for all egg white solutions. Feed flow rate was 160 ml/min.....	127
Table 24. Total solids balances around the egg white precipitation process	130
Table 25. Process stream total protein and volume data for the separation of ESEW at 0 kPa, trial 2	135

Table 26. Static binding concentrations, membrane volumes, and static binding capacities according to binding pH and NaCl concentration for the time-dependent static binding curves in Figure 9 136

List of Abbreviations

Roman Letters

A	Lysozyme Activity (U/ml)
c	Concentration (mol L ⁻¹)
C _f	Final Total Protein Concentration (mg/ml)
C ₀	Initial Total Protein Concentration (mg/ml)
K	Binding Rate Coefficient (min)
l	Light Path Length (cm)
n _i	Sample Size of Component i
P	Total Protein Concentration (mg/ml)
q	Static Total Protein Binding Capacity (mg/ml membrane)
q _{max}	Maximum Total Protein Binding Capacity (mg/ml membrane)
Q(DBC _{10%})	Dynamic Binding Capacity at 10 % Breakthrough (mg/ml membrane)
Q(SBC)	Static Binding Capacity (mg/ml membrane)
S _i ²	Sample Variance of Component i
t	Time (min)
t ₀	Student's T Test Statistic
V	Volume (ml)
V _{10% DBC}	10 % Breakthrough Volume
V _{DV}	Dead Volume of System (ml)
V _{membrane}	Membrane Volume (ml)
\bar{y}_i	Sample Mean of Component i

Greek Letters

ϵ	Molar Extinction Coefficient (M ⁻¹ cm ⁻¹)
$\epsilon^{1\%}$	Molar Extinction Coefficient of 1 % protein solution at 280 nm (% ⁻¹ cm ⁻¹)

Other Abbreviations

Abs	Absorbance of UV light (-)
AEW	Aqueous Egg White
ASEW	Aqueous Egg White containing Salt
ESEW	Ethanol Soluble Egg White
HEW	Hen Egg White
LYS	Lysozyme
NaCl	Sodium Chloride
OA	Ovalbumin
OG	Ovoglobulin
OM	Ovomucoid
OT	Ovotransferrin
Per	Permeate
pI	Isoelectric Point

Ret	Retentate
SDS	Sodium Dodecyl Sulfate
SDS-PAGE	Sodium Dodecyl Sulfate Poly(Acrylamide) Gel Electrophoresis
SEC-HPLC	Size Exclusion High-Performance Liquid Chromatography
UV	Ultraviolet

1. Introduction

1.1. Research Motivation

The increase of cell culture volumes and concentrations has led to greater productivities in upstream, or fermentation processes in biomanufacturing. These processes may be scaled-up to produce larger volumes with minimal changes to operating costs [1-4]. Due to limitations in the cell culture volumes that are able to be processed at a time, the purification and recovery of proteins has been unable to match the rapid technological advances of upstream fermentation [1]. The downstream purification processes, such as packed-bed chromatography, face disadvantages, such as significant pressure drops, poor bed utilization, low loading volumes and throughputs, and mass transfer limitations [1,3-5]. As such, alternative protein purification methods are necessary to overcome many of the limitations of traditional packed-bed chromatography while retaining high protein selectivity and purity.

Membrane chromatography is an alternative method to packed-bed chromatography for protein purification. Mass transfer is driven through convective flow [1,2,4-7], allowing high throughputs and low residence times while retaining protein selectivity through the addition of functional groups, such as ion-exchange ligands [1,4,7,8]. With ion-exchange chromatography, separation is induced through electrostatic attraction between charged surfaces, such as a protein and membrane [1,4,7,9,10] allowing for high protein selectivity according to the relative surface charges of the protein mixture.

Lysozyme is a well-understood protein commonly chosen for the characterization of biotechnological, food, or pharmaceutical applications [6,7,11-19]. In this study, lysozyme was selected as a model protein to aid in the binding capacity characterization of a weak cation-exchange hydrogel membrane material. Through the manipulation of pH and salt concentration, the binding and elution of lysozyme to and from the membrane material may be monitored and controlled. Selective separation using the membrane material may also be determined using lysozyme as it is naturally present in egg white in low concentrations [19].

Published work has focused on protein binding capacity quantification and characterization of ion-exchange membrane chromatography materials [6,7,9,11,20]. The

separation of lysozyme from egg white has also been investigated with membrane chromatography materials [7,12,17,21], although these materials typically utilize strong cation-exchange functional groups and a dynamic binding set-up.

1.2. Project Objectives

1.2.1. Goals

The overall goals of this project were to investigate binding characteristics of a weak cation-exchange hydrogel membrane material using lysozyme as a model protein; based on a given set of conditions, determine the pH and salt concentrations that will maximize lysozyme binding and elution from the membrane material and the overall recovery of lysozyme; compare differences in protein binding and electrostatic interaction behaviour for static membrane incubation and a dynamic cross-flow set-up; and evaluate the effect of protein impurities on the binding of lysozyme to the membrane materials using egg white solutions of varying initial lysozyme purity.

1.2.2. Hypotheses

The following hypotheses were tested in this project:

1. Increasing the pH of the binding step from 4.5 to 7.5 should increase the lysozyme binding capacity of the weak-cation-exchange membrane due to an increase in electrostatic interactions between protein and the membrane surface. Conversely, increasing the pH of the elution step from 4.5 to 7.5 should decrease the recovery of protein from the membrane surface since the stronger electrostatic interactions would keep bound protein retained on the membrane.
2. Increasing the ionic strength of the binding solution by the addition of 300 mM NaCl should decrease lysozyme binding capacity and the overall recovery of lysozyme activity due to a decrease in electrostatic interactions via charge shielding. In a similar manner, increasing the ionic strength of the elution solution through the addition of 1 M NaCl should increase the recovery of lysozyme activity from the membrane surface.
3. Higher total protein binding capacity and overall recovery of lysozyme activity should be achieved through the static membrane incubation process than in a dynamic, cross-flow set-up. Since the weak cation-exchange membrane should reach equilibrium during

incubation, the membrane should be saturated with protein allowing for maximum protein binding to be achieved. In contrast, the high flow rates of the dynamic set-up should reduce contact time between protein and the membrane surface, reducing binding site utilization.

4. Lysozyme specificity of the weak cation-exchange membrane should be independent of initial lysozyme purity as lysozyme should be the only positively-charged protein present in egg white. Although the concentration of negatively-charged protein impurities present in the binding solution may vary, they should not bind to the membrane surface due to their similar charges.
5. The application of 14 kPa feed-side pressure to the membrane during dynamic flow operation should decrease the overall recovery of lysozyme activity and lysozyme purity in the elution stream. Although increasing operational pressure should decrease processing time, the membrane would be in contact with the elution solution for a shorter period of time, reducing the amount of protein that may be recovered.

1.2.3. Objectives

In order to test the proposed hypotheses, total protein and lysozyme activity recovery from the membrane and process recovery, lysozyme purity, and protein selectivity will be studied. These will be covered in two studies.

1. Examine the total protein and lysozyme activity recovery, yield, and selectivity from weak cation-exchange hydrogel membranes under static binding conditions for ethanol soluble egg white and a pure lysozyme solution as a control. Suitable pH and salt concentration binding and elution conditions to maximize lysozyme activity recovery, yield, and purity will be identified.
 - a. The pH of the binding step will be varied between three values: 4.5, 6.0 and 7.5.
 - b. The ionic strength of the binding, through NaCl concentration, will be investigated at two NaCl concentrations: 0 mM and 300 mM.
 - c. Two different pH strategies for binding and elution will be investigated: (1) binding and elution at a constant pH, and (2) binding at a constant pH (pH 4.5) followed by variable pH elution. The elution step for both strategies will be performed with a 1 M NaCl solution.

2. Examine the total protein and lysozyme activity recovery and yield, protein selectivity, and protein purity under dynamic binding conditions for ethanol soluble egg white, aqueous egg white solutions, and pure lysozyme. Total protein and lysozyme activity recovery and process recovery, protein selectivity, and protein purity will be measured.
 - a. Investigate changes to total protein and lysozyme activity recovery and process recovery, protein selectivity, and protein purity based on the addition of salt and ethanol to the protein precipitation process and the lysozyme binding step. A pure lysozyme solution will be compared as a control for binding at pH 7.5. Four different lysozyme sources will be tested: (1) pure lysozyme in 50 mM phosphate citrate, (2) ethanol soluble egg white, (3) aqueous egg white solution (50 mM phosphate citrate, pH 4.8), and (4) aqueous egg white solution with salt addition (50 mM phosphate citrate at pH 4.8 and 100 mM NaCl).
 - b. Examine the total protein and lysozyme activity recovery and yield, and lysozyme purity changes at two feed-side pressures during lysozyme separation of ethanol soluble egg white: 0 kPa and 14 kPa.
 - c. Evaluate the dynamic binding capacity, lysozyme recovery, and lysozyme yield for three lysozyme concentrations: 0.35 mg/ml, 1.0 mg/ml, and 5.0 mg/ml.
 - d. Investigate the effect of membrane regeneration with 0.1 M NaOH by determining the total protein and lysozyme activity recovery and process recovery after each generation cycle.

1.3. Thesis Organization

Chapter 2 provides fundamental principles, background theory, and literature review regarding protein purification, membrane and ion-exchange chromatography, hen egg white proteins, and properties of lysozyme.

Chapter 3 presents the investigation of pH and NaCl binding and elution conditions of lysozyme from ethanol soluble egg white with a weak cation-exchange membrane for static conditions. The impacts of binding pH, ionic strength (obtained by NaCl addition), and elution pH according to total protein and lysozyme activity recovery from the membrane and process recovery and lysozyme selectivity are presented. This chapter was prepared as a manuscript for the Journal of Agricultural and Food Chemistry.

The investigation of the lysozyme activity breakthrough for four different sources of pure lysozyme, ethanol soluble egg white, aqueous egg white, and aqueous NaCl egg white with a weak cation-exchange membrane in a dynamic system is discussed in Chapter 4. The separation of lysozyme from the four sources is discussed through their total protein and lysozyme activity recovery from the membrane and process recovery, protein selectivity and protein purity. The effects of lysozyme concentration, pressure and membrane regeneration cycles on lysozyme purification are also presented. This chapter was prepared as a manuscript for the Journal of Membrane Science.

A summary of the most significant findings of this project and proposed future works are discussed in Chapter 5.

2. Literature Review

2.1. Protein Purification

Proteins are biological molecules consisting of long chains of amino acids connected by peptide bonds and folded into complex three-dimensional structures. The numerous applications of proteins have led to increasing demands of protein quantities. Proteins can be produced *in vivo*, relying on gene expression to manufacture large quantities. The production of high purity proteins requires separation of the target molecule from other chemical or biological contaminants that may be harmful to the end product. Often, a process stream will require several purification steps to obtain the desired purity. While upstream processes such as protein translation and cell growth benefit from an economy of scale, increases in separation volumes correlate directly with increased costs [1,4]. This limitation creates a bottleneck in protein production, as chromatography and other separation-based techniques are unable to match the resources necessary to process greater volumes. Consequently, there has been a shift in focus to protein purification processes in order to keep up with advances in cell culture technology [1,14,22].

2.1.1. Packed-Bed Chromatography

Stemming from the need to selectively recover a target protein, packed-bed chromatography is commonly used in protein purification due to its highly selective nature. The desired process stream is fed into a glass or steel column filled with porous bead resins composed of functionalized polysaccharide, mineral, or synthetic materials. Molecules are separated out by functional groups in the resin pores according to properties such as size, charge, hydrophobicity, or affinity [1,4]. Depending on the desired application, the resin can bind the target molecule while allowing impurities to elute through the column, or can bind impurities in order to purify the process stream [1]. Adsorbed molecules may be eluted by manipulating the pH and ionic strength conditions of the buffer.

There are several limitations to packed-bed chromatography despite its common application in industrial protein purification. In larger columns, physical limitations of the resin beads can hinder separation effectiveness. Increased force exerted on the packed-bed

results in large pressure drops. As well, uneven packing can result in dispersion issues, channelling, and resin collapse, which limit binding site usage within the resin pores. [1,4,23]. Chromatography columns can also suffer from resin fouling and microbial contamination with insufficient cleaning and sanitization [1,23]. Packed-bed chromatography is expensive in comparison to the cost of other separation techniques; especially Protein A affinity, for which the resin material can be an order of magnitude greater than other traditional resins [24].

The most significant drawback of packed-bed resins arises from mass transfer limitations. The binding of particles relies upon diffusion of the solutes into pores of the resin. The use of packed-bed chromatography processes is therefore limited by the speed of diffusion and the target molecule size; larger molecules are slower to diffuse and may actually block pores [1,4,5]. Pore diffusion limitations can lower column efficiency and loading capacity, requiring longer residence times for processing. In order to offset these mass transfer problems, larger column heights or slower flow rates may be implemented leading to a further increase in operation costs [1].

2.2. Ion-Exchange Chromatography

Ion-exchange chromatography is the most widely used chromatographic separation technique due to its ease-of-use, versatility, and wide variety of available adsorbent surfaces and buffers. Ion-exchange materials also have the added benefits of high binding capacity and minimal reduction in biological activity [25]. A stationary phase, often comprised of charged functional ligands grafted to bead resins or membrane materials, is used to separate out oppositely charged particles dissolved in a mobile phase through electrostatic interactions [25,26]. There are two main classifications of ion-exchange materials: cation-exchangers and anion-exchangers. In cation-exchange, a negatively charged surface is used to bind positively charged solutes, whereas anion-exchange reverses the polarity of the two species [26,27]. Certain materials have the ability to perform both cation- and anion-exchange processes, and are known as amphoteric ion exchangers [27]. Each ion-exchange group can be further divided into weak and strong exchangers, based on their ligands. Strong exchangers will retain their charged form over the entire pH range. Weak ion-exchange materials, on the other hand, have a limited range over which they are in a charged state [26,27].

The binding of proteins to the resin surface is a reversible exchange process through which proteins, salt counter-ions, and other charged particles displace similarly charged ions on the resin surface [26,27]. An example of this stoichiometric exchange of ions is shown in Figure 1. An elution step is necessary to recover adsorbed protein from the resin surface. Generally, this is accomplished by increasing the ionic strength of the solution, although for weak-exchangers, solution pH may be changed to promote elution [25]. Dissolved ions compete with the bound protein for oppositely charged ligands on the stationary surface. Depending on counter-ion affinity, salt may displace the bound protein on the stationary surface [25]. As well, salt will reduce electrostatic interactions of the charged surfaces, weakening affinity for the bound protein.

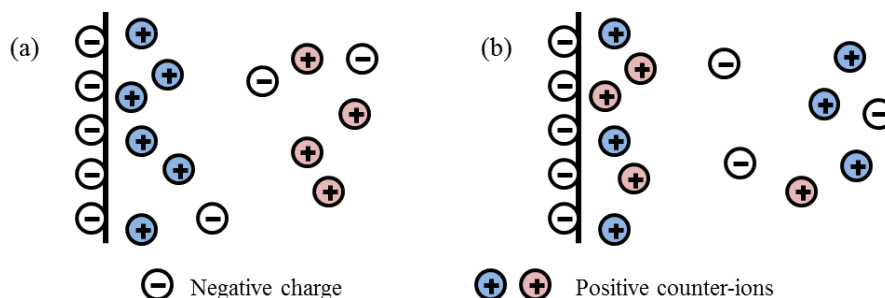


Figure 1. The ion exchange process of a cation exchanger. (a) Blue counter-ions surround the negatively charged surface; (b) Red counter-ions displace blue counter-ions on the exchanger surface.

When considering the solution from which a protein needs to be recovered, the interaction between dissolved proteins and the ion-exchange surface is influenced by a number of factors. Salt and pH will similarly alter both surfaces and can change protein adsorption [9,10,20,25]. Increasing the ionic strength of solution will increase the presence of ions surrounding both the charged surface and dissolved proteins. These ions will decrease the Debye length of the electrical double layer extending out from the surfaces, effectively reducing the strength of electrostatic interactions between solutes and surfaces [28]. Consequently, the attraction between the charged side groups of protein and the oppositely charged group of the ion-exchange surface will be reduced and protein will be less likely to adsorb onto the surface. This effectively reduces the maximum binding capacity of protein to the ion-exchange material surface [20]. Increased salt concentrations will also introduce increased competition for the oppositely charged ion-exchange material surface, reducing available active binding sites [10,25].

The pH of the binding buffer is another factor that will influence the ability of a protein to bind to a charged surface. Since proteins are zwitterions, they carry both positive and negative charges. Based on the pH of solution, protein side groups can protonate or deprotonate, thereby changing their net charge [29]. The total charge of the protein is an accumulation of all of the individual surface charges. In a pH environment below the isoelectric point (pI) of a protein, the protein will have a net positive charge, while a negative charge will be carried at pH above the pI [29]. By modifying the pH of the buffer of a protein solution, the molecular charge can be controlled. Protein shape, conformation, and distribution of charges are all influenced by electrostatic interactions within the polypeptide chain of the protein [9].

As a protein approaches its pI, its affinity for an oppositely charged surface decreases [20]. Theoretically, a protein should not bind to a charged surface at its pI. However, local concentration of charges can lead to an affinity for the charged ligands of the surface [25]. According to the Donnan effect, protons in solution will be attracted to cation-exchange groups on the protein surface, lowering the local pH surrounding the molecule. Likewise, hydroxide ions will be drawn to positively charged side chains, raising the local pH [25]. Although the net charge on the protein is zero, the pH around a protein may be up to one pH unit higher or lower than the buffer pH [20,25]. This may explain why proteins can still adsorb onto ion-exchange surfaces at their isoelectric point.

Protein concentration and surface coverage of the chromatography material can have a negative impact on the retention of proteins. As the concentration of bound protein increases, further retention may be inhibited due to steric hindrances [9]. Proteins that bind to the material surface can cover other binding sites, limiting their capacity to participate in a binding reaction. For example, lysozyme occupies an average of 2.5 binding sites per molecule [20]. According to the steric mass action model describing protein adsorption to ion-exchange materials, proteins will actually block more active sites than they interact with [20]. The binding orientation of proteins may also be negatively impacted by steric hindrances, and poor activity recovery may result.

2.2.1. Membrane Chromatography

With the limitations and rising costs of packed-bed chromatography, alternative chromatography techniques have been developed for the recovery and purification of proteins. One such technology is membrane chromatography. Membranes are traditionally thin, synthetic materials comprised of cellulose, polyethersulfone, or polyvinyl fluoride [5,22], and are commonly used for a wide array of separation applications, such as the recovery of macromolecules and buffer exchange [22]. Through the addition of functional groups to the membrane material, selectivity may be enhanced to allow for capture and polishing applications. Functional group chemistries common for membrane adsorber materials include ion-exchange, affinity, hydrophobic interactions, and reversed-phase interactions [4,22]. There are three main types of membrane set-ups: flat sheet, hollow fibre, and radial flow. Flat sheet is the most common configuration, and introduces the liquid solution perpendicularly or tangentially with respect to the membrane surface [4,5,22]. Stacks of several flat sheet membranes are common to increase adsorbent volume in comparison to a single sheet. In a hollow fibre configuration, bundles of small diameter tubular membranes are grouped together in a shell and tube arrangement. Despite high surface area-to-volume ratio and a reduction in membrane fouling, hollow fibre membranes are not as well-suited for membrane chromatography processes due to poor adsorbent utilization [4]. In a radial flow configuration, flat sheet membranes are wrapped around a porous cylindrical core. Radial flow adsorbers suffer from flow distribution limitations and are not widely reported in membrane chromatography literature [4].

Membrane chromatography processes are highly advantageous compared to packed-bed chromatography columns as mass transfer limitations are not a significant factor. While solutes must diffuse into and out of porous resin materials for separation to occur in packed-bed chromatography, mass transfer for membrane materials is driven through convective flow (Figure 2). Thus, solutes are brought into direct contact with functional groups that may line the pore structure, allowing for higher feed rates through the chromatography material [1,2,4,5]. Increasing laminar flow rates through the membrane may decrease operation costs, due to lower processing times and buffer requirements. Similar separations may be performed with membranes of a significantly smaller size compared to chromatography columns. The need for additional separation steps is also reduced, as cross-contamination and

ligand leaching is not as prevalent in membrane chromatography [1,4]. Due to their low bed height-to-volume ratio, membranes do not suffer from the high pressure drop commonly reported with packed-bed resins [1,5]. Scale-up to larger separation volumes is consequently much easier to implement.

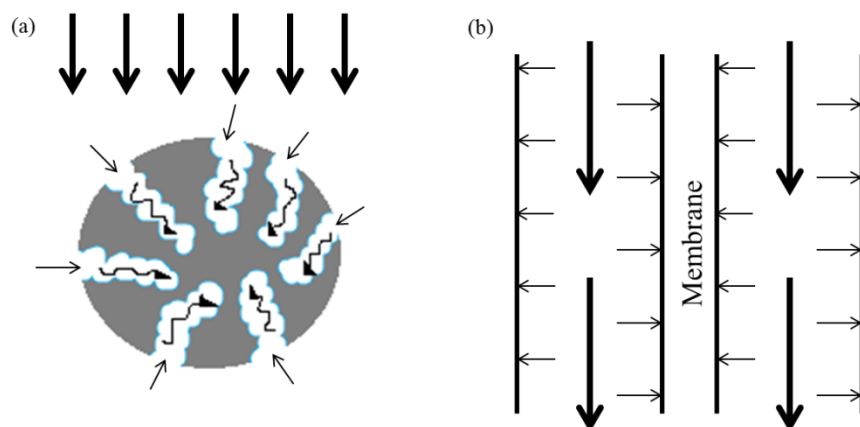


Figure 2. Comparison of mass transport mechanisms between (a) packed-bed chromatography and (b) membrane chromatography operations. Thick arrows represent bulk convection, thin arrows represent film diffusion, and curly arrows represent pore diffusion

Despite its advantages, membrane chromatography shares a number of issues that prevent its use as a protein purification and recovery method. Membrane chromatography materials typically have lower binding capacity and selectivity when compared to packed-bed chromatography resin materials, which can limit their effectiveness in separation processes [2,5,23]. Membrane chromatography materials are also restricted to simple binding and elution applications and are better suited for the purification of large volumes with a low concentration of target molecules [1,4]. Uneven flow distribution across the membrane chromatography material can limit their utilization [4,22]. Heterogeneous pore size and thickness of membrane chromatography can also impact the utilization of the membrane chromatography material, as liquid will pass quickly through larger pores and thinner sections [4]. Stacks of membrane chromatography materials are often placed atop one another to reduce the diameter to length ratio and increase flow distribution uniformity, but require mesh spacers to promote turbulence [4,22,30].

2.2.1.1. Membrane chromatography review for lysozyme purification

A review of novel membrane chromatography studies reveal several flow-through set-ups aimed at the determination of lysozyme dynamic binding capacity [6,11,14,16,31].

The materials used in these studies are predominantly cation-exchange membranes [11,14,31], or ultrafiltration membranes prepared with ion-exchange or affinity functional groups for improved binding and separation [6,7,16,32,33]. As well, the majority of cation-exchange materials contain sulphuric acid ligands or other strong cation-exchangers, where the membrane will retain a constant surface charge density. Weak cation-exchange materials have not been examined in detail.

Throughout the dynamic binding methodologies, a similar adsorption pattern is followed: the chromatography material is equilibrated with buffer, the sample volume is introduced into the system, the material is washed with buffer, and the bound protein is desorbed using an elution buffer of either higher pH or salt concentration. In some cases, the chromatography material is then regenerated to allow further processing. Many equilibration buffers have been used for dynamic binding studies including sodium phosphate [31,33], deionized water [7], citrate [34], and potassium phosphate [6]. Most equilibrium buffers are adjusted to approximately pH 7.0 [6,7,11,31]

Table 1. Comparison of dynamic binding capacity ($Q(\text{DBC})_{10\%}$) and static binding capacity ($Q(\text{SBC})$) for lysozyme separation between cation-exchange membrane chromatography materials

Reference	Separation Material	Static Binding [mg protein/ml membrane]	Dynamic Binding [mg protein/ml membrane]	$Q(\text{DBC})_{10\%}/$ $Q(\text{SBC})$
[6]	Weak cation-exchange membranes prepared via UV-initiated graft copolymerization	62.6 (5 mg lysozyme/ml solution)	23.9 (1 mg lysozyme/ml solution; pH 7, 1 ml/min)	0.38
[11]	Commercial strong cation-exchange hydrogel membrane	29 (lysozyme concentration not given, pH 7.0)	24.8 (5 mg lysozyme/ml solution; pH 7.0, 0.25-2.5 ml/min)	0.86
[12]	Hollow-fibre membranes loaded with weak cation-exchange resin particles	60 (lysozyme concentration, conditions not given)	65.7 (lysozyme concentration, conditions not given)	1.1
[17]	Strong cation-exchange hydrogel hollow-fibre membranes	140 (1-2 mg lysozyme/ml solution, pH 7.0)	~ 90 (1 ml lysozyme/ml solution; pH 7.0, 10 ml/min)	0.65
[31]	Strong cation-exchange hollow-fibre membranes	84 ± 9 (2 mg lysozyme/ml solution; pH 7.0)	~ 50.4 (1 mg lysozyme /ml solution; 1 ml/min, 0.1 bar)	0.60

Table 1 presents a comparison of the static binding and dynamic binding capacities for pure lysozyme solutions of several cation-exchange membrane materials. For most materials, the dynamic binding capacity is lower than the static binding capacity, as the membrane does not have enough time to reach saturation. Table 2 shows a summary of lysozyme activity recovery for the separation of lysozyme as well as end lysozyme purity for different cation-exchange membranes. The lysozyme activity process recovery ranges from 51.1 % to 82.7 % for ethanol soluble egg white solutions, while the lysozyme purity tends to vary between 60 % and 95 % [7,12,17,21].

Table 2. Comparison of lysozyme purity and lysozyme purification factor for the separation of lysozyme from egg white with different cation-exchange chromatography materials.

Ref.	Separation Material	Loading Solution and Conditions	Lysozyme Activity Process Recovery (%)	Lysozyme Purity (%)	Lysozyme Purification Factor
[7]	Prepared polysulfone strong cation-exchange membrane	Ethanol soluble egg white, pH 8.0, 1 ml/min	72.6	78.9	31.6
		Ethanol soluble egg white, pH 8.0; 10 ml/min	68.8	76.9	30.8
	ICE 450 unsupported commercial strong cation-exchange membrane	Ethanol soluble egg white; pH 8.0; 1 ml/min	82.7	60.4	24.2
		Ethanol soluble egg white, pH 8.0, 10 ml/min	76.1	63.6	25.4
[12]	Hollow-fibre membranes loaded with weak cation-exchange resin particles	Filtered, aqueous egg white, pH 7.4	95	95	27
[17]	Strong cation-exchange hollow-fibre hydrogel membrane	Filtered, aqueous egg white, pH 6.5, 10 ml/min, recycled	N/A	95	N/A
[21]	Prepared polysulfone strong cation-exchange membrane	Ethanol soluble egg white, pH 8.0; 10 ml/min	51.1	N/A	N/A
[35]	Alcohol-insoluble cross-linked pea pod solid (AI-CLPPS) ion-exchange chromatography resin	Ethanol soluble egg white, pH 8.0	71.1	N/A	4.7

2.2.1.2. Cation-Exchange Membrane Chromatography

Similar to many other chromatography operations, there are three phases: (1) sample loading; (2) binding and (3) elution. In cation-exchange membrane chromatography, the charged ligands of the membrane material possess a net negative charge. For protein separation (Figure 3), after sample loading, the proteins will be in contact with the negatively charged functional groups. Positively charged proteins adsorb to the negative surface, while negatively charged proteins will permeate through the membrane (Figure 3b and Figure 3c). The positively charged proteins may be eluted from the membrane by manipulating buffer conditions to alter electrostatic interactions (Figure 3d).

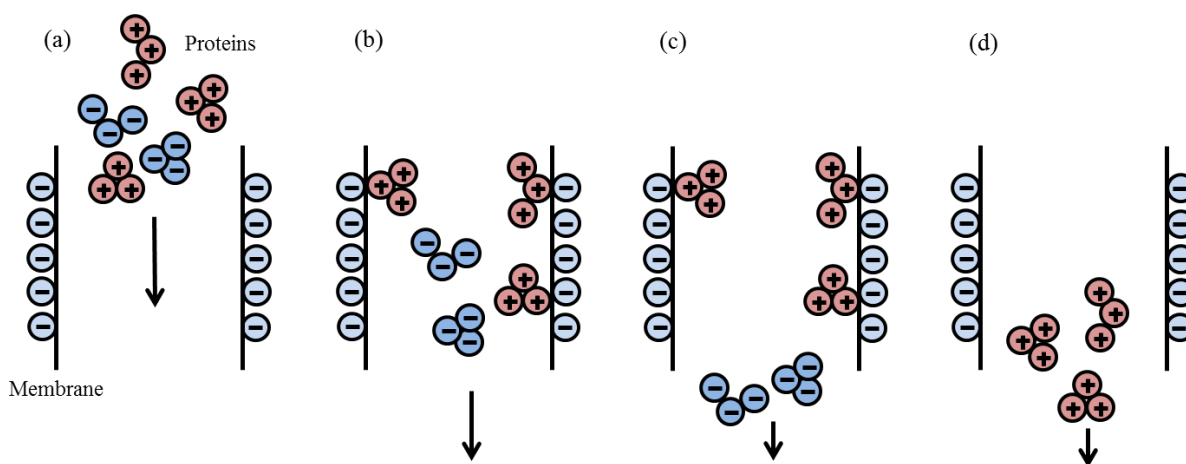


Figure 3. Cation-exchange membrane chromatography operation. (a) A mixture of proteins is passed through the membrane with negatively charged pores; (b) positively charged proteins bind to the negatively charged ligands; (c) negatively charged proteins pass through the membrane in solution; (d) positively charge proteins are eluted from the membrane surface and collected.

There are two main methods for the elution of bound protein from a cation-exchange membrane material, as outlined in Figure 4. The first method is to increase the salt concentration of the elution buffer, so that an increased ion concentration will surround the membrane and the bound protein. Oppositely charged ions will align themselves in the vicinity of the two charged surfaces, producing a charge shielding effect and reducing electrostatic interactions [28,36]. For high salt (ionic strength) solutions, effective binding no longer occurs and bound protein is eluted from the membrane (Figure 4b). The second method is to increase the pH of the elution buffer and reduce electrostatic interactions (Figure 4c). In cation-exchange membrane chromatography, increasing the pH of the solution above a protein's pI will bestow a net negative surface charge on the protein, while the

anionic membrane surface will become more negative [29,36]. As a result, electrostatic repulsion between the two similar charges will lead to the elution of the bound protein from the negatively charged ligands on the membrane surface.

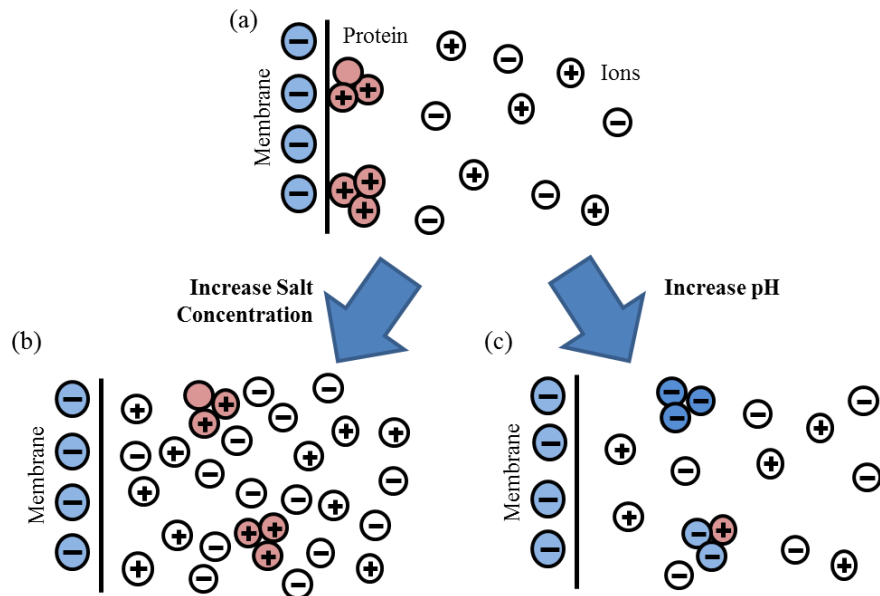


Figure 4. Effect of environmental conditions on protein binding in cation-exchange membrane chromatography. (a) Proteins bound to the membrane in solution; (b) effect of increasing salt concentration; (c) effect of increasing pH

As discussed previously, most cation-exchange membrane materials are strong exchangers, which will retain a constant surface charge throughout the entire pH range [7,11,17,21,31]. These materials are generally polysulfone ligands affixed to a polymeric backbone, such as cellulose, to provide structural support and the pore structure. Weak cation-exchange membranes are susceptible to changes in solution pH, as variations in pH may alter the deprotonation state of the charged ligands [4,22]. The charged function groups for weak cation-exchange chemistry are typically carboxylic acid, although other weak exchangers such as acetic acid are possible [6]. Cation-exchange membranes are typically operated in a flat sheet configuration in a cross-flow set-up [6,7,11,21], although hollow-fibre cartridges are also encountered [12,17].

2.2.1.3. *Natrix adsept*TM Weak Cation-Exchange Membrane Material

The weak cation-exchange hydrogel membrane utilized in this study is comprised of a functionalized hydrogel layer supported by a polyolefin matrix backbone, as shown in Figure 5. The porous support provides mechanical strength and structure to the membrane material. An environment-responsive macroporous hydrogel is grafted to the polymeric

support containing carboxylic acid ligands which offer ion-exchange capabilities and produces the pore structure when exposed to an aqueous solution. With a pK_a of 4.7, the carboxylic acid ligands will deprotonate and carry a net negative surface charge in neutral and basic pH conditions [26,37]. In pH conditions below pH 4.7, the membrane will be a neutral material, and electrostatic interactions will not be prevalent. The weak cation-exchange hydrogel is comprised of approximately 90 mol % carboxylic acid and 9 mol % crosslinker, with the remainder 1 % consisting of filler materials for improving membrane hydrophilicity [38]. The average pore size of the weak cation-exchange membrane ranges between 0.1 μm and 25 μm , while the volume porosity may vary between 40 % and 90 % according to pH or salt concentration [38].

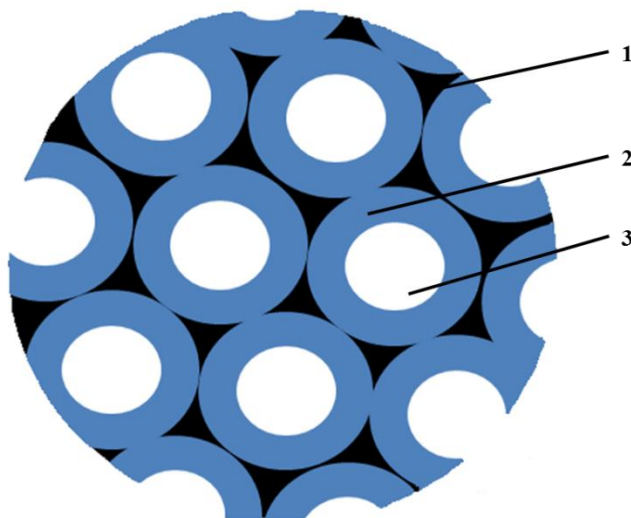


Figure 5. Structure of weak cation-exchange membrane: (1) Porous polyolefin support; (2) hydrogel layer affixed to support; (3) membrane pores.

2.3. Egg White

Hen eggs are widely used as ingredients in the food industry due to their high nutritional value and unique functional characteristics, such as emulsification, water binding, foaming, and gelation [19]. Egg white represents approximately 60 % of total egg weight, most of which is predominantly water. The remaining dry weight is divided between proteins, trace minerals, fats, vitamins, and glucose [19,39].

2.3.1. Egg White Proteins

There are nearly 40 different proteins found in egg white, contributing to 10-15 % of its total mass. The major proteins include ovalbumin, ovotransferrin, ovomucoid, ovomucin,

lysozyme, ovoglobulins, flavoprotein, and avidin [19,39]. These major proteins contribute much of the foaming and gelling properties of egg white, and possess a wide range of functional properties due to complex interactions between different peptide chains [19]. The protein composition of hen egg white (HEW) is given in Table 3.

Table 3. Hen Egg White Protein Components [19]

Protein	Composition [%] (w/w)	Molecular Weight [kDa]	pI
Ovalbumin	54	45	4.5-4.9
Ovotransferrin	12-13	77.7	6.0-6.1
Ovomucoid	11	28	4.1
Ovomucin	1.5-3.5	$5.5-8.3 \times 10^3$	4.5-5.0
Lysozyme	3.4-3.5	14.3-14.6	10.7
G2 ovoglobulin	1.0	47-49	4.9-5.5
G3 ovoglobulin	1.0	49-50	4.8, 5.8
Ovoflavoprotein	0.8	32-35, 80	4.0
Ovostatin	0.5	760-900	4.5-4.7
Cystatin	0.05	12	5.1
Avidin	0.05	55-68.3	10.0

Nearly all of the major protein constituents of HEW have an isoelectric point (pI) close to 4.5-5.0, with lysozyme and avidin being the only components with basic pI. Therefore, most HEW proteins will carry a similar charge as the weak cation-exchange membrane and electrostatic interactions between the two surfaces will not be significant. The majority of the hen egg white proteins have molecular weight below 100 kDa.

Hen egg white proteins are classified as globular proteins due to their round, spherical shapes. Globular proteins contain secondary structures that induce close packing of amino acid residues and a more compact arrangement. Egg white proteins are typically separated according to anion- and cation-exchange chromatographies, ethanol precipitation, or size-exclusion techniques [34,40,41]

Ovalbumin is well known for its foaming properties and is the most abundant egg white protein, representing 54 % of the total protein weight. Due to this high content, ovalbumin will predominate during egg white fractionation. Ovalbumin is a relatively small phosphoglycoprotein with a 45 kDa molecular weight [19,41]. Ovalbumin has high thermal

stability, with a denaturation temperature of approximately 84 °C, and is responsible for being one of the main egg allergens [19].

Ovotransferrin is a glycoprotein with a 77 kDa molecular weight. Also known as conalbumin, it represents 12-13 % of the total protein weight. Ovotransferrin is capable of reversibly binding ferric Fe^{3+} ions and carries anti-microbial properties [19,34,41,42]. Due to its iron binding properties, ovotransferrin has potential as an iron-fortification ingredient; however, it is also a major egg allergen [19].

Ovomucoid is a thermally-stable glycoprotein with antiviral, anti-tumor, and immunomodulating abilities [19,34,42]. It is highly resistant to heat degradation in acidic conditions but loses its thermal stability in alkaline environments. With a 28 kDa molecular weight, ovomucoid represents 11 % of the total protein weight. Ovomucoid is responsible for inducing the most significant immune response of all egg white protein allergens [19].

Ovomucin is a sulphated glycoprotein which contains two subunits (α - and β -) that differ in carbohydrate composition. The proportions of these subunits will define the physicochemical characteristics and molecular weight of ovomucin [19]. Ovomucin can be classified as either soluble or insoluble, with the higher molecular weight soluble ovomucin containing a higher proportion of β -subunits. Ovomucin is typically found in its insoluble form at neutral pH, but may be solubilised using mechanical or chemical treatments [19]. The protein also serves as an antiviral compound [34,42].

Other minor egg white proteins have their own unique characteristics. G2 and G3 globulins share similarities with ovalbumin by coagulating under heat treatment and solubilising in low salt solution [19]. Avidin can be used as a carrier for vitamins and for anti-microbial purposes, while flavoprotein is a vitamin stabilizer [34,42].

2.4. Lysozyme

Lysozyme is one of the most important egg white proteins for pharmaceutical, biotechnological, and food applications. Lysozyme can hydrolyse the β -1,4-linkage between muramic acid and *N*-acetyl glucosamine of mucopolysaccharides found in bacterial cells [19,43,44]. Lysozyme has widespread use as an antimicrobial agent and can provide structural, antigenic, antiviral, and anti-inflammatory functions and is an excellent preservative of milk-related products [19,34,42,44]. Formerly known as ovoglobulin G1, lysozyme consists of 129 amino acids distributed in two domains (α and β). Lysozyme is also

known to readily form electrostatic complexes with other HEW proteins, such as ovomucin, ovalbumin, and ovotransferrin,

Approximately 40% of the lysozyme polypeptide chain is in the α -helix configuration. These helices line a long active site for substrate binding located on the protein side [45]. Six lysine residues and four disulfide bonds are distributed throughout the peptide chain to stabilize protein structure [9,43,45]. The secondary structure of lysozyme is thermally stable up to 65 °C, especially in acidic conditions, although this stability may be modified through the addition of organics, such as ethanol [44,46].

As lysozyme is a small protein, possesses a unique pI, and has a well-studied structure, it is widely used as a model protein for the characterization of systems. Hen egg white, is its most abundant source [19,41].

2.4.1. Lysozyme Surface Charge

Twenty-nine different charged groups line the surface of lysozyme and contribute to its net charge. These side chains consist of both basic groups (arginine, lysine, and histidine), and acidic residues in the form of glutamic and aspartic acids [9]. All charged amino acid side groups have a different deprotonation tendency according to pH conditions, which will give a protein net surface charge dependence on environmental pH. The pI of lysozyme, is typically reported as 10.7 and independent of salt concentration, although some sources have reported pI to be as high as 11.3 [9,19,47]. Due to the basic nature of the isoelectric point, lysozyme carries a positive charge for a significant pH range. Increasing the pH decreases the surface charge of the protein with a slight plateau between pH 7-9. In this pH range, pH changes will not significantly alter electrostatic interactions between amino acid side groups and protein conformation will remain relatively stable [29,45].

The net charge of local regions of a protein can vary from that of the whole protein. For lysozyme, although the charge distributions for local regions and the whole protein follow a similar pattern, the active sites shows a higher relative net charge at all pH and was reported to have an isoelectric point of 12.1 [9]. The charge differences of binding sites may contribute to a stronger affinity for negatively charged surfaces compared to other areas of the lysozyme surface. Hence, even at the pI for lysozyme, some locations along the surface may still carry a positive charge, allowing for potential electrostatic interactions.

2.4.2. Effect of Salt

Lysozyme charge is also influenced by the presence of salt in solution. Due to the close proximity between charged amino acid ligands along the polypeptide chain, electrostatic interactions may occur within a protein's tertiary structure. These interactions between charged groups can promote deprotonation, thereby raising or lowering the resulting tendency to lose a proton compared to normal amino acid values. For example, the six lysine groups spread throughout the lysozyme surface will encourage acidic residues with a low pK_a to give up a proton through electrostatic attraction [47]. These interactions will cause a shift of the pK_a of the acidic groups towards lower pH values. The presence of ions in solution decreases the strength of electrostatic interactions through charge shielding, as the thickness of the diffuse layer of oppositely charged ions extending away from the surface is reduced [28]. This reduces the negative shift in the acidic side group pK_a . Thus, for pH values less than the lysozyme pI (10.7), the net charge of lysozyme increases with ionic strength [47]. For pH conditions above the lysozyme pI (pH 10.7), where basic side groups are similarly perturbed upwards, the opposite phenomenon is observed. Shifts in the pK_a towards higher pH values are minimized in the presence of salt, and the net surface charge of lysozyme is decreased [47].

When salts are present in aqueous solution, they will dissociate into their ions that can interact with lysozyme. Since lysozyme exists as a positively-charged molecule over a wide pH range, negative ions, such as chloride, will be attracted to lysozyme; altering the charge and conformation of lysozyme [47]. This effect is more pronounced at low pH, where the net surface charge of lysozyme is higher and negative charges will move into the electrical double layer surrounding lysozyme. Decreasing pH or increasing ionic strength will induce increased binding of chloride ions [47]. For pH above the lysozyme pI, chloride ions are expelled from the electrical double layer, decreasing the concentration of negative ions in the diffuse layer surrounding lysozyme. Since the electroneutrality of charges is required in the electrical double layer, cations such as sodium or potassium will exhibit opposing trends to those of anionic chloride [28,47]. The binding of ions to lysozyme will produce small changes to the tertiary structure and net surface charge. These changes can indirectly influence protein interactions with other surfaces or proteins.

Ionic strength is an important factor when determining lysozyme solubility. In room temperature solutions with a low ionic strength (0.25 – 0.34 M NaCl), lysozyme has a high solubility across the neutral pH range [48]. When the ionic strength is increased (greater than 0.68 M NaCl), however, lysozyme solubility rapidly decreases under all temperature and pH conditions. Decreasing temperature and increasing pH will also decrease lysozyme solubility [48]. Under conditions with reduced solubility, such as high ionic strength or pH greater than 7.0, lysozyme is more susceptible to the formation of aggregates and insoluble precipitates.

2.4.3. Effect of Organic Solvents

Since lysozyme is only naturally present in egg white in low concentrations, the need to increase lysozyme purity as a pre-treatment step may arise. Additives such as organic solvents are one such method through the selective precipitation of protein. Therefore, interactions between organic solvents and lysozyme are important factors to consider. Alcohols promote the formation of protein aggregates and insoluble precipitates by altering the tertiary structure of proteins through increased hydrophobic interactions and the disruption of ionic and hydrogen bond interactions [49]. Alcohols can bind to lysozyme, influencing its tertiary structure and protein activity. There are two main areas at which alcohol-lysozyme interactions tend to occur: the amino terminal of the polypeptide chain and at the sugar-binding cleft region known as the C site [49]. As the length of the alcohol chain increases (C₄ and up), greater interactions with the C site are observed. This has an inhibitory effect on lysozyme activity and also decreases the temperature at which lysozyme is denatured [49]. Therefore, when the addition of alcohol is necessary, short-chain alcohol such as ethanol may be utilized in order to minimize the impact of alcohol binding on activity and conformation of lysozyme [49].

2.4.4. Lysozyme Binding Properties

There are several potential active sites on the lysozyme surface responsible for the interaction with charged surfaces, proteins, and other solution compounds [9,20]. These sites tend to lie in close proximity to six lysine groups. In these active sites, the local areas of hydrophobicity can vary significantly. Therefore, the location and binding orientation of lysozyme may depend on the charge and hydrophobicity of the opposing surface [9]. Charges of different binding sites may also vary from one another at different pH values, which can

lead to preferential binding depending on the pH of the buffer. Sites with greater affinity dominate interactions and will be more likely to bind over lower affinity active regions.

Lysozyme is well-known for its ability to form complexes with other proteins. Of those present in hen egg white, electrostatic complexes with ovalbumin, ovotransferrin, and ovomucoid are the most common [44,50,51]. These complexes are predominant in low salt conditions and tend to have lower stability in extreme pH conditions. The positively charged residues of the lysozyme are vital in complex formation, as the addition of negative amine or guanidine groups have minimal impact on protein interactions [52]. Binding to ovalbumin produces a complex with a low degree of aggregation, although lysozyme activity is hindered as a consequence [44,51]. Interaction between lysine residues of lysozyme and sialic acid of ovomucoid is a frequent phenomenon due to the large pH range between the isoelectric points of the respective proteins [52]. The two oppositely charged proteins form a soluble electrostatic complex that is difficult to separate. The resulting particles are often too small to be precipitated out via centrifugation [51]. Although the application of heat treatment will induce aggregation of ovomucoid-lysozyme complexes, their formation can be mitigated with salt due to its ability to shield electrostatic attraction between the proteins [51].

2.5. Protein Precipitation

A common separation method for proteins is the induction of aggregates and precipitates through the manipulation of protein environment. The process typically consists of four-steps: (1) destabilization of the feed solution by altering the environment or adding a precipitating agent; (2) appearance of small solid particles of protein; (3) formation of flocs by convective transport; and (4) production of smooth, uniform precipitates due to hydrodynamic disruption and limits to floc size [53]. Precipitates can be removed via filtration or centrifugation and solubilized in solvent for purification of the target protein [54]. Precipitation is traditionally used as an initial step in protein purification due to its relatively low selectivity; however, recent developments with high selectivity affinity ligands have improved on this property [53,54].

2.5.1. Ethanol Precipitation

Ethanol is a common organic solvent used for lysozyme precipitation and separation. Due to its short chain length and relatively hydrophilic behaviour, ethanol

minimizes reduction in lysozyme activity [49]. Ethanol precipitation is often used with other techniques, such as isoelectric precipitation, as the addition of ethanol alone has negligible protein selectivity. At pH values close to the lysozyme isoelectric point (pH 10.7), less ethanol is required to induce precipitation as electrostatic repulsion between molecules is reduced [53,55,56]. Salt addition will also impact the effectiveness of precipitation, as low salt concentrations will result in a finer precipitate difficult to separate out, while at higher salt concentration lysozyme is more susceptible to denaturation effects [56]. Solubility in organic solvents is an important consideration with ethanol precipitation as some proteins other than lysozyme will actually have an increased solubility in ethanol, which can limit protein selectivity [56]. Thus, the use of ethanol to induce aggregation formation may not be suitable for all applications.

Ethanol concentration is a critical factor in determining the extent of lysozyme destabilization and aggregation. For example, solubilised lysozyme will repel similarly charged proteins or surfaces in an ethanol concentration less than 60 % (v/v), preventing the formation of aggregated protein clusters. As a result, solubility increases compared to that of an aqueous solution [57]. Low ethanol concentrations can increase hydrophobicity and induce tighter folding of lysozyme [43,46]. As the ethanol concentration increases, hydrophobic interactions alter the conformation of lysozyme through the formation of α -helices. Lysozyme eventually becomes entangled with other chains, and large, stable aggregates are formed [57]. When the ethanol concentration is above 90 % (v/v), lysozyme precipitates out into a gel-like structure. Based on these properties, the ideal ethanol concentration for retaining lysozyme in solution is less than 45 % (v/v) [57]. Although ethanol concentrations greater than 45 % (v/v) will give stable and soluble protein solutions, the temporary protein clusters formed in this range could potentially interact and become entangled with other unfolded protein aggregates in solution [57].

2.5.2. Separation of Lysozyme from Hen Egg White

Due to the differences in the surface charges between lysozyme and other major egg white proteins, precipitation techniques may be effective for separation. Aside from lysozyme, avidin, representing 0.05 % of the total egg white mass, is the only other protein present in egg white possessing a basic isoelectric point [19]. The pI of the majority of the

hen egg white proteins lies within the range of 4.0-6.0. Consequently, proteins such as ovalbumin, ovotransferrin and ovomucoid will aggregate and precipitate when exposed to pH between 4.0 and 6.0. On the other hand, lysozyme will retain a high negative charge and will remain soluble in pH conditions around 5.0 [48].

The addition of ethanol will accelerate the precipitation of egg white proteins near their isoelectric point, while lysozyme will remain solubilised in ethanol at low concentrations [57]. Thus, the precipitate formed through ethanol precipitation can be removed from solution, leaving only ethanol-soluble lysozyme. At higher ethanol concentrations, problems with the separation of lysozyme may be encountered, as the protein will aggregate in combination with other egg white proteins [57]. Since lysozyme can form complexes with other proteins, like ovomucoid, [51] any soluble complexes will also not be removed from solution.

While many of the studies focus on the binding of lysozyme, some studies incorporate the separation of lysozyme from crude egg white using novel separation techniques [7,12,14,16-18]. Most of these separation techniques consist of ion-exchange properties, and are predominantly strong-cation-exchangers [7,11,17,21,31]. Therefore, weak cation-exchange membrane materials have not been widely investigated [6,12].

The separation of lysozyme from egg white can also vary according to the pre-treatment step performed prior to the separation process. The most common egg white pre-treatment method is ethanol precipitation, where the aggregation of non-lysozyme proteins present in egg white are promoted through hydrophobic interactions in the presence of approximately 30 % (v/v) ethanol [7,21,35,40]. Alternatively, egg white solutions may be diluted with water or buffer and then filtered to remove contaminants or aggregated proteins [12,17,32].

2.6. Protein Quantitation

There exist several methods for protein quantification. These methods can determine protein concentration, distribution, and even purity in a solution, and will be discussed in the following sections.

2.6.1. UV-vis Absorbance

Proteins can absorb ultraviolet light with wavelengths in the range of 200 nm to 280 nm [58,59]. As UV light passes through a sample, photons are adsorbed by electrons, which will translate in the decrease of the light intensity reaching the detector. In proteins, different ligands and chains will absorb UV light at different wavelengths. Peptide bonds absorb photons at 210 nm, while aromatic residues such as tryptophan and tyrosine will absorb light at 280 nm. Phenylalanine will also accept photons at the 260 nm wavelength [58,59]. Although significant discrepancies may be observed when measuring protein samples, the use of UV light at 280 nm for protein concentration determination has been widely reported due to its simplicity, ease of use, and decreased chemical absorption compared to other wavelengths [58,59].

There are several factors that may influence the absorption of photons by proteins. The pH, ionic strength, and polarity may affect the protein tertiary structure and can change the absorbance spectrum of protein. As well, buffers and solubilized components may interact with the protein structure or may absorb UV light themselves, which can change the light passing through the sample [58,59]. Cuvette materials such as glass and polystyrene can also absorb UV light, although quartz minimizes this phenomenon.

Protein concentration estimation by UV spectrophotometry is based on the Beer-Lambert law shown in Equation 2-1. This law states that the fraction of light absorbed by the sample is proportional to the thickness and concentration of the absorbing solution, and is independent of light intensity [59].

$$Abs = -\log\left(\frac{I}{I_0}\right) = \epsilon cl \quad [2-1]$$

Where Abs is the absorbance of solution [-], I_0 is the intensity of light entering the solution [-], I is the intensity of light leaving the solution [-], ϵ is the molar extinction coefficient [$M^{-1} cm^{-1}$], c is the concentration [$mol L^{-1}$], and l is the light path length through the solution [cm]. In most cases, the light path length is 1 cm. While the extinction coefficient (ϵ) for most biomolecules, such as nucleic acids, lipids, and polysaccharides, is expressed in molar terms ($\epsilon_{molar}; M^{-1} cm^{-1}$), protein extinction coefficients are expressed as $\epsilon^{1\%}$ ($\%^{-1} cm^{-1}$) [59]. The $\epsilon^{1\%}$ is the absorbance of a 1 % (1 g/100 ml) solution at 280 nm wavelength. The protein extinction coefficient of lysozyme can range between 24.7 and 27.2

$\%^{-1} \text{ cm}^{-1}$ [59]. Concentration, in mg/ml, may be calculated from the protein extinction coefficient directly as shown in Equation 2-2.

$$c = \frac{A}{\epsilon^{1\%}} \times 10 \quad [2-2]$$

2.6.2. Bradford Protein Assay

Protein concentration in a solution may also be quantified from the formation of a protein-dye complex as in the Bradford method. Coomassie brilliant blue is a dye that exists in several chemical forms. The two most prominent forms are R-250 (structure shown in Figure 6) and G-250, which contains an additional two methyl groups [60,61]. Coomassie brilliant blue is known to occur in three different forms: neutral, cationic, and anionic, with the absorbance maxima of these three forms varying between 650 nm, 470 nm, and 595 nm, respectively [61-63]. The anionic species primarily binds to the side chains of arginine, tryptophan, tyrosine, histidine, and phenylalanine to form a protein-dye complex. Therefore, absorbance measurements at 595 nm can be correlated to protein concentration in solution [59,61-63].

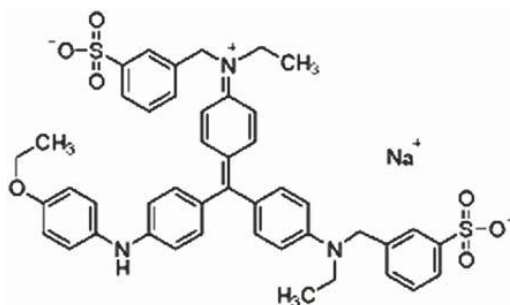


Figure 6. Structure of Coomassie brilliant blue R-250

Although the Bradford method is a rapid assay with high sensitivity, there are some limitations that may skew the calculated protein concentration. Anionic Coomassie brilliant blue has a high affinity for arginine ligands that is approximately eight times greater than other residues. As such, protein concentration tends to be overestimated for arginine-rich proteins [59]. A nonlinear relationship between absorption and protein concentration is often observed due to overlapping absorption spectra between the bound and free dye concentrations [61-63]. Since the formation of the protein-dye complex depends on the protein concentration and the free dye concentration, the ratio between absorbance at 595 nm

and absorbance at 450 nm has been reported to reduce nonlinearity for bovine serum albumin (BSA) concentrations between 0.2 and 20 $\mu\text{g/ml}$ [59,62,63].

2.6.3. Sodium Dodecyl Sulfate Poly(Acrylamide) Gel Electrophoresis (SDS-PAGE)

Electrophoresis is a rapid tool for protein identification and characterization due to its simplicity and high sensitivity. This method is based on the migration of proteins through a poly(acrylamide) support matrix subjected to an electric field. Poly(acrylamide) gel electrophoresis can determine size, quantity, purity, and isoelectric point of proteins in solution [64]. Sodium dodecyl sulfate poly(acrylamide) gel electrophoresis (SDS-PAGE) is one of the most common poly(acrylamide) gel electrophoresis methods. This method, first described by Laemmli, denatures protein and separates them according to size [64,65].

In SDS-PAGE analysis, the protein sample is heated at 100 °C in the presence of SDS and a thiol reducing reagent to break disulphide bonds, denature the polypeptide chains, and impart a uniform negative charge to the polypeptide structure. The amount of SDS bound to each polypeptide depends on the mass of the polypeptide (1.4 g SDS/g polypeptide) [64]. Therefore, the primary and secondary protein structure do not influence the formation of a SDS-protein complex, and the charge density is held constant. The length of each complex is proportional to the molecular weight of the protein, so size is the only determining factor on the mobility of the polypeptide through the support matrix [64,65]. After applying the electric field to induce protein migration through the gel, the separated polypeptides may be stained with one of several dye solutions to aid with visualization. Staining options include Commassie brilliant blue and silver staining.

There are some limitations to molecular weight estimation by SDS-PAGE. High ionic strength can inhibit SDS binding to protein, which can affect charge density and migration through the poly(acrylamide) gel. The presence of glycoproteins or high concentrations of acidic amino acid residues can lead to anomalous migration patterns due to interferences in hydrophobic and electrostatic interactions, respectively. Similarly, SDS-PAGE tends to overestimate highly basic proteins and those with high proline content [64]. Protein mixtures with the aforementioned conditions are special cases that must be accounted for when separating protein. Most protein molecular weight estimates are relatively reliable and do not require modifications.

2.6.4. Size-Exclusion High-Performance Liquid Chromatography (SE-HPLC)

Size-exclusion high-performance liquid chromatography (SEC-HPLC), also called size exclusion chromatography (SEC) separates particles according to size. The technique is based on the permeation of molecules through pores of the chromatography packing material, and depends on the size of the molecules relative to the pore size of the packing material [66,67]. When a mixture of solutes is injected into a column, smaller molecules will diffuse through the pores of the packing material, increasing retention time through the column. Large molecules, on the other hand, will not diffuse in the pores of the packing material and will be eluted first [67]. This process is demonstrated in Figure 7. A variety of quantification techniques can be used to determine concentrations of the eluting compounds, such as UV absorbance, refractive index, or fluorescence.

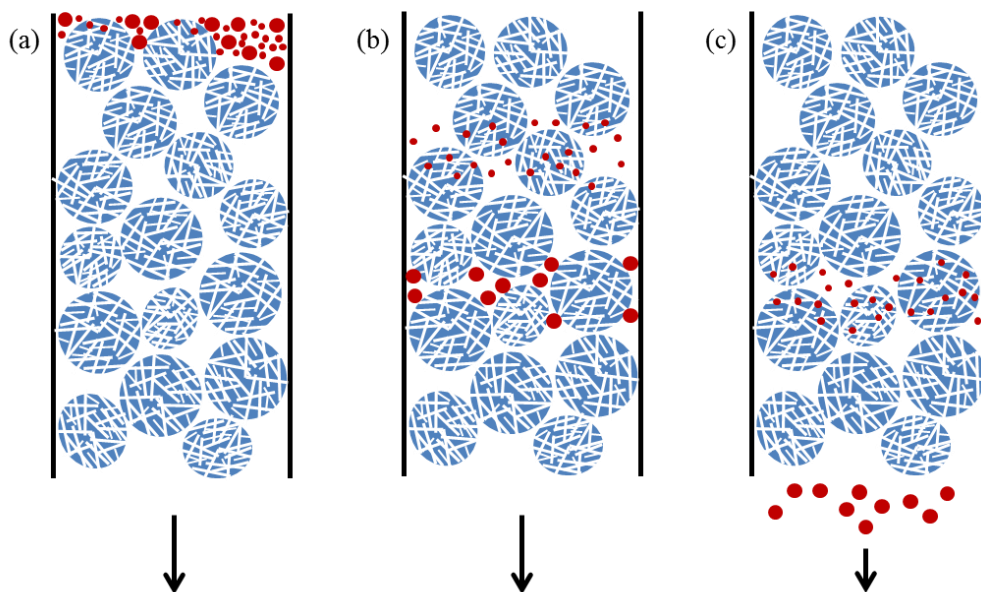


Figure 7. Separation of solutes in SEC-HPLC. (a) A mixture of solutes is injected into the column; (b) solutes are separated according to size, with small solutes diffusing into adsorbent pores; (c) large solute molecules are eluted while smaller solutes continue through the adsorbent material.

For the separation of proteins in an aqueous solution, SEC-HPLC materials include dextran, agarose, polyacrylamide, or porous silica for high pressure treatments [67]. As separation is based solely on size, pH and ionic strength should not have a significant impact on the elution times of different protein species, although hydrophobic interactions have been reported to increase elution times [66].

3. Separation of Lysozyme from Egg White through Incubation with a Novel Weak Cation-Exchange Membrane

A. Yeh, P. Fumeaux, C. Moresoli

This manuscript was guided by Dr. Christine Moresoli. Mr. Pierre Fumeaux conducted preliminary studies of static binding capacity under different pH and sodium chloride (NaCl) concentrations. The turbidimetric assay for lysozyme activity determination was adapted and developed by Ms. Katharina Hassel, while Ms. Priscilla Lai aided with the experiments. All other experiments and results included in this manuscript as well as all data analysis were performed by Mr. Andrew Yeh.

3.1. Overview

In this study, the extraction of lysozyme from egg whites was investigated through static incubation with a weak cation-exchange hydrogel membrane material. Lysozyme was chosen as a model protein due to its small size and well-understood characteristics. The egg whites were precipitated at pH 4.8 in the presence of 30 % (v/v) ethanol in order to reduce competitive binding of other proteins present in egg white to the membrane and promote lysozyme adsorption. Based on a given set of conditions, optimal pH and salt concentration of the binding step and elution step were determined through the measurement of total protein and lysozyme activity recovery from the membrane and recovery of the overall separation process. Protein selectivity of the separation process was determined through sodium dodecyl sulfate poly(acrylamide) gel electrophoresis (SDS-PAGE). The highest maximum lysozyme binding of 82.6 mg protein/ml membrane was achieved for pure lysozyme at pH 4.5 and 0 mM NaCl after 48 hours of incubation. Although high protein binding for ethanol soluble egg white (ESEW) at pH 4.5 and 0 mM NaCl was observed, poor total protein (26.7 %) and lysozyme activity (0.5 %) recovery from the membrane was achieved due to non-specific binding. The highest total protein (36.9 %) and lysozyme activity (74.0 %) process recovery was obtained when binding ESEW at pH 7.5 and 0 mM NaCl and elution at the same pH. Increasing the pH of the elution buffer after binding at pH 4.5 increased total protein and lysozyme activity process recovery, with the highest achieved at pH 7.5 and no NaCl addition (44.5 % and 68.8 %, respectively). Protein selectivity for binding at pH 4.5 and no NaCl addition was poor due to the presence of an ovomucoid polypeptide band in the elution stream, in addition to lysozyme. Therefore, a non-specific binding mechanism was confirmed under these conditions. Membrane incubation conditions for high recovery of lysozyme from ethanol soluble egg white proteins were determined as binding at pH 7.5 and 0 mM NaCl and elution with 1 M NaCl at the same pH due to high total protein and lysozyme activity recovery from the membrane and process recovery, and high lysozyme selectivity.

3.2. Introduction

The separation and purification of proteins and other biomolecules is traditionally performed through packed bed chromatography, which separates components according to their mobility through the material [1,4-8,10,11,13,20]. This separation can be based on size, charge, or affinity interactions. The resin beads are often comprised of highly porous material designed to maximize the surface area and number of binding sites on the material. Since most binding sites are positioned within resin pores, solutes must undergo a pore diffusion step to move from the surface [1,4-8,10,11,13,20]. Pore diffusion is often a slow process that can increase processing time and buffer volumes needed for effective separation. Traditional resin chromatography can be limited by poor mechanical strength of the resin material, high pressure drops, and difficult scale-up [1,4-7,11,13].

Alternative purification techniques aim at overcoming the limitations of traditional resin chromatography columns. Membrane processes are one such technology that is increasingly used for biomolecule separation and purification [1,4-7,11,13,22]. Through the chemical modification of the membrane surface, functional groups may be grafted onto a macroporous membrane support. This allows for the addition of binding sites, giving a chromatographic membrane similar resolution and selectivity to that of traditional chromatography resins. Membrane processes are also advantageous over traditional chromatography, as solute transport is dominated by convection and scale up is typically easier. Consequently, significantly shorter residence times are needed for protein separation [1,4-7,11,13,22].

Ion-exchange processes are common for protein purification due to their ease-of-use and versatility. The separation is based on electrostatic interactions between charged surfaces in which a stationary surface attracts oppositely charged solutes [1,4,5,7-10,20,22]. There are two main classifications of ion-exchange surfaces: cation-exchange and anion-exchange. Cation-exchange, which will be the focus of this study, uses a negatively charged surface to bind positively charged molecules. Cation-exchangers may be further divided into two categories: strong and weak cation-exchange materials. The surface charge of a strong exchanger will remain constant over the entire pH range. Weak cation-exchangers, however, will change surface charge density depending on the pH of solution [4,9,11,20].

This work aims to characterize the protein binding capacity of a membrane material with a weak cation-exchange hydrogel layer. Through the combination of membrane filtration and ion-exchange chemistry, high protein selectivity can be achieved at higher throughputs than in traditional resin chromatography [1,4,5,22,23]. The hydrogel layer, comprised of carboxylic acid functional groups, is environment-responsive; therefore, conditions such as pH and salt concentration can induce swelling or shrinking of the material, thereby altering pore sizes [13,68]. This changes the distribution of binding sites within membrane pores, and can alter interactions between protein and the membrane.

For this study, lysozyme was selected as a model protein to quantify protein-membrane interactions in response to different pH and sodium chloride (NaCl) conditions for a weak cation-exchange hydrogel material. Lysozyme is a small, well-characterized protein with a 14.3 kDa molecular weight that is often chosen for biotechnology and pharmaceutical applications [6,7,11-19]. As lysozyme is naturally present in egg white in low concentrations (approximately 3.5 % of egg white by mass), lysozyme is ideal for the determination of binding efficiency from a protein mixture [19]. While nearly all other egg white proteins have an isoelectric point in the range of 4.0-6.0, lysozyme has a basic pI of 10.7, allowing for the potential for high selectivity of a charge-based separation [19].

In this study, pH conditions were selected to ensure that lysozyme possessed a positive charge, while other egg white proteins and the weak cation-exchange membrane held strongly negative charges [9,19,69]. The pH of the solution and its salt concentration in the form of NaCl were varied to determine binding conditions for lysozyme present in a mixture of ethanol soluble egg white proteins. To date, literature focuses on either the quantification of the binding capacity of ion-exchange membrane chromatography materials [6,7,11,12,31] or the separation of lysozyme from egg white mixtures through more conventional methods (packed-bed chromatography, ethanol precipitation, etc.) [8,18,34,42]. For example, Wickramasinghe (2006) investigated the maximum and dynamic protein binding capacities of different ion-exchange membranes using confocal laser scanning microscopy [11]. Wang (2009) examined the pore structure of a prepared weak cation-exchange membrane material and its effect on protein binding [6]. Meanwhile, Omana (2010) developed a multi-column fractionation process for egg white proteins through a combination of anion- and cation-exchange resin materials [34]. Very few studies have

attempted to integrate both components into a single work [7,12,17,21], and most of these works utilize either a strong cation-exchange material or a hollow-fibre configuration. While lysozyme adsorption out of egg white using a weak cation-exchange membrane material has been studied by Chiu [7], the emphasis of this work was on total protein recovery from the membrane following adsorption and the overall separation process recovery for lysozyme activity.

Other egg white separation studies focus primarily on protein binding in a dynamic flow-through set-up [6-9,13,18,34,42]. In contrast, non-flow conditions were chosen for the study to allow for membrane saturation and to determine the maximum protein binding capacity of different lysozyme sources, while eliminating any protein-membrane interactions introduced directly through convective flow. This work investigated the recovery of lysozyme from the membrane after contact with an ethanol soluble egg white solution and the process recovery of the static separation process for total protein and lysozyme activity under two different modes of operation: (1) binding and elution at a constant pH, and (2) binding at pH 4.5 with a variable elution pH.

3.3. Experimental

3.3.1. Materials

The membrane chromatography materials used in this study were *Adsept*TM Weak C cation-exchange flat sheet membranes (thickness of 0.278 ± 0.019 mm) provided by Natrix Separations Inc. (Burlington, ON, Canada). Lysozyme from hen egg white (L6876), *Micrococcus lysodeikticus* ATCC No. 4698 (M3770), citric acid (C0759), bromophenol blue sodium salt (B5525), glycine (G7126), albumin from bovine serum (A3912), and N,N,N',N'-tetramethylethylenediamine (TEMED) (T9281) were purchased from Sigma-Aldrich Co. (St. Louis, MO, USA). Coomassie brilliant blue R250 (161-0400), and 30 % acrylamide/bis solution (37.5:1, 2.6 % C) (161-0158) were obtained from Bio-Rad Laboratories Inc. (Hercules, CA, USA). Ammonium persulfate (BP179), ethanol (95 % v/v) and sodium dodecyl sulfate (BP166) were purchased from Fisher-Scientific Co. (Toronto, ON, Canada). PageRuler Plus Prestained Protein Ladder, 10 to 250 kDa (26619) was purchased from Thermo Scientific (Waltham, MA, USA). Sodium phosphate dibasic heptahydrate (SX0715) was purchased from EMD Chemicals Inc. and sodium chloride

(ACS 783) was purchased from BDH Inc. (both now a division of Merck Group) (Darmstadt, Germany). Tris (X188-7) was purchased from JT Baker (now Avantor Performance Materials, Center Valley, PA, USA).

3.3.2. Egg white pretreatment with ethanol

The treatment of egg white with ethanol was adapted from Chiu et al. and Guérin-Dubiard et al. [7,42]. Fresh eggs were purchased from a local market. The egg whites of 12 eggs were manually separated from their yolks and gently stirred for 30 min on a Dyla-Dual[®] hotplate/stirrer (12620-970, VWR International, Radnor, PA, USA). The egg whites were diluted to 33.3 % (v/v) with 50 mM phosphate citrate buffer, pH 4.8 to a final total protein concentration of 15 mg/ml. The pH was adjusted to pH 4.8 with 1M HCl, and the dilution was stirred gently for another 30 min. The diluted egg whites were mixed with an equal volume of 60 % (v/v) ethanol and incubated overnight at room temperature. The precipitate was removed by centrifugation at 34 178 x g for 45 minutes at 22 °C (Sorvall WX Ultra 100 Centrifuge, 46902, Thermo Scientific, Waltham, MA, USA). The supernatant, referred to as ethanol soluble egg white (ESEW), was collected and used in subsequent static binding and characterization tests.

3.3.3. Static adsorption experiments

For each experiment, a new square sample of Natrix *adsept*[™] Weak C-type cation-exchange membrane with a length and width of 14.5 ± 0.9 mm and a thickness of 0.278 ± 0.019 mm was cut out from a flat sheet. Each membrane piece was equilibrated with 5 ml of 50 mM phosphate citrate buffer at pH 4.5, 6.0, or 7.5 under gentle shaking on a Gyrotory[®] Shaker-Model G2 (New Brunswick Scientific Co. Inc, Edison, NJ, USA) at 125 rpm for 2 hours. Upon equilibration, each membrane sample was transferred into 10 ml of binding solution. Two binding solutions were tested: ESEW diluted to a final total protein concentration of 0.363 ± 0.001 mg/ml with 50mM phosphate citrate buffer of a given pH and 0.358 ± 0.002 mg/ml lysozyme in 50 mM phosphate citrate buffer of a given pH. Membrane samples were incubated under gentle shaking at 125 rpm. Total protein concentration was measured via UV-vis spectrophotometry with a Spectronic[™] GENESYS[™] 2 UV-vis spectrophotometer (Milton Roy, now under Thermo Scientific, Waltham, MA, USA) at

280 nm. Absorbance readings of the binding solution were taken over the course of 48 hours of membrane incubation.

Following 48 hours of incubation with a given solution, the membrane samples were transferred into 15 ml of 50 mM phosphate citrate buffer at pH 4.5, 6.0, or 7.5 and 1 M sodium chloride (NaCl) to promote elution of protein. Membrane samples were incubated for 2 hours on a shaker and the UV-vis absorbance of the solution was read at 280 nm.

Static total protein binding capacity was estimated through Equation 3-1.

$$q = (C_0 - C_f) * \frac{V_{\text{solution}}}{V_{\text{membrane}}} \quad [3-1]$$

Where q represents the binding capacity [mg total protein/ml membrane], C_0 is the initial protein concentration prior to membrane incubation [mg/ml], C_f is the total protein concentration after membrane incubation [mg/ml], V_{solution} is the volume of solution [ml], and V_{membrane} represents the volume based on the dry dimensions of the membrane sample [ml membrane]. Total protein concentration was determined using a calibration curve developed from the 280 nm absorbance of lysozyme concentrations ranging from 0.1 mg/ml to 1.0 mg/ml.

The static total protein binding capacity over the 48 hour incubation period was fitted with a saturation-type model, shown in Equation 3-2, based on time. From this model, the maximum total protein binding capacity was determined at different pH and NaCl concentration conditions.

$$q = \frac{q_{\text{max}} t}{K + t} \quad [3-2]$$

Where q is the total protein binding capacity per membrane volume [mg/ml membrane], q_{max} is the estimated maximum total protein binding capacity per membrane volume [mg/ml membrane], t is the time elapsed [min], and K is the binding rate coefficient [min].

The initial total protein binding rate was determined, according to Equation 3-3, as the derivative of equation 3-2 at time $t = 0$.

$$\text{Initial Binding Rate} = \left. \frac{dq}{dt} \right|_{t=0} = \frac{q_{\text{max}}}{K} \quad [3-3]$$

Where dq/dt is the protein binding rate [mg/ml membrane·min], and q_{max} and K are as defined previously.

As a comparison, the average total protein binding rate was determined according to Equation 3-4 as the slope of a linear relationship of the protein binding capacity over the first six hours of membrane incubation.

$$\text{Average Binding Rate}_P = \frac{q_{(t=360\text{min})} - q_{(t=0\text{min})}}{360\text{min} - 0\text{min}} \quad [3-4]$$

Where $q_{(t=360\text{min})}$ and $q_{(t=0\text{min})}$ is the total protein binding capacity [mg/ml membrane] at 360 min and 0 min of incubation time.

3.3.4. Total protein recovery

Following the elution step, the total protein recovery from the membrane was calculated for both pure lysozyme and ESEW according to Equation 3-5.

$$\text{Recovery}_{\text{Membrane, P}} (\%) = \frac{C_{\text{eluted}} V_{\text{eluted}}}{C_{\text{initial}} V_{\text{initial}} - C_{\text{final}} V_{\text{final}}} * 100 \% \quad [3-5]$$

Where C_{eluted} is the total protein concentration in the elution solution [mg/ml], V_{eluted} is the volume of the elution solution [ml], C_{initial} is the total protein concentration of the protein binding solution prior to the membrane incubation step [mg/ml], V_{initial} is the volume of the protein binding solution prior to the membrane incubation step, C_{final} is the total protein concentration of the protein binding solution after 48 hour incubation [mg/ml], and V_{final} is the volume of the protein binding solution after 48 hour incubation [ml].

The total protein recovery of the process was calculated for pure lysozyme and ESEW according to Equation 3-6.

$$\text{Recovery}_{\text{Process, P}} (\%) = \frac{C_{\text{eluted}} V_{\text{eluted}}}{C_{\text{initial}} V_{\text{initial}}} * 100 \% \quad [3-6]$$

Where C_{eluted} , V_{eluted} , C_{initial} , and V_{initial} are as defined previously.

3.3.5. Determination of lysozyme activity

The lysozyme activity was determined with a turbidimetric microplate assay adapted from Helal and Melzig [70]. A suspension of *Micrococcus lysodeikticus* served as a substrate for lysozyme, as the protein hydrolyses the β -1,4-linkage between muramic acid and *N*-acetyl glucosamine in the bacterial cell wall [19,43,44,71]. A unit of activity for lysozyme (U) was defined as a decrease in absorption of 0.001 per minute at 450 nm and 37 °C. A lysozyme activity calibration curve was prepared from a series dilution of an 800 U/ml lysozyme stock solution with 0.1 M phosphate buffer, pH 6.24 in eight wells of a 96 well microplate. The

calibration curve was prepared in duplicate. Four replicates (50 μ l) of each unknown sample were added into separate wells. The reaction was started with the addition of 200 μ L of a 0.36 mg/ml *Micrococcus lysodeikticus* (substrate) solution to each well. With the addition of substrate to each well, the final diluted activities of the calibration curve ranged from 0 U/ml to 120 U/ml. Absorption was read at 450 nm with a Synergy 4 microplate reader (BioTek Instruments Inc., Winooski, VT, USA) held at 37 °C. Readings were taken every minute for ten minutes under gentle shaking.

3.3.6. Lysozyme activity recovery

The lysozyme activity recovery from the membrane and the lysozyme activity of the separation process were calculated for each lysozyme source according to Equation 3-7 and Equation 3-8, respectively.

$$\text{Recovery}_{\text{Membrane, A}} (\%) = \frac{A_{\text{eluted}} V_{\text{eluted}}}{A_{\text{initial}} V_{\text{initial}} - A_{\text{final}} V_{\text{final}}} * 100 \% \quad [3-7]$$

$$\text{Recovery}_{\text{Process, A}} (\%) = \frac{A_{\text{eluted}} V_{\text{eluted}}}{A_{\text{initial}} V_{\text{initial}}} * 100 \% \quad [3-8]$$

Where A_{eluted} is the lysozyme activity in the elution solution [U/ml], V_{eluted} is the volume of the elution solution [ml], A_{initial} is the lysozyme activity of the protein binding solution prior to the membrane incubation step [U/ml], V_{initial} is the volume of the protein binding solution prior to the membrane incubation step [ml], A_{final} is the lysozyme activity of the protein binding solution after 48 hour incubation [U/ml], and V_{final} is the volume of the protein binding solution after 48 hour incubation [ml].

3.3.7. Sodium dodecyl sulphate poly(acrylamide) gel electrophoresis (SDS-PAGE)

Sodium dodecyl sulfate poly(acrylamide) gel electrophoresis (SDS-PAGE) was performed through a resolving separation gel consisting of 15 % acrylamide with 10 % (w/v) SDS adapted from Laemmli [65]. The stacking gel for sample loading contained 4 % acrylamide. Unknown samples were diluted to a total protein concentration of 1.00 mg/ml with 50 mM phosphate citrate, pH 7.5, measured by UV absorbance at 280 nm. The diluted samples were mixed in a (1:2) ratio with an SDS reducing buffer containing β -mercaptoethanol, glycerol, and bromophenol blue. The resulting solution was heated at 95 °C for 4 minutes and a volume totalling approximately 2.5 μ g of protein was loaded into a BioRad Mini-PROTEAN[®] Tetra Cell system (165-8001, BioRad Laboratories Inc., Hercules,

CA, USA). The protein ladder comprised of undisclosed prestained recombinant proteins in a reducing agent with a range of molecular weights from 10 kDa to 250 kDa (10 kDa, 15 kDa, 25 kDa, 35 kDa, 55 kDa, 70 kDa, 100 kDa, 130 kDa, 250 kDa). Five μ l of the protein ladder was loaded into each gel in duplicate. Electrophoresis was performed in a Tris-Glycine buffer with 0.1 % SDS at 100 V through the stacking gel and 150 V for the resolving gel, for a total of 90 minutes using a PowerPacTM Basic Power Supply (164-5050, Bio-Rad Laboratories Inc., Hercules, CA, USA). The gels were incubated under shaking at 125 rpm in a methanol/acetic acid/water (2:1:2, v/v/v) staining solution containing 0.1 % Coomassie Brilliant Blue R250 for 2 hours, and destained overnight with a methanol/acetic acid/water (4:0.7:5.3, v/v/v) solution. Images of the gels were taken with an Epson Stylus CX4810 All-in-One Printer (Epson America Inc., Long Beach, CA, USA).

3.3.8. Statistical analysis

Paired two sample t-test analyses were performed to determine significance between mean values of sample sets. The test statistic t_0 was calculated according to Equation 3-9 [72].

$$t_0 = \frac{\bar{y}_1 - \bar{y}_2}{\sqrt{\frac{S_1^2}{n_1} + \frac{S_2^2}{n_2}}} \quad [3-9]$$

Where t_0 is the test statistic, \bar{y}_1 and \bar{y}_2 are the sample means of set 1 and 2, S_1^2 and S_2^2 are the sample variances, and n_1 and n_2 are the sample set sizes.

A 90 % confidence interval ($\alpha = 0.90$) was calculated with a two-tailed t test. Significance was determined when the test statistic, t_0 , was greater than the critical t value, as determined by the degrees of freedom through Equation 3-10 [72].

$$v = \frac{\left(\frac{S_1^2}{n_1} + \frac{S_2^2}{n_2}\right)^2}{\frac{\left(\frac{S_1^2}{n_1}\right)^2}{n_1 - 1} + \frac{\left(\frac{S_2^2}{n_2}\right)^2}{n_2 - 1}} \quad [3-10]$$

Where v is the degrees of freedom, and S_1^2 , S_2^2 , n_1 , and n_2 are as defined previously.

Significance is reported as either partial significance or total significance. For partial significance, the reported values are significantly different from at least one other factor under similar conditions (e.g. pH, NaCl concentration, protein source). For total significance, the reported value is statistically significant from all other factors under similar conditions.

3.4. Results and Discussion

3.4.1. Ethanol precipitation of egg whites

Crude egg white was treated with an equal volume of 60 % (v/v) ethanol to increase lysozyme concentration and reduce process volumes through the removal of competing egg white proteins [7,40,73]. The extent of protein removal by ethanol precipitation was characterized by SDS-PAGE (Figure 8). The detected molecular weight polypeptide bands were compared to literature values for major egg white proteins (

Table 4). Four significant polypeptide bands were identified, corresponding to ovotransferrin (OT), ovalbumin (OA), ovomucoid (OM) and lysozyme (LYS). Two faint polypeptide bands located between the ovotransferrin and ovalbumin bands were identified as ovoglobulin (OG) [19].

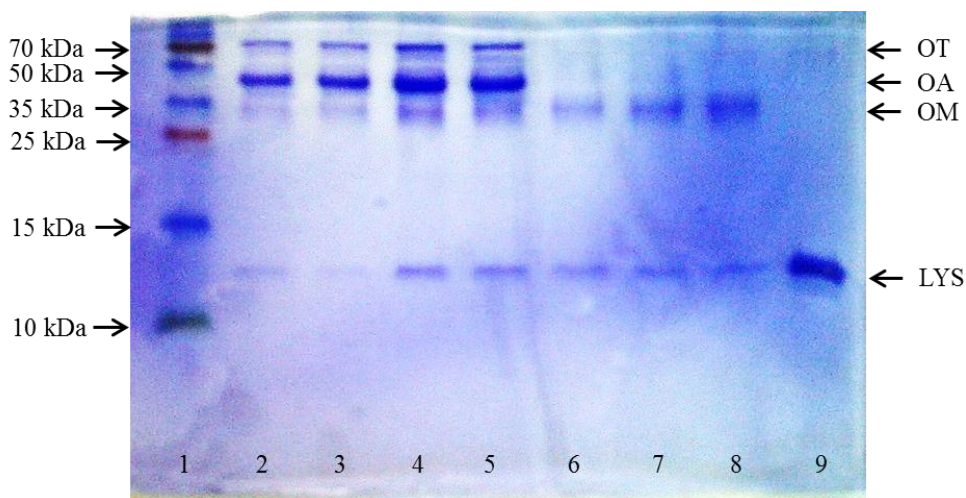


Figure 8. SDS-PAGE analysis of the ethanol precipitation process on 15 % acrylamide gel, stained with Coomassie brilliant blue. Lane 1: protein ladder (values given on the left); Lanes 2 and 3: crude egg white following storage at room temperature and -20 °C, respectively, diluted with Milli-Q water to concentration of 0.3 mg/ml (2 µg of protein loaded); Lanes 4 and 5: crude egg white diluted 33.3 % (v/v) with 50mM phosphate citrate, pH 4.8, after storage at room temperature and -20 °C, respectively, to concentration of 0.6 mg/ml (4 µg); Lanes 6, 7, and 8: ESEW after storage at room temperature, 4 °C, and -20 °C, respectively (4 µg); Lane 9: 1.0 mg/ml lysozyme (4 µg).

Table 4. Comparison of molecular weight estimates of major egg white proteins obtained by SDS-PAGE analysis. Estimates based on crude egg white after storage at room temperature (Lane 2 in Figure 8)

Egg White Protein	Ovotransferrin	Ovoglobulin	Ovalbumin	Ovomucoid	Lysozyme
Estimated Molecular Weight [kDa]	71.5	59.9, 48.8	38.7	29.8	13.2
Reported Molecular Weight [kDa] [19]	77.7	50, 47	45	28	14.3

Similar molecular weight estimates were obtained for ovomucoid and lysozyme. Differences in molecular weight were observed for ovotransferrin, ovalbumin, and ovoglobulin, with approximately 10 to 15 % relative error compared to reported values. Significant removal of ovotransferrin and ovalbumin by ethanol precipitation was obtained as shown by the polypeptide pattern of ESEW (Lanes 6, 7, and 8 in Figure 8). The polypeptide bands in the ESEW profile corresponding to lysozyme and ovomucoid had similar intensity to those in diluted egg white (Lanes 4 and 5). This suggests that their concentration remained similar before and after incubation with 30 % (v/v) ethanol. Ovomucoid did not co-precipitate with other egg white proteins likely due to its high solubility in organic solvents and its ability to form electrostatic complexes with lysozyme [51,52,73]. There was no visible effect of storage temperature on the polypeptide profile for each of the different egg white solutions.

3.4.2. Pure lysozyme and ESEW solution properties

The total protein concentration and lysozyme activity of pure lysozyme and ESEW solutions for different pH and NaCl conditions prior to membrane incubation are compared in Table 5. Total protein concentration measured by UV absorbance at 280 nm remained constant at all pH conditions. Similarly, the presence of NaCl and the source of protein did not affect the total protein content. Lysozyme activity was significantly lower when comparing the ESEW aqueous solution to pure lysozyme ($p < 0.10$). Under all pH and salt concentrations investigated in this study, the lysozyme activity of the ESEW aqueous solution was approximately 60 % lower than that of the pure lysozyme. This indicates that the ESEW solution could potentially be comprised of as much as 40 % lysozyme, based on the similar total protein concentrations of all solutions. As shown previously in Figure 8, the predominant protein contained in ESEW aqueous solution was ovomucoid, with some trace amounts of ovalbumin and ovotransferrin.

Table 5. Total protein concentration and lysozyme activity of pure lysozyme and ESEW solutions, as measured by UV-vis absorbance at 280 nm and a turbidimetric assay at 450 nm, respectively.

Protein Source	NaCl [mM]	Total Protein [mg/ml]			Lysozyme Activity [U/ml]		
		pH			pH		
		4.5	6.0	7.5	4.5	6.0	7.5
Pure Lysozyme	0	0.354 ** ^Ω (0.002)	0.348 * ^{ΩΩ} (0.002)	0.348 * ^Ω (0.002)	1815.4 (114.4)	1820.5 (128.3)	2036.8 (143.1)
	150	0.359 ** ^{ΩΩ} (0.002)	0.355 * ^Ω (0.001)	0.353 * ^Ω (0.001)	1679.3 (70.8)	1723.5 (78.9)	1727.0 (107.6)
	300	0.354 ^Ω (0.002)	0.356 ^Ω (0.003)	0.352 (0.002)	1666.5 (81.5)	1626.9 (51.1)	1727.5 (71.9)
ESEW	0	0.354 ^Ω (0.004)	0.352 ^Ω (0.003)	0.352 ^Ω (0.003)	723.4 * (34.1)	725.5 * (10.6)	833.3 ** ^{ΩΩ} (17.8)
	150	0.362 * ^Ω (0.000)	0.364 * ^{ΩΩ} (0.000)	0.363 ^{ΩΩ} (0.000)	688.5 (20.3)	705.7 (40.0)	734.1 ^Ω (35.7)
	300	0.356 (0.003)	0.355 ^Ω (0.004)	0.353 ^Ω (0.004)	715.0 (22.4)	650.3 (81.8)	696.9 ^Ω (46.3)

Note: Values in brackets represent standard error based on n = 8 (150 mM NaCl condition), and n = 16 elsewhere for total protein concentration and based on n = 4 for lysozyme activity. The significance between total protein and lysozyme activity was not investigated.

* represents partial significance according to pH for a specific NaCl concentration and a specific protein source.

** represents total significance according to pH for a specific NaCl concentration and a specific protein source.

^Ω represents partial significance according to NaCl concentration for a specific pH and a specific protein source.

^{ΩΩ} represents total significance according to NaCl concentration for a specific pH and a specific protein source.

The conductivity of 50 mM phosphate citrate buffer is shown in Table 6 for all pH conditions at 0 mM and 300 mM NaCl and reflects the presence of NaCl or the buffer ingredients. The addition of lysozyme to the buffer did not significantly impact solution conductivity at pH 6.0 and 7.5 ($p < 0.10$). Conductivity of ESEW diluted in 50 mM phosphate citrate to a total protein concentration of 33.3 % (v/v) was approximately 20 % lower than the conductivity of pure buffer at all pH with no NaCl addition, and 45 % lower at all pH in the presence of 300 mM NaCl ($p < 0.10$). The addition of salt did not show as much influence on solution conductivity for ESEW aqueous solution as for 50 mM phosphate citrate due to the presence of non-conductive ethanol in solution.

Table 6. Conductivity of 50 mM phosphate citrate, ESEW, and lysozyme solutions according to pH and NaCl conditions

Solution	Conductivity [mS/cm]			
ESEW	2.01 (0.01)			
	NaCl [mM]	pH		
		4.5	6.0	7.5
50 mM Phosphate Citrate Buffer	0	4.32 (0.01) ^{ΩΩSS}	5.49 (0.02) ^{ΩΩS}	7.01 (0.03) ^{ΩΩS}
	300	32.60 (0.10) ^{ΩSS}	33.15 (0.15) ^{ΩS}	34.45 (0.15) ^{ΩS}
Lysozyme Aqueous Solution	0	4.40 (0.01) ^{ΩΩSS}	5.53 (0.03) ^{ΩΩS}	7.03 (0.02) ^{ΩΩS}
	300	32.18 (0.29) ^{ΩΩSS}	32.98 (0.16) ^{ΩΩS}	33.95 (0.04) ^{ΩΩS}
ESEW Aqueous Solution	0	3.44 (0.09) ^{ΩΩSS}	3.99 (0.14) ^{ΩΩSS}	4.82 (0.14) ^{ΩΩSS}
	300	18.21 (0.06) ^{ΩΩSS}	18.42 (0.04) ^{ΩΩSS}	19.15 (0.05) ^{ΩΩSS}

Note: Values within brackets represent standard errors for n = 2.

All conductivity values are significant according to pH for a specific NaCl concentration and a specific solution.

^Ω represents partial significance according to NaCl concentration for a specific pH and a specific solution.

^{ΩΩ} represents total significance according to NaCl concentration for a specific pH and a specific solution.

^S represents partial significance according to solution for a specific NaCl concentration and a specific pH.

^{SS} represents total significance according to solution for a specific NaCl concentration and a specific pH.

3.4.3. Lysozyme and egg white static binding capacity

Due to the dynamic nature of the weak cation exchange membrane hydrogel layer containing the carboxylic acid ligands, different pH and NaCl concentrations were investigated.

The pH range of this study (pH 4.5-7.5) was selected to determine the effect on electrostatic interactions between protein and membrane on protein binding. At pH 4.5, lysozyme carried a highly positive surface charge, while the net surface charge of the membrane should have been negligible as operation was below the membrane pK_a (4.7). Therefore, electrostatic interactions should not be significant at this pH. As the pH of solution increased, the surface charge of the membrane increased allowing for electrostatic interactions to dominate. pH 7.5 was chosen as a midpoint between lysozyme pI and the membrane pK_a in order to maximize cation-exchange binding capacity.

The addition of NaCl to the binding solution was varied to determine the effect of NaCl on protein binding and lysozyme selectivity. High NaCl concentration (300 mM) was chosen to determine the overall relationship between NaCl and protein binding, and was compared to binding when no NaCl was added. NaCl concentrations greater than 300 mM were not investigated, as further increasing the presence of ions in solution could promote

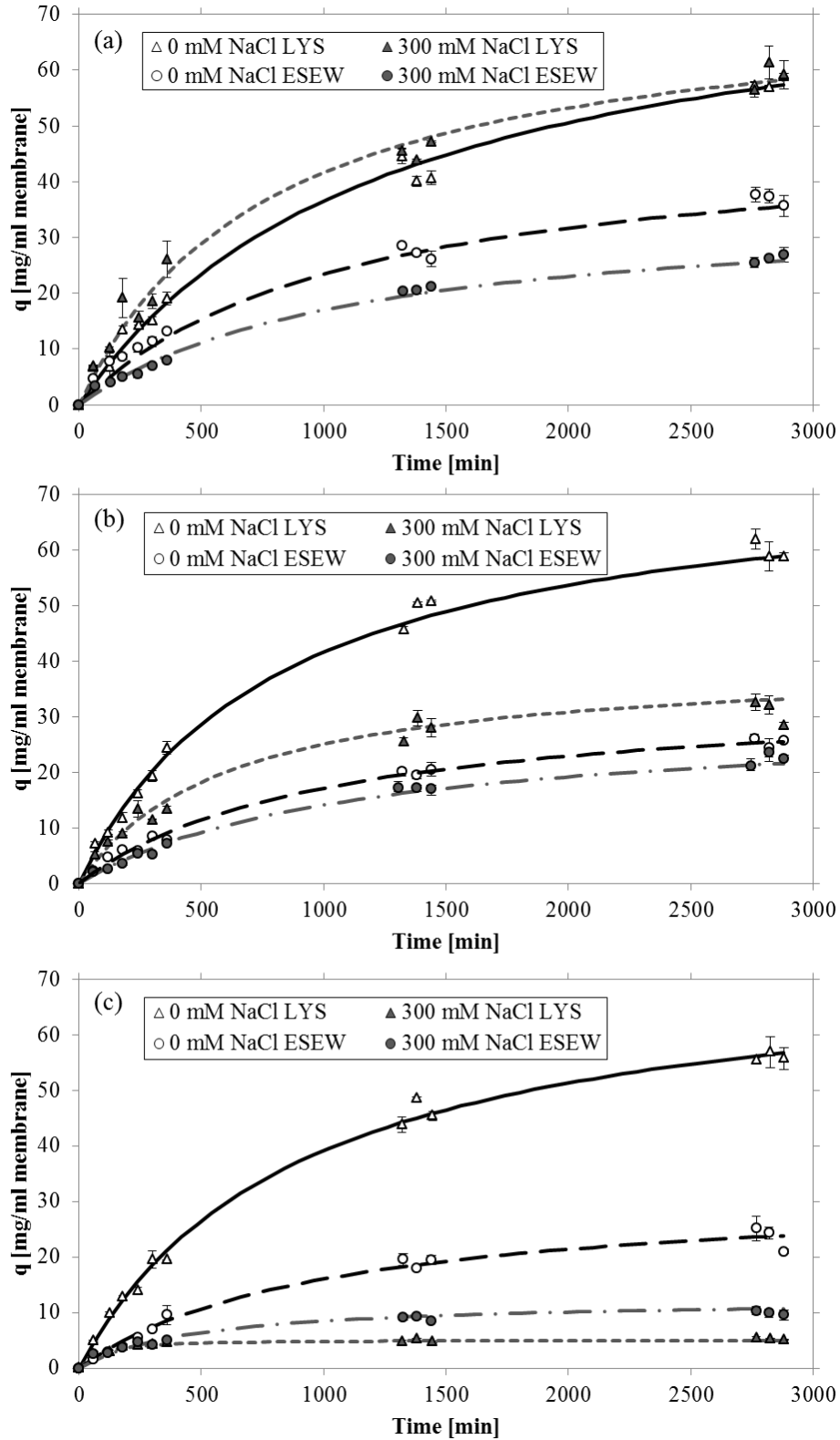


Figure 9. Time dependent total protein static binding capacity for pure lysozyme and ESEW at 0 mM and 300 mM NaCl concentrations for (a) pH 4.5, (b) pH 6.0, and (c) pH 7.5. Error bars represent standard error for $n = 4$. The lines were calculated from experimental data and equation 3-2.

protein elution from the membrane, leading to difficulties in protein retention during the binding step.

The kinetics of the static total protein binding for ESEW and lysozyme solutions to the Weak C membrane are shown in Figure 9. Maximum total protein binding capacity was not yet observed after 48 hours of incubation for most pH and NaCl conditions. The static total protein binding curves were fitted with a saturation-type model based on time (Equation 3-2). The maximum total protein binding capacities calculated from the binding curves are presented in Table 7. Overall, the highest total protein binding capacity after 48 hour incubation was observed at pH 4.5 and no NaCl addition for both ESEW and pure lysozyme, whereas the lowest total protein binding capacity was observed at pH 7.5 and 300 mM NaCl. The observed maximum binding capacities were based on the dry volume of the membrane material. This volume calculation, however, includes the void volume of the membrane pores so the actual volume of the material itself would be lower, depending on the porosity of the membrane sample. Therefore, the actual maximum binding capacity of the membrane material may be significantly higher depending on membrane porosity.

Increasing the pH of binding solution decreased the total protein binding capacity after 48 hour incubation for both protein sources, with a more pronounced effect observed when 300 mM NaCl was added to the binding solution. At the higher NaCl concentration, the total protein binding capacity of pure lysozyme decreased by 92.8 % when increasing the pH from 4.5 to 7.5, while the maximum protein binding capacity for ESEW decreased by 70.2 % over the same range. The presence of NaCl in the binding solution also decreased the maximum binding capacity for both protein sources at each pH condition. The increased presence of ions in solution would have decreased the magnitude of the opposing charges of the membrane and the protein, reducing the attraction between them. Although this phenomenon was not unexpected, the presence of salt in the binding solution revealed some remarkable observations. When operating at a pH below the membrane's pK_a , increased ion concentration in solution did not significantly influence the binding of protein to the membrane for both protein solutions ($p > 0.10$). As a result, electrostatic interactions may not be prominent at pH 4.5, and an alternative binding mechanism may be responsible to the high total protein binding to the membrane. Further investigation into this non-electrostatic binding interaction would aid in the characterization of the membrane material, and could

potentially allow for an alternative separation technique with the same membrane; however, investigation into the mechanism was beyond the scope of this project.

As the pH of the binding solution increased, the effect of increasing the NaCl concentration during membrane incubation was enhanced. For the pure lysozyme solutions, increasing the NaCl concentration decreased the maximum total protein binding capacity by 52.4 % at pH 6.0 and by 92.9 % at pH 7.5. Consequently, the presence of salt in solution was highly effective in preventing protein-membrane interactions at pH 7.5 for both ESEW and pure lysozyme solutions. Two potential elution strategies may therefore be extracted from the binding curves: the addition of salt and a pH gradient in the presence of high salt. Both of these strategies will be investigated in subsequent sections.

Table 7. Maximum protein binding capacities and initial protein binding rates to Weak C membranes according to pH and NaCl conditions after 48 hour incubation.

Protein Source	pH	NaCl (mM)	Maximum Protein Binding Capacity [mg/ml membrane]	Initial Protein Binding Rate [mg/ml membrane·min]	Average Protein Binding Rate [mg/ml membrane·min]
Lysozyme	4.5	0	82.6 (4.6)	0.067 (0.008)	0.051 (0.004)
		300	73.8 (1.5) **	0.095 (0.001)	0.065 (0.001) **
	6.0	0	79.2 (5.0) ^Ω	0.091 (0.007)	0.064 (0.002) ^Ω
		300	37.7 (2.9) ** ^Ω	0.071 (0.006)	0.041 (0.001) ** ^Ω
	7.5	0	74.8 (3.5) ^Ω	0.083 (0.007)	0.059 (0.003) ^Ω
		300	5.3 (0.1) ** ^Ω	0.071 (0.017)	0.010 (0.000) ** ^Ω
ESEW	4.5	0	46.2 (4.5)	0.053 (0.003) ^Ω	0.037 (0.003)
		300	37.9 (2.2) *	0.031 (0.000) ^Ω	0.025 (0.000)
	6.0	0	34.6 (2.1)	0.034 (0.001)	0.026 (0.000)
		300	33.3 (1.9) *	0.025 (0.003)	0.021 (0.002)
	7.5	0	32.1 (1.3) ^Ω	0.032 (0.002)	0.025 (0.001)
		300	11.3 (1.1) ** ^Ω	0.030 (0.005)	0.016 (0.002)

Note: Average protein binding rate estimated from the first 6 hours of incubation. Values in brackets represent standard errors for n = 2. The significance between maximum protein binding capacity, initial protein binding rate, and average protein binding rate was not investigated.

* represents partial significance according to pH for a specific NaCl concentration and a specific protein source.

** represents total significance according to pH for a specific NaCl concentration and a specific protein source.

^Ω represents total significance according to NaCl concentration for a specific pH and a specific protein source.

While similar patterns were observed in the time-dependent binding curves of the two different sources of lysozyme, the binding of protein from ESEW aqueous solution was shown to behave differently from a pure lysozyme solution. Although the maximum total

protein binding capacity for ESEW was approximately half compared to the pure lysozyme maximum total protein binding capacity, protein binding from the ESEW solution was observed to be more robust under varying pH and NaCl concentrations. Increasing the pH and NaCl concentration of the binding solution did not significantly affect the maximum binding capacity of total protein from ESEW, except when at pH 7.5 and 300 mM NaCl ($p > 0.01$). The more pronounced effect of pH and NaCl on protein binding for pure lysozyme compared to ESEW aqueous solution may be due to increased conductivity of the pure lysozyme aqueous solutions (Table 6); however, the more stable ESEW binding capacities indicate that other egg white proteins may be binding to the membrane. For example, when binding at pH 7.5 with 300 mM NaCl, the maximum total protein binding capacity for ESEW was higher than for pure lysozyme.

The maximum total protein binding capacity for weak cation-exchange membranes at pH 7.5 and 0 mM NaCl (74.8 ± 3.5 mg/ml membrane) was very high compared to calculated monolayer coverage of $9.6 \mu\text{g/ml}$ membrane, suggesting that a significant portion of the protein binding to the membrane was located within the pore structure [31]. The maximum total protein binding capacity was comparable to other cation-exchange materials reported in literature [6,11,12,17,31]. Maximum total protein binding capacities of 89.5 mg/ml membrane [6] and 67 mg/ml membrane [74] are reported for 24 hour incubation of UV-initiated, polymer-grafted strong cation-exchange membranes in 5.0 mg/ml lysozyme solutions at pH 7. Similarly, maximum total protein binding capacity of 60 mg/ml for an unknown lysozyme concentration in a hollow-fibre membrane loaded with weak cation-exchange resin particles [12] and 84 ± 9 mg/ml for 2 mg/ml lysozyme at pH 7 with a tentacle-based strong cation-exchange hollow fibre membrane [31] have also been achieved. Static incubation of membrane materials in egg white solutions has not been studied elsewhere, as the implementation of a dynamic set-up was favoured [7,12,17,21].

The initial protein binding rates for pure lysozyme and ESEW are shown in Table 7 according to pH and NaCl concentration. The initial protein binding rates for ESEW showed similar trends to those of the maximum binding capacity with a decreased rate of protein binding observed with increasing NaCl concentration. Protein binding rate decreased with increasing pH when no NaCl was present in the binding solution. As with the maximum total protein binding capacity, the highest initial protein binding rate for ESEW aqueous solutions

was at pH 4.5 and 0 mM NaCl, while the lowest initial total protein binding rate was observed at pH 7.5 and 300 mM NaCl. With the initial binding rate of pure lysozyme, a lower initial total protein binding rate was observed at pH 4.5 in the absence of NaCl than when 300 mM NaCl was added to the binding solution, further reinforcing the notion of a non-electrostatic binding interaction.

The initial total protein binding rates were compared to average protein binding rates calculated over the first six hours of membrane incubation. For all pH and NaCl concentration conditions, the average protein binding rate was lower than the initial binding rate. The average binding rates for ESEW aqueous solution were approximately 25 % lower than the initial protein binding rates indicating a decrease in protein binding over time. With the average protein binding rate of pure lysozyme solutions, a decrease of approximately 30 % was observed for all conditions except binding at pH 7.5 with 300 mM NaCl. In that experiment, the average binding rate was 86 % lower than the initial protein binding rate. The significant decrease was likely a result of the membrane surface achieving saturation within the first four hours of membrane incubation.

3.4.4. Total protein and lysozyme recovery from the membrane

Two different recovery calculations were determined for the membrane incubation process. Recovery from the membrane represents the ability to recover total protein or lysozyme activity from the membrane surface during the elution step. Process recovery represents the overall separation of total protein or lysozyme activity by comparing concentrations in the elution stream to the concentrations in the initial feed. Process recovery is the more common calculation in literature and is commonly referred to as recovery.

Total protein elution and recovery from the membrane was obtained by contacting the membrane samples with a 50 mM phosphate citrate buffer and 1 M NaCl. Two pH elution strategies were examined: (1) binding and elution at the same pH, and (2) binding at pH 4.5 and elution at a different pH. The total protein and lysozyme activity recovery from the membrane for both strategies will be discussed in the next sections.

3.4.4.1. Binding and elution at the same pH

The total protein recovery from the membrane for binding and elution at the same pH (Table 8) for pH 6.0 and 7.5 was at least 97 % for all NaCl conditions and the two

lysozyme sources. Although the highest maximum total protein binding capacity was observed at pH 4.5 for the ESEW and pure lysozyme solutions, the resulting total protein recovery from the membrane was 70 % lower than at pH 6.0 and 7.5. Since operation was below the pK_a (4.7) of the membrane, it is theorized that binding occurred due to non-electrostatic interaction. At pH 4.5, the membrane hydrogel layer carries a net neutral charge due to the protonization of carboxylic acid groups. While lysozyme will possess a high positive relative net surface charge of 0.9 at pH 4.5, ovalbumin and ovomucoid will carry either a net neutral or small negative surface charge under similar conditions according to their pI values (between 4.5-4.9 and at 4.1, respectively) (Table 3). Since most surfaces will not be charged at pH 4.5, protein-membrane electrostatic interactions would be negligible while non-electrostatic forces would be significant. Therefore, increasing the ionic strength of the elution buffer would be ineffective in promoting protein elution.

Table 8. Total protein and lysozyme activity recovery from the membrane and process recovery for binding at different pH and NaCl concentrations and elution at 1 M NaCl and the same pH.

Binding Condition		Elution	Total Protein		Lysozyme Activity	
pH	NaCl [mM]	pH	Membrane Recovery [%]	Process Recovery [%]	Membrane Recovery [%]	Process Recovery [%]
Aqueous Lysozyme						
4.5	0	4.5	5.3 (0.5) **	4.5 (0.4) **	0.5 (0.1) * Ω	0.4 (0.1) * Ω
	300		6.5 (1.2) **	5.4 (0.9) **	5.1 (0.6) Ω	4.8 (0.5) Ω
6.0	0	6.0	98.5 (0.7) *	88.3 (1.1) * Ω	28.9 (6.7) *	27.9 (6.4) *
	300		103.8 (3.2) **	47.7 (1.9) ** Ω	15.6 (7.4)	11.3 (4.7)
7.5	0	7.5	98.4 (1.1) * Ω	85.7 (1.3) * Ω	136.4 (14.3) ** Ω	114.4 (11.0) ** Ω
	300		136.1 (8.1) ** Ω	8.7 (0.6) ** Ω	0.7 (1.8) Ω	1.6 (0.7) Ω
ESEW Aqueous Solution						
4.5	0	4.5	26.7 (2.9) ** Ω	13.8 (1.4) ** Ω	0.5 (0.0) **	0.4 (0.0) ** Ω
	300		17.9 (1.9) ** Ω	7.0 (0.7) ** Ω	15.1 (2.3)	14.6 (2.2) Ω
6.0	0	6.0	98.0 (3.4) *	39.1 (0.8) ** Ω	27.1 (1.9) *	26.9 (1.9) * Ω
	300		98.3 (3.7) *	33.2 (0.9) ** Ω	[-23.9] (16.8)	6.2 (1.7) Ω
7.5	0	7.5	97.3 (1.1) *	36.9 (0.9) ** Ω	88.9 (12.4) *	74.0 (11.5) *
	300		97.7 (7.2) *	12.4 (0.1) ** Ω	28.2 (8.4)	5.2 (0.1)

Note: Values in brackets are standard error with $n = 8$ for total protein and $n = 2$ for lysozyme activity. The significance between total protein and lysozyme activity, and between membrane recovery and process recovery was not investigated.

* represents partial significance according to pH for a specific NaCl concentration and a specific protein source.

** represents total significance according to pH for a specific NaCl concentration and a specific protein source.

Ω represents total significance according to NaCl concentration for a specific pH and a specific protein source.

The recovery of lysozyme activity from the membrane was influenced by pH and NaCl concentration for binding and elution at constant pH (Table 8). Lysozyme activity recovery from the membrane at pH 4.5 was less than 15 % for both NaCl concentrations and protein sources, as expected from the low total protein recovery from the membrane observed under these conditions. However, while nearly 100 % of the total protein bound to the membrane was recovered at pH 6.0, the lysozyme activity recovery from the membrane was significantly lower, likely due to a deactivation effect on lysozyme activity in pH conditions below 7.0 [75]. Since the activity assays were performed on the individual elution conditions, some of the lysozyme activity may be able to be recovered by readjusting the pH of the elution solution. It should be noted that the negative lysozyme activity membrane recovery observed for binding at pH 6.0 in the presence of 300 mM NaCl was due to similar activity values obtained before and after the membrane incubation step. Slightly higher lysozyme activity was reported following membrane incubation, which led to a negative amount of bound lysozyme activity (according to equation 3-7). Consequently, this negative term propagated through to the final membrane recovery value. It may be concluded that the recovery of lysozyme activity from the membrane under these conditions are negligible. Elution at pH 7.5 after binding at pH 7.5 and 0 mM NaCl retained lysozyme functionality, having the highest lysozyme activity recovery from the membrane for both lysozyme sources. Conversely, lysozyme activity recovery from the membrane for binding at pH 7.5 and 300 mM NaCl decreased by at least 60 % for ESEW and was negligible for the pure lysozyme solution when compared to binding at pH 7.5 and no NaCl addition.

3.4.4.2. Binding at pH 4.5 with a variable elution pH

The observed non-electrostatic binding and limited total protein recovery from the membrane at pH 4.5 was confirmed when the pH of the elution solution was increased to pH 6.0 and pH 7.5; pH conditions above the pK_a of the membrane material (Table 9). The increased total protein recovery from the membrane with increasing elution pH was independent of NaCl concentration ($p < 0.10$), similar to the behaviour observed in experiments with binding and elution at the same pH for pH 6.0 and pH 7.5. The highest total protein recovery from the membrane for binding at pH 4.5 was observed for elution at pH 7.5 with no NaCl addition, approximately 10 % lower than the maximum total protein recovery

from the membrane when the pH remained constant during binding and elution for ESEW under the same pH and NaCl conditions ($p < 0.10$). The total protein recovery from the membrane for the pure lysozyme solution at pH 7.5 after binding at pH 4.5 (94.0 % and 98.3 %), was not statistically different from the total protein recovery from the membrane obtained for binding and elution at constant pH 7.5 (98.4 % and 136.1 %) at both NaCl binding concentrations ($p > 0.10$).

Table 9. Total protein and lysozyme activity recovery from the membrane and process recovery for binding at pH 4.5 and different NaCl concentrations and elution at 1 M NaCl and variable pH.

Binding Condition		Elution	Total Protein		Lysozyme Activity	
pH	NaCl [mM]	pH	Membrane Recovery [%]	Process Recovery [%]	Membrane Recovery [%]	Process Recovery [%]
Aqueous Lysozyme						
4.5	0	4.5	5.2 (0.4) **	4.3 (0.0) **	0.3 (0.2) **	0.2 (0.1) *
	300		4.7 (0.4) *	4.0 (0.4) *	0.2 (0.1) *	0.2 (0.1) *
6.0	0	6.0	47.5 (5.6) **	40.9 (3.3) **	24.3 (2.1) *	21.2 (0.6) *
	300		76.7 (23.9)	63.9 (18.2)	41.9 (10.0)	36.2 (7.6)
7.5	0	7.5	94.0 (0.4) **	80.2 (2.3) **	62.9 (8.8) *	54.6 (10.3)
	300		98.3 (2.4) *	82.2 (2.0) *	68.3 (9.0) *	60.4 (7.9) *
ESEW Aqueous Solution						
4.5	0	4.5	27.6 (1.3) *	14.3 (0.2) ** ^Ω	5.5 (4.6) *	4.9 (4.2) *
	300		16.0 (1.8) **	6.0 (0.2) * ^Ω	0.2 (0.3) *	0.2 (0.2) *
6.0	0	6.0	61.9 (5.5)	32.3 (2.5) *	34.7 (1.4) *	29.9 (1.7) *
	300		69.4 (8.1) *	26.5 (4.1)	47.3 (3.9) *	42.6 (3.4) *
7.5	0	7.5	87.0 (0.7) *	44.5 (0.0) * ^Ω	80.0 (1.6) **	68.8 (0.8) **
	300		87.9 (0.7) *	33.0 (0.1) * ^Ω	82.1 (23.4)	69.3 (20.0)

Note: Values in brackets are standard error with $n = 2$ for total protein and for lysozyme activity. The significance between total protein and lysozyme activity and between membrane recovery and process recovery was not investigated.

* represents partial significance according to pH for a specific NaCl concentration and a specific protein source.

** represents total significance according to pH for a specific NaCl concentration and a specific protein source.

^Ω represents total significance according to NaCl concentration for a specific pH and a specific protein source.

Increasing the pH for the elution after binding at pH 4.5 increased the recovery of lysozyme activity from the membrane in a similar pattern to the total protein recovery from the membrane (Table 9). The highest lysozyme activity recovery from the membrane for ESEW was achieved at pH 7.5 elution conditions, with no significant difference when compared to the maximum lysozyme activity recovery from the membrane for binding and

elution at a constant pH. While less than 30 % of the lysozyme activity was recovered for binding and elution at constant pH 7.5 and 300 mM NaCl for the two lysozyme sources, the lysozyme activity recovery from the membrane increased three-fold for ESEW and almost 100-fold for pure lysozyme solution for binding at pH 4.5 and 300 mM NaCl and eluting at pH 7.5. The improved lysozyme recovery from the membrane with increasing elution pH was in agreement with literature showing increasing lysozyme activity with increasing pH under all salt conditions [75].

3.4.5. Total protein and lysozyme process recovery

The total protein and lysozyme activity process recovery, estimated according to Equation 3-6 and Equation 3-8, are shown in Table 8 for binding and elution at constant pH and in Table 9 for binding at pH 4.5 with variable elution pH. The total protein process recovery and lysozyme activity process recovery reflected the combined effect of the total protein recovery and the maximum protein binding capacity.

3.4.5.1. Binding and elution at the same pH

The total protein process recovery at constant pH 4.5 for binding and elution was low (less than 15 %) regardless of whether NaCl was present, reflecting the poor protein recovery from the membrane (Table 8). At constant pH 6.0 and pH 7.5 for binding and elution, the total protein process recovery decreased with NaCl addition reflecting the NaCl effect observed for the maximum protein binding capacity. The highest protein process recovery was observed at pH 6.0 and pH 7.5 when no NaCl was added in the binding stage for the two sources of lysozyme. The total protein process recovery after binding at pH 6.0 and pH 7.5 and no NaCl addition was significantly lower for the ESEW aqueous solution at only 56 % of the total protein process recovery for the pure lysozyme solutions ($p < 0.10$). The presence of NaCl in the binding solution had a greater influence on the binding of pure lysozyme to the membrane compared to the binding of ESEW (Figure 9). Due to the presence of ethanol in ESEW, the addition of NaCl to solution did not increase the solution conductivity to the same extent as for the lysozyme aqueous solution (Table 6). This reduced the charge shielding effect produced by increasing ion concentrations in solution, which reduced electrostatic interactions between protein and the membrane [28,47]. Therefore, despite similar total protein recovery from the membrane at pH 6.0 and 7.5, the presence of

salt in solution had a greater impact on the binding of pure lysozyme to the membrane. Similar total protein process recovery was observed for binding and elution at pH 4.5 for both protein sources, as operation was below the pK_a of the membrane and electrostatic interactions were not dominant.

The lysozyme activity process recovery at constant pH for binding and elution (Table 8) reflected the recovery of lysozyme activity from the membrane. The process recovery of lysozyme activity was less than 15 % at pH 4.5 and when NaCl was present at all pH conditions, similar to the low lysozyme activity recovery from the membrane at these conditions. The highest lysozyme activity process recovery, 74.0 ± 11.5 % (ESEW aqueous solution) and 114.4 ± 11.0 % (lysozyme solution), was obtained at pH 7.5 when no NaCl was present during binding.

3.4.5.2. Binding at pH 4.5 with a variable elution pH

When the pH of the elution buffer was varied for binding at pH 4.5 (Table 9), the total protein process recovery increased and provided a means to recover significant amounts of protein bound to the membrane. Increasing the pH of the solution from pH 4.5 to pH 7.5 increased the negative charge of the membrane surface and of any protein impurities present in solution. Therefore, electrostatic interactions between the membrane surface and positively charged lysozyme (pI 10.7) were allowed to dominate, and the addition of NaCl to solution increased the elution of bound protein from the membrane. The presence of NaCl in the binding solution did not affect total protein process recovery of the pure lysozyme aqueous solution at all pH ($p > 0.10$). For ESEW aqueous solution, however, the addition of NaCl to the binding solution significantly decreased the total protein process recovery at pH 4.5 (14.3 % with no NaCl addition, 6.0 % at 300 mM NaCl) and pH 7.5 (44.5 % and 33.0 %, respectively) ($p < 0.10$). Increasing total protein process recovery was observed with increasing elution pH at both NaCl binding concentrations. Higher total protein process recovery was observed in ESEW for binding at pH 4.5 with no NaCl addition and elution at pH 7.5 (44.5 %) compared to binding and elution at pH 7.5 and 0 mM NaCl (36.9 %), indicating the potential for multiple strategies for the static separation of lysozyme from egg white ($p < 0.10$).

Lysozyme activity process recovery for binding at pH 4.5 and elution under variable pH (Table 9) increased with pH, similar to the recovery of lysozyme activity from the membrane. Maximum lysozyme activity process recovery of at least 50% was observed at pH 7.5, with no statistically significant effect of NaCl or lysozyme source ($p < 0.10$). Adjusting the pH above 4.7, the pK_a of the membrane, during the elution step increased the process recovery of lysozyme activity due to the reintroduction of electrostatic interactions between lysozyme and the membrane surface.

The lysozyme activity process recovery observed for static operation should have been near its maximum after 48 hour membrane incubation. The lysozyme activity process recovery for constant pH binding and elution at pH 7.5 and no NaCl addition for ESEW (74.0 %) was similar to previously reported lysozyme recovery [7,21,35]. Chiu obtained lysozyme activity recovery of ethanol-treated egg whites at pH 8.0 ranging from 68.8 % to 82.7% for prepared and commercial strong cation-exchange membranes under flow rates of 1 ml/min and 10 ml/min [7]. A maximum lysozyme recovery of 51.1 % was reported for the isolation of lysozyme from egg white treated with ethanol at pH 8 with a permeate flow rate of 10 ml/min using a strong cation-exchange membrane [21]. The observed lysozyme activity process recovery from ESEW when binding and elution steps were at pH 7.5 was also comparable to lysozyme activity recovery of ESEW at pH 8 using a novel alcohol-insoluble cross-linked pea pod solid (AICPPS) ion-exchange resin chromatography system (71.7 %) [35].

3.4.6. Specific lysozyme activity after elution

The specific activity of lysozyme recovered after elution with 1 M NaCl for the two different binding and elution strategies is presented in Table 10. When binding and elution steps were performed at the same pH, the specific activity of lysozyme decreased when pH was increased from 6.0 to 7.5 and when the NaCl concentration of the binding solution increased from 0 mM to 300 mM NaCl for both protein sources. At pH 4.5, however, high specific activity was observed when binding in the presence of 300 mM NaCl, despite very low process recoveries. Similar to the lysozyme activity process recovery, the highest specific activity was obtained following binding at pH 7.5 with 300 mM NaCl while the lowest specific lysozyme activity was at pH 4.5 in the absence of NaCl. Despite lower total

protein process recoveries from ESEW solutions, similar specific lysozyme activities were observed compared to the binding and elution of a pure lysozyme stream. Thus, the presence of other egg white proteins in solution does not appear to influence the lysozyme activity during the static recovery of lysozyme.

Table 10. Specific lysozyme activity in the elution solution after membrane incubation according to pH and NaCl concentration for two different binding and elution pH strategies with 1 M NaCl elution.

Elution pH	Binding NaCl [mM]	Binding and Elution at Same pH		Binding at pH 4.5, Elution with Variable pH	
		Binding pH	Specific Activity [U/mg]	Binding pH	Specific Activity [U/mg]
Aqueous Lysozyme					
4.5	0	4.5	283 (48) ^{*Ω}	4.5	347 (139)
	300		3761 (54) ^{**Ω}		296 (104) *
6.0	0	6.0	1518 (62) ^{*Ω}	4.5	2519 (608)
	300		648 (97) ^{*Ω}		2714 (468)
7.5	0	7.5	5034 (1071)	4.5	3280 (1106)
	300		396 (0) *		3362 (356) *
ESEW Aqueous Solution					
4.5	0	4.5	54 (4) ^{*Ω}	4.5	820 (736)
	300		4324 (482) ^{**Ω}		48 (82) ^{**}
6.0	0	6.0	1523 (37) ^{*Ω}	4.5	1781 (36) ^Ω
	300		429 (126) ^{**Ω}		3399 (241) ^{*Ω}
7.5	0	7.5	4719 (1091) ^{**Ω}	4.5	2967 (430)
	300		1052 (27) ^{**Ω}		4192 (596) *

*Values in brackets are standard errors, n = 2. The significance between total protein and lysozyme activity and between membrane recovery and process recovery was not investigated.

* represents partial significance according to pH for a specific NaCl concentration and a specific protein source.

** represents total significance according to pH for a specific NaCl concentration and a specific protein source.

^Ω represents total significance according to NaCl concentration for a specific pH and a specific protein source.

When the pH of the elution solution was varied after membrane incubation at pH 4.5, increasing specific lysozyme activity was observed when the elution pH was increased from pH 4.5 to pH 7.5. As well, similar to the trends observed with the lysozyme activity process recovery for the same elution strategy, the addition of 300 mM NaCl to the binding solution at pH 6.0 and 7.5 increased the specific activity of the elution stream. Low specific activity was observed for binding and elution at pH 4.5 with 300 mM NaCl unlike in the previous elution study. Therefore, although a low amount of high activity lysozyme may be

recovered after binding at pH 4.5 with 300 mM NaCl, it is not always consistent. Further investigation into the binding mechanism at pH 4.5 may allow for a more reproducible recovery of high specific activity lysozyme.

3.4.7. Protein binding selectivity (SDS-PAGE)

The selectivity achieved during the static binding and elution process was investigated through the examination of SDS-PAGE gels of the different solutions. The ESEW aqueous solution prior to exposure to the membrane contained four main polypeptide bands (Figure 10a). These polypeptides were identified in Section 3.4.1 as ovotransferrin (estimated 71.5 kDa molecular weight), ovalbumin (38.7 kDa), ovomucoid (29.8 kDa), and lysozyme (13.2 kDa) [19]. Lysozyme and ovomucoid (OM) appeared to be in high concentrations, represented by larger and brighter polypeptide bands, while ovalbumin (OA) and ovotransferrin (OT) appeared to be present at lower concentrations with faint bands. The purity of the pure lysozyme solutions was confirmed with only one polypeptide band present. Similar polypeptide patterns were obtained for all pH and NaCl conditions (Figure 10a and Figure 10b).

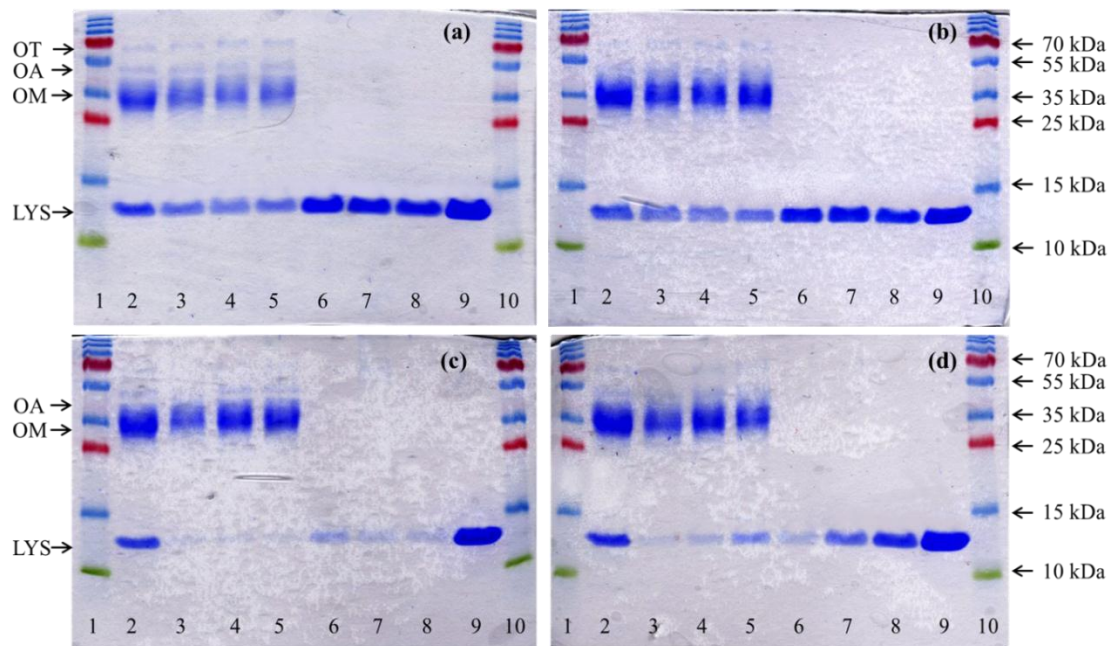


Figure 10. SDS-PAGE analysis on 15 % acrylamide gel, stained with Coomassie brilliant blue. (a) 0 mM NaCl binding solutions prior to the static binding process; (b) 300 mM NaCl binding solutions prior to the static binding process; (c) 0 mM NaCl protein binding solutions following 48 hour membrane incubation; (d) 300 mM NaCl protein binding solutions following 48 hour membrane incubation. Lanes 1 and 10: protein ladder; Lane 2: ESEW; Lanes 3, 4, and 5: ESEW aqueous solutions at pH 4.5, 6.0 and 7.5, respectively; Lanes 6, 7, and 8: aqueous lysozyme solutions at pH 4.5, 6.0, and 7.5, respectively; Lane 9: 1.0 mg/ml lysozyme. Approximately 2 μ g of protein was loaded into each well.

The polypeptide band pattern of the residual solution after membrane incubation is presented in Figure 10c and Figure 10d according to NaCl addition. When no NaCl was present, the lysozyme polypeptide band had nearly disappeared indicating the removal of the majority of lysozyme under all pH conditions and both protein sources (Figure 10c). The intensity of the OM polypeptide band for the ESEW solution at pH 4.5 and no NaCl present was less intense than at pH 6.0 and pH 7.5, suggesting the binding of ovomucoid to the membrane at pH 4.5.

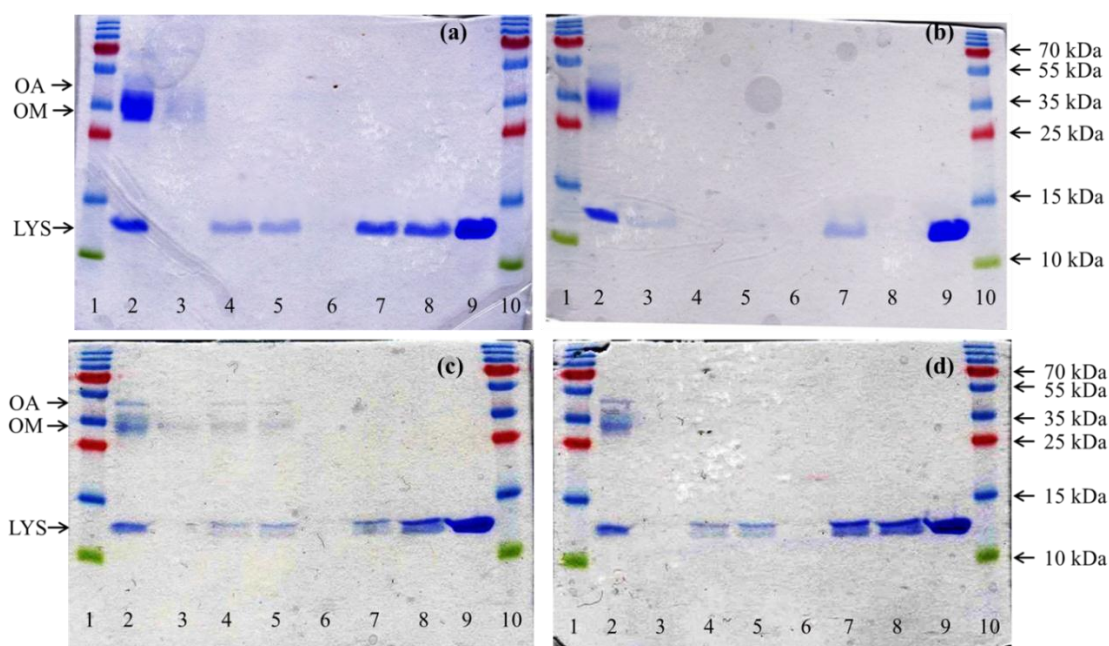


Figure 11. SDS-PAGE analysis of elution solutions on 15 % acrylamide gel, stained with Coomassie brilliant blue. (a) After binding with 0 mM NaCl when binding and elution are at the same pH; (b) after binding with 300 mM NaCl when binding and elution are at the same pH; (c) after binding at pH 4.5 with 0 mM NaCl and elution at variable pH; (d) after binding at pH 4.5 with 300 mM NaCl and elution with variable pH. Lanes 1 and 10: protein ladder; Lane 2: ESEW; Lanes 3, 4, and 5: ESEW aqueous solutions at pH 4.5, 6.0 and 7.5, respectively; Lanes 6, 7, and 8: aqueous lysozyme solutions at pH 4.5, 6.0, and 7.5, respectively; Lane 9: 1.0 mg/ml lysozyme. Approximately 2 μ g of protein was loaded into each well.

The polypeptide band profile of the elution solution for binding and elution at a constant pH confirmed the differences in total protein process recovery according to pH and NaCl conditions (Figure 11a and Figure 11b). At pH 6.0 and pH 7.5, lysozyme was present in the elution streams for the two lysozyme sources when no NaCl was present, with higher polypeptide band intensity for pure lysozyme solution representing a higher lysozyme concentration. At pH 4.5, no lysozyme polypeptide band was visible with or without NaCl addition, confirming the low total protein recovery from the membrane and process recovery for these conditions (Table 8). In the ESEW elution stream at pH 4.5, a faint OM band was visible indicating that the total protein recovered was not lysozyme but undesired ovomucoid

instead. The presence of the OM polypeptide band provided further evidence that binding at pH 4.5 was not through electrostatic forces, as ovomucoid was not present in the elution solutions of pH 6.0 and pH 7.5. With a pI of 4.1 [19], ovomucoid should carry a small net negative charge at pH 4.5, while the membrane should not be charged, being near its pK_a . Therefore, electrostatic interactions between ovomucoid and the membrane hydrogel should be negligible. At 300 mM NaCl, faint lysozyme bands were present for ESEW at pH 4.5 and for pure lysozyme solution at pH 6.0 (Figure 11b). Although the highest total protein process recovery at 300 mM NaCl for ESEW was observed at pH 6.0 (33.2 %), no lysozyme polypeptide band was detected, suggesting that trace amounts of other proteins were recovered but not detected by SDS-PAGE. No visible ovomucoid polypeptide band was observed in the elution solution of ESEW at pH 4.5 and 300 mM NaCl, in contrast to the 0 mM NaCl condition. Consequently, the addition of NaCl during binding reduced the interaction between ovomucoid and the weak cation-exchange membrane material and prevented the binding of ovomucoid.

Improved total protein and lysozyme activity process recovery with increasing pH during elution after binding at pH 4.5 was confirmed through SDS-PAGE gels (Figure 11c and Figure 11d). The intensity of the lysozyme polypeptide band increased when elution pH was increased to pH 6.0 and pH 7.5 at both NaCl conditions and for the two lysozyme sources. Similar to the binding and elution at constant pH and no NaCl addition (Figure 11a), a faint OM band was present for all pH conditions. The intensity of the ovomucoid polypeptide band remained constant for all elution pH conditions while the intensity of the lysozyme band increased with increasing elution pH. The presence of the ovomucoid band at pH 6.0 and pH 7.5, indicated that the lysozyme separation was not as effective under these conditions as an additional separation step would be required to remove the ovomucoid and produce a pure lysozyme stream. Therefore, despite higher total protein process recovery observed when binding at pH 4.5 with no NaCl addition and elution at pH 7.5, compared to binding and elution at pH 7.5, the purity of lysozyme in the former case would be considerably lower. Thus, the highest total protein process recovery with high lysozyme purity was achieved for binding and elution of ESEW at pH 7.5 and no NaCl addition during binding.

Based on the total protein and lysozyme activity process recovery and SDS-PAGE analysis, the conditions which produce high total protein and lysozyme activity process recovery and a pure lysozyme product from egg white were binding and elution at pH 7.5 and no NaCl addition during binding. Although binding at pH 4.5 and no NaCl addition with elution at pH 7.5 produced similar total protein and lysozyme activity process recovery, a mixture of lysozyme and ovomucoid was observed in the elution stream, reducing the effectiveness of the separation process.

As previously discussed, binding in pH conditions below the membrane's pK_a was observed to involve a non-electrostatic binding interaction that should be investigated further. This alternative mechanism may allow for a potential orthogonal separation process using the same weak cation-exchange membrane material. The selective binding of two different egg white proteins was demonstrated, as ovomucoid was bound at pH 4.5 in the absence of NaCl. Therefore, by manipulating the pH and salt concentration in the binding solution, different platform approaches may be applied to separate out different proteins. Further protein separation may be enhanced by altering the elution buffer, as both pH and NaCl gradients can effectively be applied to promote the elution of lysozyme.

In this study, a Weak C membrane was investigated for its ability to separate lysozyme from ethanol soluble egg white (ESEW) aqueous solution under different pH and NaCl concentrations, and two types of binding and elution patterns. Maximum total protein binding capacity of 82.6 mg/ml membrane was achieved after 48 hours of incubation at pH 4.5 and no NaCl addition for an ESEW aqueous solution; however, the total protein and lysozyme activity recovery from the membrane at pH 4.5 and no NaCl addition was less than 30 % and 0.5 % of lysozyme respectively. Consequently, increasing the pH of the elution buffer was necessary to promote the elution of protein as electrostatic interactions between positively charged lysozyme and negatively charged membrane were reintroduced. In contrast, at least 85 % total protein and lysozyme activity recovery from the membrane was obtained at pH 7.5 with no NaCl addition during binding and elution at constant pH. SDS-PAGE analysis indicated the presence of ovomucoid in the elution stream at pH 4.5 and no NaCl addition during binding, suggesting a non-electrostatic mode of interaction between egg white proteins and the weak cation-exchange membrane material, and a less efficient lysozyme separation overall. Of the conditions tested, the optimal conditions for the static

separation of lysozyme from ESEW were determined to be pH 7.5 and 0 mM NaCl when binding and eluting at the same pH, although similar total protein process recovery (33.0 % compared to 36.9 % for constant pH 7.5 binding and elution; $p < 0.10$) and lysozyme activity process recovery (69.3 % compared to 74.0 %, $p > 0.10$) results were obtained for binding at pH 4.5 and 300 mM NaCl and pH 7.5 during elution.

Both elution strategies were shown to be effective in the recovery of lysozyme activity. For the manipulation of electrostatic interactions through NaCl addition, increasing total protein and lysozyme activity process recoveries were observed for binding and elution at pH 7.5. Likewise, pH 7.5 was demonstrated to be the best elution pH of the tested conditions after binding in conditions below the pK_a of the membrane, where electrostatic interactions are minimal. While adjusting both the pH and NaCl of the elution buffer achieved results that were independent of salt concentration, poor selectivity of bound proteins was attained, leading to lower lysozyme purity in the elution stream.

Significant flexibility of the weak cation-exchange membrane material was demonstrated as multiple binding mechanisms were shown to produce different protein selectivity. A thorough investigation into the non-electrostatic interaction between protein and membrane at pH 4.5 could open a new avenue of protein separation, allowing for an orthogonal separation process with the same membrane. As well, multiple lysozyme binding and elution strategies were possible with the membrane material, with the application of a pH gradient and NaCl producing high lysozyme recovery with high specific activity. Thus, the weak cation-exchange membrane may be useful in many different applications, including separations involving varying conditions.

Future work will consider these binding and elution conditions for the operation of a dynamic flow system amenable to scale-up and industrial operation.

4. Dynamic Separation of Lysozyme from Egg White Through Weak Cation-Exchange Membrane Chromatography

A. Yeh, C. Moresoli

This manuscript was guided by Dr. Christine Moresoli. The turbidimetric assay for lysozyme activity determination was adapted and developed by Ms. Katharina Hassel. Assistance with the HPLC system was provided by Ms. Sarah Meunier. Aqueous egg white solutions (AEW and ASEW) were prepared by Mr. Stephen Wei. All other experiments and results included in this manuscript as well as all data analysis were performed by Mr. Andrew Yeh.

4.1. Overview

The dynamic binding characteristics of a weak cation-exchange hydrogel membrane material were investigated through the isolation of lysozyme from egg white using a tangential flow cell in recycle mode at pH 7.5. Lysozyme was chosen as a model protein due to its well-characterized nature and its natural occurrence in a mixture of proteins.

Three different egg white treatments were prepared and compared to a pure lysozyme solution to evaluate lysozyme binding and selectivity for protein mixtures of varying lysozyme concentrations: (1) egg white precipitated with 30 % (v/v) ethanol (ESEW), (2) aqueous egg white (AEW), and (3) aqueous egg white precipitated with 100 mM sodium chloride (NaCl) (ASEW). The protein concentration of the feed, feed-side pressure applied to the membrane, and the number of regeneration cycles were varied to determine their effects on lysozyme binding. Protein purity was determined through size-exclusion high performance liquid chromatography (SEC-HPLC). Dynamic binding capacity at 10 % breakthrough of 167.3 mg lysozyme/ml membrane was observed for a 0.35 mg/ml lysozyme feed solution at pH 7.5, and was independent of feed concentration up to 5.00 mg/ml lysozyme. The ratio of dynamic binding capacity to static binding capacity for pure lysozyme solutions at pH 7.5 was 2.2 under similar conditions. Based on the tested conditions, optimal conditions for lysozyme separation from egg white using the hydrogel membrane material were determined to be ESEW at pH 7.5 and 0 kPa. These conditions yielded the highest total protein (48.0 %) and lysozyme activity (75.7 %) recovery from the membrane, and lysozyme purity (73.4 %) after elution for all the egg white solutions. Increasing the feed-side pressure (14 kPa) to increase the permeate flow rate decreased lysozyme activity process recovery in the elution stream (51.7 %), while maintaining similar lysozyme purity to operation at 0 kPa (73.4 %). Egg white treatment with ethanol increased the lysozyme purity. Lower protein purity, total protein and lysozyme activity process recovery was observed in AEW and ASEW separations. The weak cation-exchange membrane was demonstrated to be effective in the dynamic separation of lysozyme from egg whites and may be extended to the recovery of other proteins.

4.2. Introduction

The separation and purification of proteins is traditionally performed through packed-bed chromatography, which exploit physical properties to isolate individual components in a process stream [1,4-7,11,22]. Packed-bed resin beads are often designed to maximize the surface area-to-volume ratio and to incorporate a large number of binding sites. As a result, resin beads are generally made of highly porous media, requiring a pore diffusion step to promote contact between biomolecules and binding sites. Pore diffusion is a slow process that can increase processing times, as large column volumes are required for effective separation [1,4,5,7,13,16,22,32,74]. As well, bead chromatography can be further limited by mechanical strength issues, as the resin material can be subjected to high pressure drops, and column scale-up is often difficult [1,4-7,11,13].

Membrane chromatography is a promising alternative technology for protein purification and separation. During operation, solutes are brought into direct contact with binding sites that line the membrane pores through convective flow. Since mass transport is driven by convection, higher volume throughputs can be processed while retaining protein selectivity through functionalization [1,4,5,7,9,11,16,22,74]. Functional groups including those that separate proteins according to size, charge, hydrophobicity, or affinity interactions can be grafted to a membrane backbone to promote further separation [4,6,7,9,11,13,14,16,22,74].

Ion-exchange can be used in conjunction with membrane chromatography to separate proteins according to surface charge [6,7,9,11,12,17,31]. Electrostatic interactions between charged surfaces cause charged solutes to attract to an oppositely charged stationary surface. Modifying the charge of the membrane can be used to manipulate these electrostatic interactions, and cause bound solutes to be eluted into solution, thereby recovering a desirable product [7,9,11,17,31]. In cation-exchange chromatography, a negatively charged chromatography material will bind positively charged solutes present in a mobile phase. A strong exchanger will retain a constant surface charge over the entire pH range, while the charge density of weak exchange materials will change with pH [4,9,11,20]. Strong cation-exchange flat-sheet membrane [7,11,21], weak cation-exchange flat-sheet membrane [6], and cation-exchange hollow-fibre membrane [12,17] technology have all been investigated for binding throughout literature. However, most of these focus on polymeric materials that are

limited in their binding capacity relative to membrane incubation [6,11,12,21,31]. As well, strong cation-exchangers are often examined due to their ability to retain a charged surface across the entire pH range.

Lysozyme was selected as a model protein to determine the extent of protein binding under different pH and NaCl conditions for a weak cation-exchange membrane chromatography material. Lysozyme is a well-characterized protein that is often used in biotechnology and pharmaceutical applications [6,7,11-18]. As lysozyme is naturally present in egg white, lysozyme is ideal for the determination of binding efficiency from a protein mixture [19].

While lysozyme recovery from egg white using cation-exchange membranes has been studied previously [7,12,17,21,31], special emphasis of this work is placed on the entire protein binding process, including protein recovery from the membrane after the loading step and the overall separation process recovery for lysozyme.

In this study, the dynamic binding characteristics of a weak cation-exchange membrane were investigated in a tangential flow set-up at pH 7.5. Three types of hen egg white solutions were contacted with the membrane material to evaluate and compare the lysozyme binding and selectivity for protein mixtures of varying lysozyme concentrations. Feed protein concentration, feed-side pressure, and the number of separation cycles were also altered to demonstrate their effects on lysozyme binding.

4.3. Experimental

4.3.1. Materials

The membrane chromatography materials used in this study were *Adsept*TM Weak C cation-exchange flat sheet membranes (thickness of 0.278 ± 0.019 mm) provided by Natrix Separations Inc. (Burlington, ON, Canada). Lysozyme from hen egg white (L6876), *Micrococcus lysodeikticus* ATCC No. 4698 (M3770), citric acid (C0759), bromophenol blue sodium salt (B5525), glycine (G7126), and N,N,N',N'-tetramethylethylenediamine (TEMED) (T9281) were purchased from Sigma-Aldrich Co. (St. Louis, MO, USA). Coomassie brilliant blue R250 (161-0400) and 30 % acrylamide/bis solution (37.5:1, 2.6 % C) (161-0158) were obtained from Bio-Rad Laboratories Inc. (Hercules, CA, USA). Ammonium persulfate (BP179), ethanol (95 % v/v), and sodium dodecyl sulfate (BP166)

were purchased from Fisher-Scientific Co. (Toronto, ON, Canada). PageRuler Plus Prestained Protein Ladder, 10 to 250 kDa (26619) was purchased from Thermo Scientific (Waltham, MA, USA). Sodium phosphate dibasic heptahydrate (SX0715) was purchased from EMD Chemicals Inc. and sodium chloride (ACS 783) was purchased from BDH Inc. (both now a division of Merck Group) (Darmstadt, Germany). Tris (X188-7) was purchased from JT Baker (now Avantor Performance Materials, Center Valley, PA, USA).

4.3.2. Egg white solutions

The treatment of egg white with ethanol was adapted from Chiu et al. and Guérin-Dubiard et al. [7,42]. Fresh eggs were purchased from a local market. The white of 12 eggs were manually separated from their yolks and gently stirred for 30 min on a Dyla-Dual[®] hotplate/stirrer (12620-970, VWR International, Radnor, PA, USA). The egg whites were diluted to 33.3 % (v/v) with 50 mM phosphate citrate buffer, pH 4.8 to a final total protein concentration of 15 mg/ml. The pH was adjusted to pH 4.8 with 1M HCl, and the dilution was stirred gently for another 30 min. The diluted egg whites were mixed with an equal volume of 60 % (v/v) ethanol and incubated overnight at room temperature. The precipitate was removed by centrifugation at 34 178 x g for 45 minutes at 22 °C (Sorvall WX Ultra 100 Centrifuge, 46902, Thermo Scientific, Waltham, MA, USA). The supernatant, referred to as ethanol soluble egg white (ESEW), was collected, adjusted to pH 7.5 with 1 M HCl, and used in subsequent dynamic binding and characterization tests.

Two other egg white solutions were prepared as follows. The white of 12 eggs were manually separated from their yolks and gently stirred for 30 minutes. The egg whites were diluted to 12.5 % (v/v) with 50 mM phosphate citrate buffer solution at pH 4.8 and either 0 mM NaCl or 100 mM NaCl. The addition of salt to the aqueous egg white solution was to promote the precipitation of protein, producing an intermediary lysozyme concentration solution [76,77]. The pH of the aqueous egg white solution was readjusted to pH 4.8 with 1 M HCl and stirred for 30 minutes. Protein precipitate was removed by centrifugation at 34 178 x g for 45 minutes at 22 °C. The supernatant of the aqueous egg whites (AEW) and the aqueous egg whites in the presence of salt (ASEW) were collected, diluted to 1.35 mg/ml total protein concentration with 50 mM phosphate citrate, pH 7.5, and pH adjusted to 7.5 with 1 M HCl.

4.3.3. Tangential flow set-up

The tangential flow set-up (Figure 12) consisted of a variable-flow gear pump (R-75211-10, Cole-Parmer, Vernon Hills, IL, USA) and A-mount cavity style pump head (R-73011-08, 0.64 ml/rev, PEEK gears, PTFE seals, Micropump, a unit of IDEX Corp., Oak Harbour, WA, USA), a flow meter (RK-03267-30, 150 mm correlated aluminum, Cole-Parmer, Vernon Hills, IL, USA), pressure gauges (Duralife industrial, 0 to 30 psi, Ashcroft Inc., Stratford, CT, USA), a tangential flow filtration cell holder (CF042 Delrin cross-flow cell, 42 cm² active area, Sterlitech Corp., Kent, WA, USA), a screw clamp (delrin, Cole-Parmer, Vernon Hills, IL, USA), and a Symmetry PR Precision toploading balance (4200 g x 0.01 g, Cole-Parmer, Vernon Hills, IL, USA).

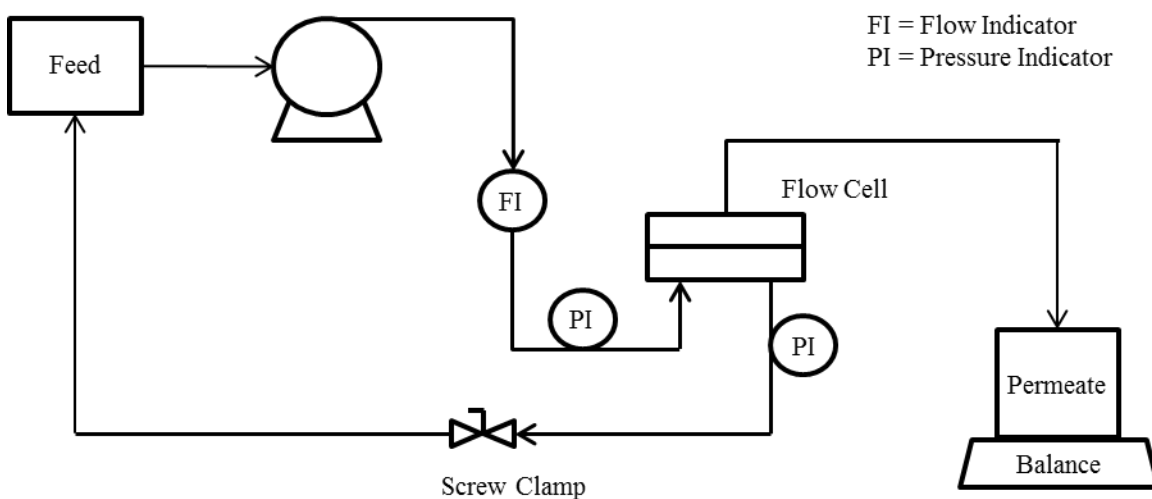


Figure 12. Schematic diagram of the tangential flow set-up.

For each experiment, a new Weak C membrane sample 6 cm by 10 cm in dimension was cut out from a flat sheet and placed in the tangential flow cell holder. The active area of the membrane was 42 cm² and a thickness was 0.278 ± 0.019 mm, giving a total membrane volume of 1.168 ml. A thin mesh permeate carrier membrane (1142817, Sepa CF, GE Osmonics, Minnetonka, MN, USA) was used as a support beneath the membrane material. For all experiments, a feed flow rate of 160 ml/min was maintained. The retentate solution was recirculated back to the feed tank. The permeate flow rate was not controlled, and was determined by the change in collected permeate mass over time. Each membrane was initially regenerated by passing 25 ml of 0.1 M NaOH through the system for 10 minutes in order to ensure complete deprotonation of the carboxylic acid functional groups in the membrane

hydrogel layer [78]. Following regeneration, the membrane was equilibrated by permeating 50 ml of 50 mM phosphate citrate, pH 7.5 through the membrane over 25 minutes to condition the material to the conditions of the binding solutions. After membrane equilibration, sample loading was performed where a binding solution was introduced into the system. The binding solution and permeate rate was varied and will be discussed in further detail in subsequent sections. Following sample loading, a wash step was performed by collecting in the permeate 10 ml of 50 mM phosphate citrate, pH 7.5 over 7 minutes. An elution step was subsequently performed to remove bound protein from the membrane by collecting in the permeate 150 ml of a 50 mM phosphate citrate, pH 7.5 and 1 M NaCl buffer over the course of 1 hour. Elution permeate was measured through UV absorbance every 3 minutes over the first 15 minutes and then in 5 minute intervals thereafter. The above process was performed in duplicate, using new membrane material for each experiment.

Slight discrepancies were observed between permeate flow rates due to varying conductivity of the feed solution during the sample loading, elution, and cleaning steps. The permeate flow rate was dependent on membrane permeability, which was found to increase with increasing conductivity. Since a constant feed flow rate was maintained for each experiment and no feed-side pressure was applied, the permeate flow rate could not be held constant for all steps.

4.3.4. Breakthrough curves

Breakthrough curves were determined off-line with a Spectronic™ GENESYS™ 2 UV-vis spectrophotometer (Milton Roy, now under Thermo Scientific, Waltham, MA, USA) set at 280 nm. In the sample loading step, varying volumes of pure lysozyme solutions of 0.35 mg/ml, 1.00 mg/ml, and 5.00 mg/ml (all at pH 7.5) were passed through the equilibrated membrane (980 ml, 380 ml, and 150 ml, respectively) with permeate collected over 280 minutes, 190 minutes, and 100 minutes, respectively. The screw clamp was opened such that no feed-side pressure was applied to the membrane. Permeate samples were measured through UV absorbance at 280 nm every five minutes. The feed solution was recirculated until the permeate concentration reached 70 % of the total protein concentration of the feed.

4.3.5. Membrane regeneration analysis

For the membrane regeneration experiments, a single membrane material was tested through five protein binding and elution steps to determine any changes to membrane performance over time. No feed-side pressure was applied to the membrane during operation, as the screw clamp was opened. The equilibrated membrane was loaded by passing approximately 150 ml of 0.35 mg/ml lysozyme, pH 7.5 into the permeate in 37.5 minutes. Permeate samples were collected and their absorbance measured off-line at 280 nm every 5 minutes. Following sample loading, the membrane was washed with 10 ml of 50 mM phosphate citrate, pH 7.5, with permeate collection over 2 minutes. Bound protein was eluted by permeating 150 ml of 50 mM phosphate citrate, pH 7.5 and 1 M NaCl for 20 minutes. Total protein concentration in the elution permeate was measured offline through UV absorbance at 280 nm at 5 minute intervals. Residual protein was cleaned off of the membrane material by passing a 2 M NaCl solution through the tangential flow cell. Fifty milliliters of the 2 M NaCl solution were collected permeate-side over 5.5 minutes. The process was then repeated, starting with membrane regeneration.

4.3.6. Dynamic separation of egg white

ESEW, AEW, and ASEW solutions containing 1.35 mg/ml total protein concentration at pH 7.5 were used. A higher total protein concentration than the static binding capacity experiments was selected for the dynamic binding capacity study to ensure saturation of the higher membrane volume of the tangential flow cell and to decrease processing times. For the sample loading step, no feed-side pressure was applied and 150 ml of a protein solution was fed through the membrane with permeate collected over 150 minutes. The permeate was collected and measured for UV absorbance at 280 nm in 5 minute intervals.

The effect of pressure on lysozyme separation was investigated. Following the membrane regeneration and equilibration steps, ESEW loading was performed with the screw clamp closed, producing a feed-side pressure of 14 kPa. The collected permeate volumes remained constant for the sample loading, wash, and elution steps, as discussed previously. However, increasing the feed pressure decreased the permeation times to 15 minutes, 1 minute, and 6 minutes, respectively. The feed flow rate was held constant at

160 ml/min. The volumes of the different steps for the separation of lysozyme from different egg white sources are presented in Table 11. The volume lost to the system includes the residual volume remaining in the dynamic set-up tubing upon the completion of each step.

Table 11. Breakdown of the volumes during the dynamic separation of lysozyme from egg white

Separation	Loading				Wash	Elution		
	Initial volume (ml)	Permeate volume collected (ml)	Residual Feed solution volume (ml)	Volume loss (ml)	Wash solution volume (ml)	Permeate volume collected (ml)	Residual Elution solution volume (ml)	Volume loss (ml)
ESEW – 0 kPa	422.5 (7.5)	206.5 (3.5)	188.0 (2.0)	28.0 (13.0)	7.5 (1.5)	203.0 (1.0)	42.0 (10.0)	55.0 (9.0)
ESEW – 14 kPa	287.5 (32.5)	204.0 (4.0)	69.5 (38.5)	14.0 (10.0)	11.5 (0.5)	200.5 (2.5)	33.0 (4.0)	66.5 (1.5)
AEW	425.0 (25.0)	206.0 (4.0)	179.5 (25.5)	39.5 (4.5)	10.0 (0.0)	202.0 (4.0)	23.5 (15.5)	74.5 (11.5)
ASEW	447.5 (17.5)	204.0 (2.0)	201.0 (25.0)	42.5 (9.5)	10.5 (0.5)	200.0 (2.0)	30.0 (10.0)	70.0 (8.0)
Pure Lysozyme	246.0	207.0	16.0	23.0	11.0	201.0	23.0	76.0

*The initial volume of the elution stream for all protein sources is 300 ml

**Values in brackets represent standard error, where n = 2

No dead volume was assumed in the dynamic binding capacity calculations. As the first 50 ml of each solution was purged to eliminate the risk of contamination or feed dilution, the dead volume of 17 ml between the feed and the tangential flow cell would have been eliminated prior to the start of each trial.

Dynamic binding capacity was calculated based on 10 % breakthrough of total protein according to Equation 4-1.

$$Q(\text{DBC}_{10\%}) = \frac{C_0 \cdot (V_{10\% \text{ BT}})}{V_{\text{membrane}}} \quad [4-1]$$

Where $Q(\text{DBC}_{10\%})$ represents the dynamic binding capacity at 10 % breakthrough [mg total protein/ml membrane], C_0 is the initial total protein concentration prior to the loading step [mg/ml], $V_{10\% \text{ BT}}$ is the volume of collected permeate at which 10 % breakthrough occurs [ml], V_{DV} is the dead volume of the system [ml], and V_{membrane} is the active volume of the

membrane [ml membrane]. As discussed, the dead volume of the system was assumed to be negligible.

4.3.7. Total protein recovery

The amount of protein loosely bound to the membrane material during the sample loading step and recovered during the wash step was calculated according to Equation 4-2.

$$\text{Washed}_P (\%) = \frac{C_{WR}V_{WR} + C_{WP}V_{WP} + (C_{Purge}V_{Purge} - C_{LR}V_{Lost})}{C_{initial}V_{initial} - C_{LR}V_{LR} - C_{LP}V_{LP} - C_{LR}V_{Lost}} * 100 \% \quad [4-2]$$

Where C_{WR} is the total protein concentration in the retentate collected after the wash step [mg/ml], V_{WR} is the volume of the retentate stream collected after the wash step [ml], C_{WP} is the total protein concentration in the permeate collected during the wash step [mg/ml], V_{WP} is the volume of permeate collected during the wash step [ml], C_{Purge} is the total protein concentration in the purged solution collected when switching feeds during the wash step [mg/ml], V_{Purge} is the volume of purged solution collected when switching feeds during the wash step [ml], $C_{initial}$ is the total protein concentration in the protein solution prior to the loading step [mg/ml], $V_{initial}$ is the volume of the solution prior to the loading step [ml], C_{LR} is the total concentration in the recycled retentate collected after the loading step [mg/ml], V_{LR} is the volume of the recycled retentate collected after the loading step [ml], C_{LP} is the total protein concentration in the permeate collected during the loading step [mg/ml], V_{LP} is the volume of permeate collected during the loading step [ml], and V_{lost} is the estimated volume of feed collected in the retentate when switching feeds during the wash step [30 ml].

The total protein recovery from the membrane during the elution step was calculated according to Equation 4-3. For total protein, the mass of protein eluted was compared to the estimated mass of protein bound to the membrane material after sample loading.

$$\text{Recovery}_{\text{Membrane, P}} (\%) = \frac{C_{ER}V_{ER} + C_{EP}V_{EP}}{C_{initial}V_{initial} - C_{LR}V_{LR} - C_{LP}V_{LP} - C_{LR}V_{Lost}} * 100 \% \quad [4-3]$$

Where C_{ER} is the total protein concentration in the retentate stream after elution [mg/ml], V_{ER} is the volume of retentate collected after elution [ml], C_{EP} is the total protein concentration in the permeate collected during elution [mg/ml], and V_{EP} is the volume of permeate collected during elution [ml]. $C_{initial}$, $V_{initial}$, C_{LR} , V_{LR} , C_{LP} , V_{LP} , and V_{lost} are as defined previously.

The total protein process recovery was calculated according to Equation 4-4.

$$\text{Recovery}_{\text{Process, P}} (\%) = \frac{C_{ER}V_{ER} + C_{EP}V_{EP}}{C_{initial}V_{initial} - C_{LR}V_{LR}} * 100 \% \quad [4-4]$$

Where C_{ER} , V_{ER} , C_{EP} , V_{EP} , $C_{initial}$, $V_{initial}$, C_{LR} , and V_{LR} are as defined previously.

4.3.8. Lysozyme activity

The lysozyme activity was determined with a turbidimetric microplate assay adapted from Helal and Melzig [70]. A suspension of *Micrococcus lysodeikticus* served as a substrate for lysozyme, as the protein hydrolyses the β -1,4-linkage between muramic acid and *N*-acetyl glucosamine in the bacterial cell wall [19,43,44,71]. A unit of activity for lysozyme (U) was defined as a decrease in absorption of 0.001 per minute at 450 nm and 37 °C. A lysozyme activity calibration curve was prepared from a series dilution of an 800 U/ml lysozyme stock solution with 0.1 M phosphate buffer, pH 6.24 in eight wells of a 96 well microplate. The calibration curve was prepared in duplicate. Four replicates (50 μ l) of each unknown sample were added into separate wells. The reaction was started with the addition of 200 μ L of a 0.36 mg/ml *Micrococcus lysodeikticus* (substrate) solution to each well. With the addition of substrate to each well, the final diluted activities of the calibration curve ranged from 0 U/ml to 120 U/ml. Absorption was read at 450 nm with a Synergy 4 microplate reader (BioTek Instruments Inc., Winooski, VT, USA) held at 37 °C. Readings were taken every minute for ten minutes under gentle shaking.

4.3.9. Lysozyme activity recovery

The lysozyme activity present in the wash solution, the recovery of lysozyme activity from the membrane, and the process recovery of lysozyme activity were calculated for each lysozyme source according to Equation 4-5, Equation 4-6, and Equation 4-7, respectively.

$$\text{Washed}_A (\%) = \frac{A_{WR}V_{WP} + A_{WR} + V_{Purge}A_{Purge}V_{WP} - A_{LR}V_{lost}}{A_{initial}V_{initial} - A_{LR}V_{LR} - A_{LP}V_{LP} - A_{LR}V_{lost}} * 100 \% \quad [4-5]$$

$$\text{Recovery}_{\text{Membrane, A}} (\%) = \frac{A_{ER}V_{ER} + A_{EP}V_{EP}}{A_{initial}V_{initial} - A_{LR}V_{LR} - A_{LP}V_{LP} - A_{LR}V_{lost}} * 100 \% \quad [4-6]$$

$$\text{Recovery}_{\text{Process, A}} (\%) = \frac{A_{ER}V_{ER} + A_{EP}V_{EP}}{A_{initial}V_{initial} - A_{LR}V_{LR}} * 100 \% \quad [4-7]$$

Where A_{WR} is the lysozyme activity in the retentate collected after the wash step [U/ml], V_{WR} is the volume of the retentate stream collected after the wash step [ml], A_{WP} is the lysozyme activity in the permeate collected during the wash step [U/ml], V_{WP} is the volume of permeate collected during the wash step [ml], V_{lost} is the estimated volume of feed collected

in the retentate when switching feeds during the wash step [30 ml], A_{initial} is the lysozyme activity in the solution prior to the loading step [U/ml], V_{initial} is the volume of the solution prior to the loading step [ml], A_{LR} is the lysozyme activity in the recycled retentate collected after the loading step [U/ml], V_{LR} is the volume of the recycled retentate collected after the loading step [ml], A_{LP} is the lysozyme activity in the permeate collected during the loading step [U/ml], V_{LP} is the volume of permeate collected during the loading step [ml], A_{Purge} is the lysozyme activity in the purged solution collected when switching feeds during the wash step [U/ml], V_{Purge} is the volume of purged solution collected when switching feeds during the wash step [ml], A_{ER} is the lysozyme in the retentate stream collected after elution [U/ml], V_{ER} is the volume of retentate collected after elution [ml], A_{EP} is the lysozyme activity in the permeate collected during elution [U/ml], and V_{EP} is the volume of permeate collected during elution [ml].

4.3.10. Membrane staining

A virgin membrane, a membrane after regeneration and equilibration, and membranes exposed to 5.00 mg/ml lysozyme (sample loading steps of 15 seconds, 30 seconds, and 5 minutes) were stained with Coomassie Brilliant Blue R250. Membranes were incubated in a methanol/acetic acid/water (2:1:2, v/v/v) staining solution containing 0.1 % Coomassie Brilliant Blue R250 for 2 hours under gentle shaking at 125 rpm on a Gyrotory® Shaker-Model G2 (New Brunswick Scientific Co. Inc, Edison, NJ, USA), and destained overnight with a methanol/acetic acid/water (4:0.7:5.3, v/v/v) solution under shaking at 125 rpm.

The staining procedure was repeated for membranes bound with pure lysozyme or egg white proteins following the elution step to visualize any proteins that remained bound to the membrane surface.

4.3.11. Sodium dodecyl sulphate poly(acrylamide) gel electrophoresis (SDS-PAGE)

Sodium dodecyl sulfate poly(acrylamide) gel electrophoresis (SDS-PAGE) was performed through a resolving separation gel consisting of 15 % acrylamide with 10 % (w/v) SDS adapted from Laemmli [65]. The stacking gel for sample loading contained 4 % acrylamide. Unknown samples were diluted to a total protein concentration of 1.00 mg/ml with 50 mM phosphate citrate, pH 7.5, measured by UV absorbance at 280 nm. The diluted

samples were mixed in a (1:2) ratio with an SDS reducing buffer containing β -mercaptoethanol, glycerol, and bromophenol blue. The resulting solution was heated at 95 °C for 4 minutes and a volume totalling approximately 2.5 μ g of protein was loaded into a BioRad Mini-PROTEAN[®] Tetra Cell system (165-8001, BioRad Laboratories Inc., Hercules, CA, USA). The protein ladder comprised of undisclosed prestained recombinant proteins in a reducing agent with a range of molecular weights from 10 kDa to 250 kDa (10 kDa, 15 kDa, 25 kDa, 35 kDa, 55 kDa, 70 kDa, 100 kDa, 130 kDa, 250 kDa). Five μ l of the protein ladder was loaded into each gel in duplicate. Electrophoresis was performed in a Tris-Glycine buffer with 0.1 % SDS at 100 V through the stacking gel and 150 V for the resolving gel, for a total of 90 minutes using a PowerPac[™] Basic Power Supply (164-5050, Bio-Rad Laboratories Inc., Hercules, CA, USA). The gels were incubated under shaking at 125 rpm in a methanol/acetic acid/water (2:1:2, v/v/v) staining solution containing 0.1 % Coomassie Brilliant Blue R250 for 2 hours, and destained overnight with a methanol/acetic acid/water (4:0.7:5.3, v/v/v) solution. Images of the gels were taken with an Epson Stylus CX4810 All-in-One Printer (Epson America Inc., Long Beach, CA, USA).

4.3.12. Size-exclusion high-performance liquid chromatography (SE-HPLC)

Size-exclusion chromatography was carried out on a Varian ProStar HPLC system (Varian Inc., now Agilent Technologies, Santa Clara, CA, USA). Egg white solutions and elution permeates were passed through 20 μ m syringe filters. Samples (20 μ l) were injected through a ZORBAX Bio Series GF-250 separation column (4.5 μ m pore size, 250 mm x 9.4 mm). The mobile phase through the column was 0.1 M phosphate buffer, pH 7.0 set for 25 minutes per sample at a flow rate of 1.0 ml/min. Separated proteins were detected on-line through UV-vis spectrophotometry at 280 nm. Protein molecular weights were estimated based the elution times of known MW proteins: BSA (66.5 kDa), lipase (35 kDa), and lysozyme (14.3 kDa). A lysozyme calibration curve between 0.15 mg/ml and 1.5 mg/ml was performed for protein quantification.

Lysozyme purity was calculated according to Equation 4-8

$$\text{Lysozyme Purity (\%)} = \frac{\text{Peak Height}_{\text{Lysozyme}}}{\sum_i \text{Peak Height}_i} * 100 \% \quad [4-8]$$

Where $\text{Peak Heights}_{\text{Lysozyme}}$ is the height count of the lysozyme peak, and Peak Height_i is the height count for the peak of component i.

The purification factor for the separation gave the increase in lysozyme purity by comparing final lysozyme purity to the lysozyme purity in the initial solution. Purification factor was calculated according to Equation 4-9.

$$\text{Purification Factor}(\%) = \frac{\text{Lysozyme Purity}_{\text{final}}}{\text{Lysozyme Purity}_{\text{initial}}} \quad [4-9]$$

Where Lysozyme Purity_{final} is the lysozyme purity in the permeate collected after elution, and Lysozyme Purity_{initial} is the lysozyme purity of the protein solution prior to the loading step.

4.3.13. Statistical analysis

Paired two sample t-test analyses were performed to determine significance between mean values of sample sets. The test statistic t_0 was calculated according to Equation 3-9. A 90 % confidence interval ($\alpha = 0.90$) was prepared for a two-tailed t test. Significance was determined when the test statistic, t_0 , was greater than the critical t value, as determined by the degrees of freedom through Equation 3-10 [72].

Significance is reported as either partial significance or total significance. For partial significance, the reported values are significantly different from at least one other factor under similar conditions (e.g. protein source). For total significance, the reported value is statistically significant from all other factors under similar conditions.

4.4. Results and Discussion

4.4.1. Dynamic Binding Capacity

Breakthrough curves for the dynamic binding of lysozyme solutions at pH 7.5 with no NaCl addition on Natrix Weak C membranes are shown in Figure 13. The feed pH was based on static binding studies corresponding to maximum total protein and lysozyme activity recovery from the membrane and process recovery (Section 3.4.4 and Section 3.4.5), while maintaining a high lysozyme purity in the elution stream (Section 3.4.6). The breakthrough of protein through the membrane was not influenced by initial inlet lysozyme concentration according to the relative volume of collected permeate. For each initial inlet lysozyme concentration, 10 % breakthrough was achieved after approximately 55 % of the final permeate volume had circulated through the membrane. As shown in Table 12, dynamic binding capacity of over 160 mg protein/ml membrane was achieved for each inlet lysozyme concentration.

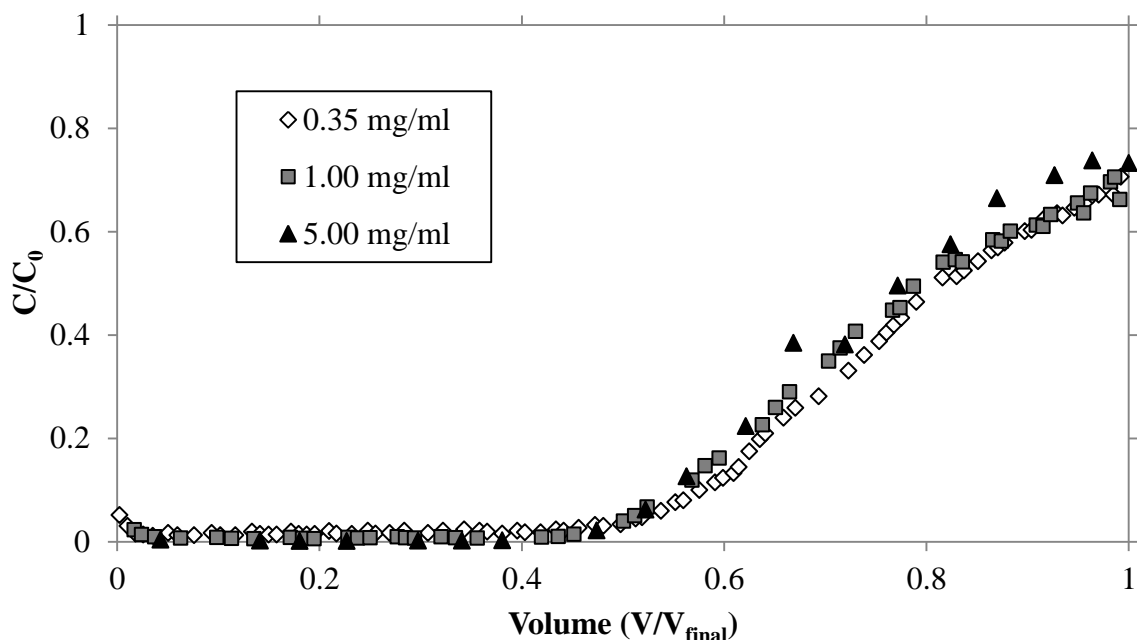


Figure 13. Breakthrough curves for different initial inlet lysozyme concentrations in 50 mM phosphate citrate buffer at pH 7.5 and no NaCl addition for Natrix Weak C membranes versus the normalized permeate volume. Feed flow rate was 160 ml/min. Total protein concentration (C) measured by UV absorbance at 280 nm was normalized based on the initial inlet total protein concentration (C_0). Volume (V) was normalized based on the final volume of collected permeate (V_{final}), as described in Section 4.3.4.

Table 12. Effect of pure lysozyme initial inlet concentration on dynamic binding capacity

Pure Lysozyme Feed Concentration (mg protein/ml solution)	Dynamic Binding Capacity (DBC _{10%}) (mg protein/ml membrane)
0.35	167.3
1.00	170.5
5.00	183.1

The dynamic binding capacity at 10 % breakthrough for the weak cation-exchange material studied in this study was significantly higher than those reported elsewhere (Table 1), despite a lower lysozyme feed concentration. Unlike many other cation-exchange membrane materials, superior lysozyme binding was observed for a 0.35 mg/ml lysozyme solution at pH 7.5 in a dynamic set-up, with the dynamic binding capacity at 10 % breakthrough 2.2 times greater than the static binding capacity at equilibrium. In comparison, most cation-exchange membrane materials demonstrate a dynamic binding capacity of less than 70 mg/ml membrane and a dynamic to static binding ratio less than or equal to 1 [7,11,12,17,31]. This increase in binding capacity during cross-flow operation may be a

consequence of the unique hydrogel layer. Since pore size and structure in the hydrogel layer is dependent on solution conditions, the arrangement of carboxylic ligands may change depending on the pH or NaCl concentration during the loading step. Therefore, at pH 7.5, it is possible that most of the cation-exchange residues will lie within the pores rather than on the membrane surface. While static binding capacity is based on equilibrium binding under stagnant conditions and may be limited to the surface, convective flow during dynamic operation will bring proteins in contact with the carboxylic acid residues located within membrane pores. Consequently, ligand utilization may be increased compared to in the no-flow condition.

4.4.1.1. Membrane Regeneration

The effect of membrane regeneration on lysozyme separation was investigated by performing a series of binding and elution steps with the same membrane material sample. Total protein and lysozyme activity recovery from the membrane with pure lysozyme are shown in Figure 14. Lysozyme recovery from the membrane was constant over five regeneration cycles with the same material, demonstrating the reusability of the membrane material for the binding and elution of simple protein solutions. Approximately 75 % of the bound protein was recovered from of the membrane, and 72 % of the activity was retained over the first five regeneration cycles.

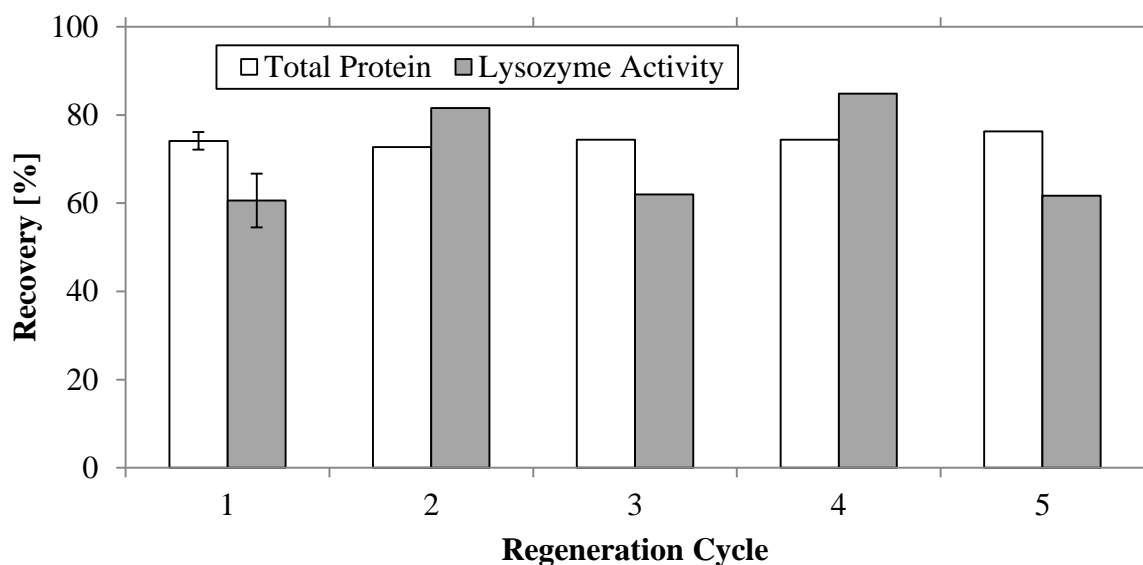


Figure 14. Effect of regeneration cycles on the total protein and lysozyme activity recovery from the membrane for the dynamic binding of 0.35 mg/ml lysozyme in 50 mM phosphate citrate at pH 7.5 to Natrx Weak C membranes. Feed flow rate was 160 ml/min. Error bars represent standard error where $n = 3$ for regeneration cycle 1, otherwise $n = 1$.

4.4.2. Lysozyme recovery from egg white

4.4.2.1. Loading step

Breakthrough curves for all egg white solutions during the loading step are given in Figure 15. While breakthrough was not observed for pure lysozyme during the loading step, protein was present in the permeate almost immediately for all egg white solutions. The proteins present in the permeate were those that did not interact with the membrane material and should have possessed a charge similar to the membrane material. For the ethanol soluble egg white (ESEW) proteins, the protein concentration in the permeate represented 40 % of the total protein concentration in the feed. Similar profiles of the breakthrough curves were observed for ESEW at two different pressures, 0 kPa and 14 kPa, indicating that pressure did not impact the protein loading step. In contrast, approximately 90 % of the initial feed total protein concentration for the two aqueous egg white solutions (AEW and AEW) was contained in the permeate during the loading step. As the feed had similar total protein concentration, the differences in breakthrough curve reflect differences in total protein interaction with the membrane. The higher relative total protein concentration achieved in the permeate for the two aqueous egg white solutions (AEW and AEW) indicates that a lower proportion of the feed proteins adsorbed on the membrane during the loading step compared to the ethanol soluble egg white solution (ESEW). There was no significant effect of NaCl addition on protein breakthrough, although a lower relative permeate concentration was observed when NaCl was present in the feed (AEW) during the loading step. Membrane saturation for all egg white solutions was quickly achieved over the first 30 ml of collected permeate ($V/V_{\text{final}} = 0.2$).

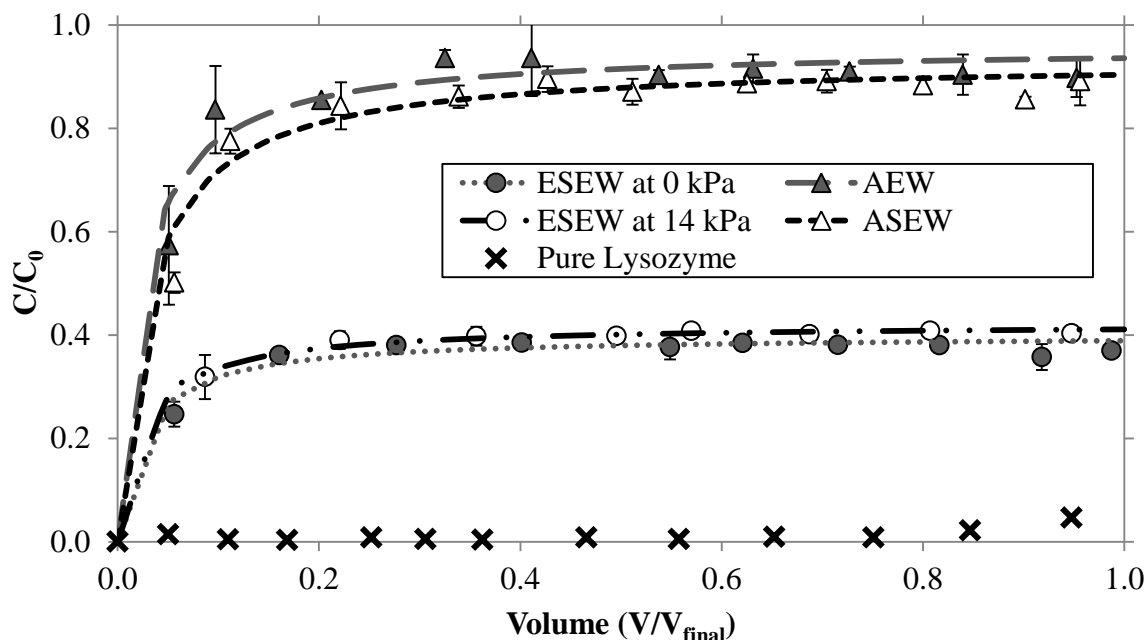


Figure 15. Normalized total protein concentration breakthrough curves for different egg white solution at pH 7.5 for Matrix Weak C membranes. Feed flow rate was 160 ml/min. Total protein concentration (C) measured by UV Absorbance at 280 nm was normalized based on the initial total protein concentration (C_0). Permeate volume (V) was normalized based on the final volume of collected permeate (V_{final}), shown in Table 11, column 3. Error bars represent standard error for $n = 2$.

Figure 31 shows the breakthrough curve of the lysozyme activity in the permeate during the loading step. Despite extensive contact time between the solution and the membrane due to the recycling of the retentate back into the feed stream and high relative total protein concentration breakthrough (Figure 15), 10 % breakthrough was not observed for lysozyme activity during the loading step for all egg white solutions. The low lysozyme activity in the permeate suggested that most of the feed lysozyme activity was bound to the membrane during the loading step. Feed-side pressure and NaCl addition to the feed did not affect lysozyme binding. As the initial lysozyme concentration decreased, lysozyme activity in the permeate during the loading step increased (8 % of the initial feed lysozyme activity for ASEW compared to less than 2 % for ESEW), likely due to increased competitive binding to the membrane; egg white proteins other than lysozyme may have been occupying binding sites on the membrane despite a similar negative charge to the membrane material at pH 7.5. This effect, however, was not significant due to high standard error for the two aqueous egg white solutions, particularly when NaCl was present. The pH and conductivity of all egg white solutions remained constant after loading. The conductivity of the aqueous

egg white solutions (AEW and ASEW) was three and four times higher, respectively, when compared to the conductivity of ESEW aqueous solution (Table 13).

Table 13. Effect of the sample loading process on egg white solution physical properties

Protein Source	pH		Conductivity [mS/cm]	
	Before Loading	After Loading	Before Loading	After Loading
Lysozyme	7.50 (0.00)	N/A	7.00 (0.01)	N/A
ESEW	7.50 (0.00)	7.48 (0.02)	2.33 (0.00)	2.69 (0.06)
AEW	7.50 (0.003)	7.53 (0.00)	6.64 (0.00)	6.69 (0.33)
ASEW	7.50 (0.001)	7.56 (0.05)	8.90 (0.00)	8.61 (0.10)

4.4.2.2. Elution Profiles

As expected, a burst of protein was observed in the collected permeate volume early during the elution step and was associated with high lysozyme activity for all sources of lysozyme (Figure 16 and Figure 17). The magnitude of the total protein concentration and lysozyme activity elution peak varied according to pressure and lysozyme source. While it is likely that some of the eluted protein bound to the membrane surface was collected in the retentate stream, the permeate elution profiles provide an indication of the extent of protein and lysozyme binding within the membrane pores. Lower peak total protein was observed in the elution for ESEW at 0 kPa, with the peak total protein concentration representing only 46 % of the total protein concentration at the pure lysozyme elution peak. The peak lysozyme activity was further decreased at 26.7 % of the maximum pure lysozyme activity value. For ESEW at 14 kPa, the peak total protein concentration and lysozyme activity were 10.1 % and 21.6 % relative to the peak pure lysozyme concentrations. Therefore, operating at a higher pressure resulted in lower peak total protein concentrations (12.27 mg/ml at 0 kPa versus 5.77 mg/ml at 14 kPa) and peak lysozyme activity (27500 U/ml at 0 kPa compared to 14500 U/ml at 14 kPa) in the elution stream.

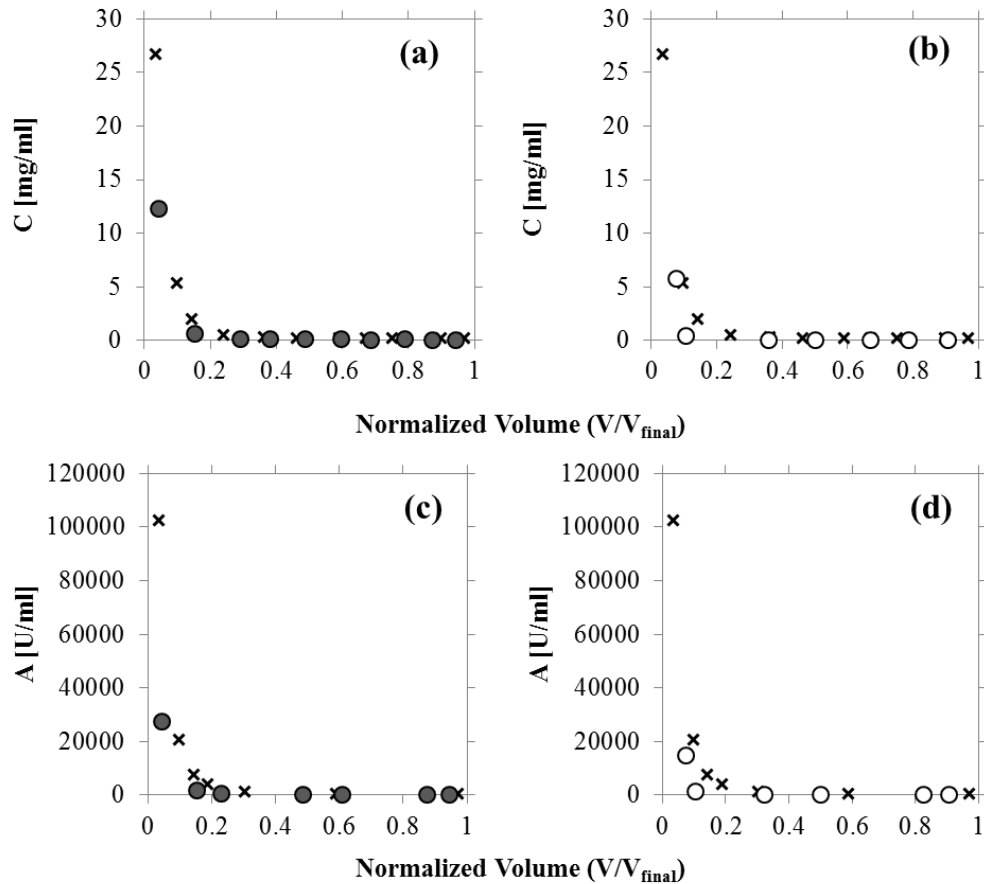


Figure 16. Elution curves for ESEW proteins at pH 7.5 from Matrix Weak C membranes based on total protein concentration following binding at (a) 0 kPa and (b) 14 kPa. Lysozyme activity elution curves are shown for (c) ESEW binding at 0 kPa, and (d) ESEW binding at 14 kPa. Pure lysozyme elution curves (x). Feed flow rate was 160 ml/min. Permeate volume (V) was normalized based on the final volume of collected permeate (V_{final}), shown in Table 11, column 7.

Figure 17 presents the total protein concentration and lysozyme activity elution curves for the AEW and ASEW feeds from Weak C membrane material. For AEW, the highest total protein concentration and lysozyme activity represented approximately 2 % of those of the pure lysozyme source indicating significantly lower protein elution from the membrane. The peak total protein concentration for ASEW was 14.3 % of the maximum total protein concentration eluted for pure lysozyme, while the highest lysozyme activity was 10.1 %. The presence of NaCl content in the egg white binding solution increased the total protein concentration (1.0 mg/ml to 3.8 mg/ml) and lysozyme activity (2400 U/ml to 10400 U/ml) during elution when comparing AEW and ASEW, respectively. Lower total protein and lysozyme activity was recovered during the elution of AEW and ASEW compared to ESEW. The peak total protein concentration for ASEW (3.8 mg/ml) was approximately one-third the peak total protein concentration of the ESEW at 0 kPa

(12.2 mg/ml). Likewise the highest peak lysozyme activity of ASEW (10400 U/ml) was only 37 % of the peak lysozyme activity for ESEW (27500 U/ml).

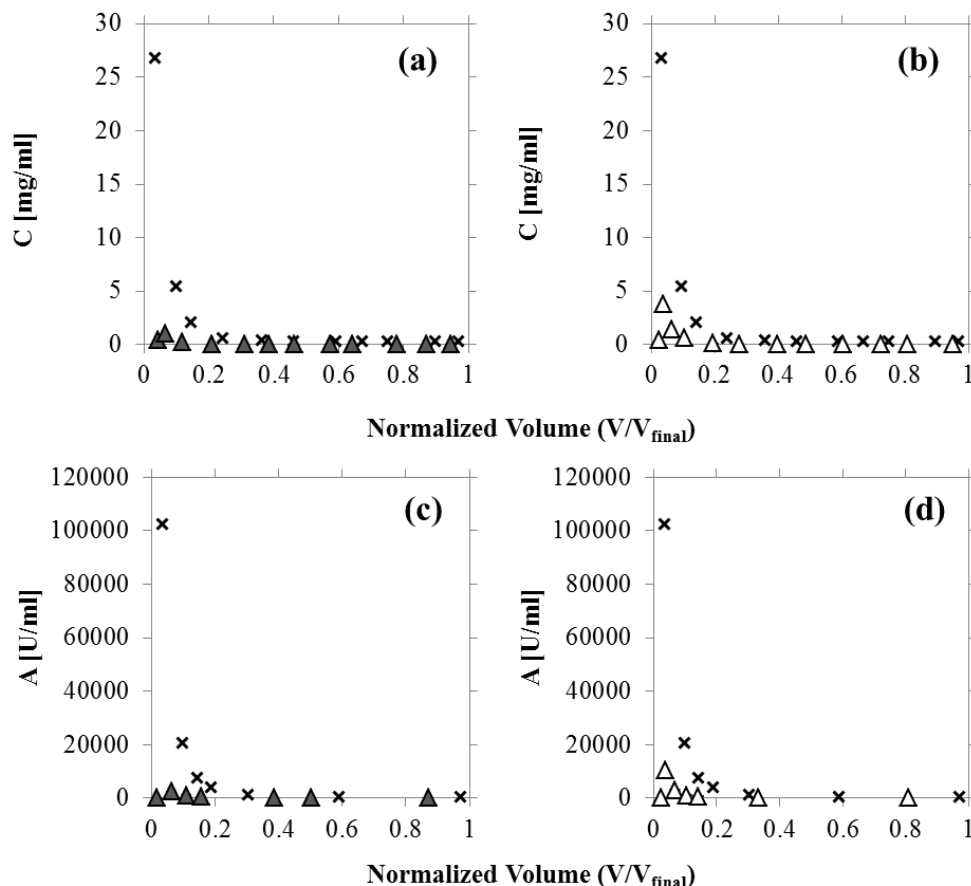


Figure 17. Total protein elution curves for (a) AEW proteins at pH 7.5 and (b) ASEW proteins at pH 7.5 from Natrix Weak C membranes. Lysozyme activity elution curves are shown for (c) AEW proteins and (d) ASEW proteins. Pure lysozyme elution curves (x). Feed flow rate was 160 ml/min. Permeate volume (V) was normalized based on the final volume of collected permeate (V_{final}), shown in Table 11, column 7.

Figure 18 shows the specific lysozyme activity of the permeate and retentate streams collected after the elution step. For each egg white source, the specific activity of lysozyme recovered in the retentate stream was approximately 1500 U/mg, reflecting the lysozyme eluted from the membrane surface. The specific activity of lysozyme eluted into the permeate demonstrated greater variability with lysozyme concentration. The highest specific activity was observed for ESEW bound under no pressure at approximately 3000 U/mg, representing half of the eluted lysozyme specific activity following the binding of pure lysozyme. For the two aqueous egg white solutions, which contained a lower initial lysozyme concentration, a slight decrease in specific activity in the elution permeate was observed. However, this decrease was not significantly different from the ESEW at 0 kPa specific activity ($p > 0.10$).

The addition of NaCl to the binding solution reduced the specific activity of the elution stream by approximately 30 %, suggesting the deactivation of lysozyme with increasing ionic strength. Increasing the operational pressure applied to the membrane during elution to 14 kPa decreased the specific lysozyme activity in the permeate to approximately 2200 U/mg, indicating a lower lysozyme recovery with accelerated processing times.

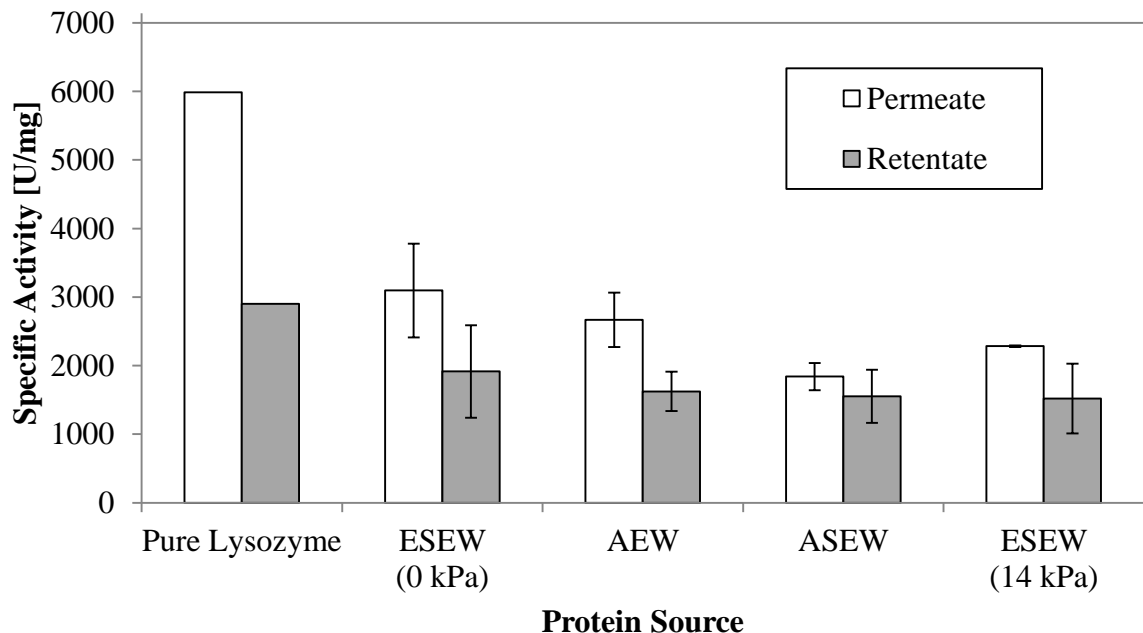


Figure 18. Specific lysozyme activity observed in the permeate and retentate streams collected after the elution step. Error bars represent standard error, where $n = 2$.

4.4.3. Material balance around the dynamic binding process

A material balance was performed around the dynamic binding process to determine losses incurred through binding and elution. Table 14 presents the total protein and lysozyme activity bound to the membrane during the loading step, and the total protein and lysozyme activity recovered in the wash and elution streams for each lysozyme source. For pure lysozyme aqueous solution, nearly all of the total protein and lysozyme activity bound to the membrane was recovered in the elution stream (88.2 % and 99.3 %, respectively). As well, minimal total protein and lysozyme activity losses were observed for the pure lysozyme solution.

For ESEW at 0 kPa, 36.6 % of the total protein bound to the membrane was not recovered, indicating approximately 67 mg of protein remained on the membrane surface after elution. However, despite these high losses, most of the lysozyme activity was

recovered with only 7.7 % of the lysozyme activity bound to the membrane remaining after elution, confirming that the unbound protein was predominantly other proteins found in egg white. While 37.3 % of total bound protein remained on the membrane for ESEW at 14 kPa, a similar proportion of lysozyme activity was lost (31.5 %). Therefore, increasing the pressure decreased the recovery of lysozyme activity from the membrane.

Table 14. Total protein and lysozyme activity recovery in the wash and elution streams for dynamic separation of lysozyme

		Total Protein [mg]	Total Protein Recovery [%]	Lysozyme Activity [U]	Lysozyme Activity Recovery [%]
Pure Lysozyme	Bound	255		1217633	
	Wash	26	10.2	94285	7.7
	Elution	225	88.2	1208564	99.3
	Lost	4.1	1.6	-85216	-7.0
ESEW (0 kPa)	Bound	183		272186	
	Wash	41	22.5	47748	17.5
	Elution	75	40.9	203390	74.7
	Lost	67	36.6	21048	7.7
AEW	Bound	96.46		139332	
	Wash	60.81	63.05	16247	11.7
	Elution	39.28	40.73	96433	69.2
	Lost	-3.6	-3.8	26651	19.1
ASEW	Bound	95.36		166754	
	Wash	51.59	54.1	18143	10.9
	Elution	38.27	40.1	64599	38.7
	Lost	5.5	5.8	84012	50.4
ESEW (14 kPa)	Bound	168		266728	
	Wash	29	17.3	18213	6.8
	Elution	76	45.4	164562	61.7
	Lost	62	37.3	83952	31.5

*Negative total protein or lysozyme activity loss signifies increase in recovery from membrane

For the aqueous egg white solutions (AEW and ASEW), nearly all of the total protein bound to the membrane was recovered by the wash and elution steps (-3.8 % for AEW and 5.8 % for ASEW). However, significant losses in lysozyme activity were observed for AEW, with 19.1 % of lysozyme activity bound to the membrane remaining on the surface

after elution. The addition of NaCl in the binding solution significantly decreased the recovery of lysozyme activity in the wash and elution streams, as over 50 % of the lysozyme activity bound to the membrane remained on the surface following the elution step. The amount of total protein bound to the membrane for AEW and ASEW was significantly lower than the observed bound ESEW protein content (approximately 70 mg lower), confirming the total protein breakthrough curves (Figure 15) where nearly 90 % of the initial total protein concentration of the two aqueous egg white solutions passed through the membrane.

The discrepancies observed in the mass balances for different egg white solutions may also be attributed to the estimation of protein held within the system after the loading step. When switching feeds, the first 50 g of retentate was collected to eliminate feed contamination or dilution during recycle operation. Following the sample loading step, an unknown quantity of feed solution remained in the lines of the dynamic set-up. The quantity of protein in the lines at this point was estimated based on the protein concentration of the collected retentate, and the known dead volume of the system. This estimation will affect the amount of protein bound to the membrane, and may account for the high total protein losses observed following the elution step.

4.4.4. Membrane Staining

Figure 19 shows the stained images of the membrane material at different stages of the dynamic binding process. While the virgin membrane (Figure 19a) showed a uniform light staining, a darker staining surrounding the active membrane area was observed after regeneration with 0.1 M NaOH (20 membrane volumes) and equilibration with 50 mM phosphate citrate at pH 7.5 (40 membrane volumes) (Figure 19b). Regeneration with 0.1 M NaOH is to ensure deprotonation of the carboxylic acid residues present in the membrane, thereby maximizing protein binding [78]. Coomassie brilliant blue is present in a cationic form under acidic conditions [61,63]. By increasing the deprotonation of carboxylic acid on the membrane surface, Coomassie brilliant blue binding to the membrane should increase. Membrane regeneration could also affect hydrophobic interactions within the membrane hydrogel, another potential binding mechanism of Coomassie brilliant blue [61,79]. The effect of contact time with a 5.00 mg/ml lysozyme solution (Figure 19c, Figure 19d, and Figure 19e) increased the intensity of the uniform staining which could be associated with

increased bound protein. Uniform staining indicated even flow distribution across the tangential flow filtration cell during the loading step.

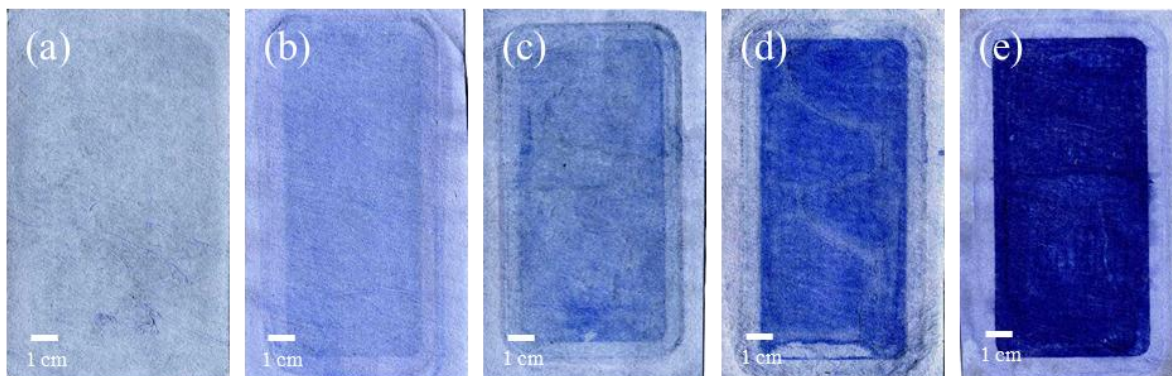


Figure 19. Stained images of the feed side of weak cation-exchange membrane material (a) new; (b) after regeneration and equilibration; (c) after 15 seconds contact time with 5.00 mg/ml lysozyme solution recirculation in the tangential flow cell; (d) after 30 seconds contact time with 5.00 mg/ml lysozyme solution recirculation in the tangential flow cell; (e) after 5 minutes contact time with 5.00 mg/ml lysozyme solution recirculation in the tangential flow cell.

4.4.5. Dynamic separation of lysozyme from ethanol soluble egg white at 0 kPa

Lysozyme was separated from different egg white solutions using the weak cation-exchange membrane to determine the dynamic binding capabilities of the material. Separation characteristics, process recovery, lysozyme selectivity, and lysozyme purity will be discussed in the following sections.

Crude egg white was treated with equal volumes of 60 % (v/v) ethanol, which would increase the concentration of lysozyme through the removal of other egg white proteins. The precipitation process produced a mixture of egg white proteins with an initial lysozyme concentration of approximately 20 %, up from its natural concentration of 3.5 % [19].

4.4.5.1. Membrane staining

Following the dynamic binding and elution process, the weak cation-exchange membrane samples were stained with a Coomassie brilliant blue solution in order to visualize any deformations or residual protein on the membrane surface. Stained membranes after elution with 50 mM phosphate citrate buffer at pH 7.5 and 1 M NaCl are shown in Figure 20. A light uniform staining on the permeate-side of each membrane was observed (Figure 20a), indicating negligible protein bound to the membrane surface. Membrane staining after binding with 1.35 mg/ml pure lysozyme solution and its subsequent elution (Figure 20b) revealed stronger staining intensity compared to the stained membrane prior to sample loading (Figure 19b), which indicates bound protein on the membrane surface. The

remaining bound protein after the elution step was estimated from the mass balance around the dynamic binding process (Table 14), and represented only 1.56 % of the total bound protein. In contrast, stronger staining intensity of the membrane surface was observed for ESEW bound at 0 kPa (Figure 20c). Uniform staining intensity, indicating a homogeneous bound protein distribution, was observed and represented the remaining bound protein after elution (approximately 36.6 % of the total bound protein).

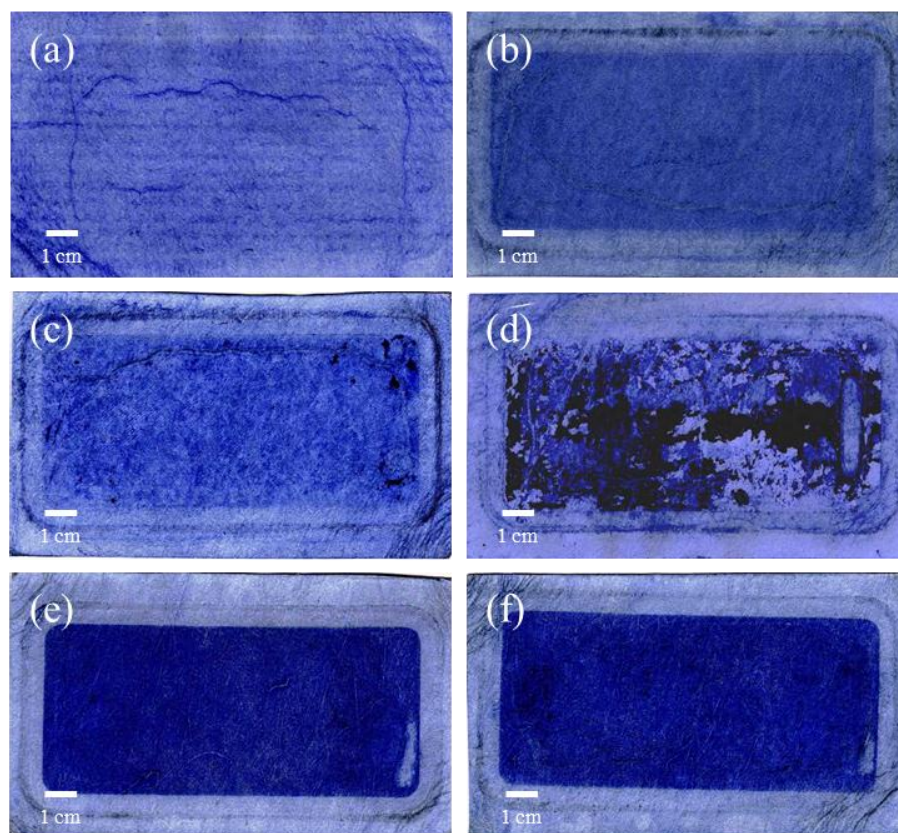


Figure 20. Stained images of weak cation-exchange membrane material after the elution step. (a) Permeate side; (b) feed side and 1.35 mg/ml lysozyme; (c) feed side and ESEW proteins at 0 kPa; (d) feed side and ESEW proteins at 14 kPa; (e) feed side and AEW; (f) feed side and ASEW.

4.4.5.2. Lysozyme membrane recovery and process recovery

Table 15 summarizes the recovery from the membrane, process recovery, and purity for the dynamic separation of lysozyme from egg white in comparison to pure lysozyme. The wash was the liquid solution collected after the binding step and before elution and represented the loosely bound proteins removed from the membrane when no NaCl was present at pH 7.5. At pH 7.5, lysozyme carries a net positive surface charge while other egg white proteins will possess a negative surface charge similar to the membrane material. Based on electrostatic interactions between protein and the membrane hydrogel, the wash

should only contain these negatively-charged proteins. For ESEW bound in the absence of feed-side pressure, the wash solution contained approximately 30 % of the total protein. Only a small proportion of the lysozyme activity bound to the membrane was recovered in the wash solution (7.6 %), indicating that the majority of the total protein present in the wash were negatively-charged egg white proteins.

Table 15. Total protein and lysozyme activity recovery from the membrane and process recovery during dynamic binding and elution operation for different egg white protein solutions

		Lysozyme	ESEW (0 kPa)	AEW	ASEW	ESEW (14 kPa)
Wash (%)	Total Protein	10.2 *	29.5 (6.2)	63.0 (2.2) *	54.1 (0.0) *	17.3 (0.7) *
	Lysozyme Activity	7.7	7.6 (3.5)	11.7 (7.1)	11.1 (6.2)	6.8 (1.1)
Membrane Recovery (%)	Total Protein	88.2 **	48.0 (0.5) *	41.6 (3.1) *	42.9 (3.0) *	46.3 (2.6) *
	Lysozyme Activity	99.3 *	75.7 (5.1) *	40.7 (4.0) *	40.1 (0.2) *	45.4 (1.7) *
Process Recovery (%)	Total Protein	75.2 **	23.1 (3.3) *	11.7 (1.2) *	12.7 (0.3) *	26.0 (0.6) *
	Lysozyme Activity	88.6 **	64.1 (3.1) *	57.1 (0.8) *	33.4 (6.3) *	51.7 (3.7) *
Eluted Lysozyme Purity (%)		N/A	73.4	28.8	33.9	73.4
Purification Factor		N/A	6.5	9.6	9.4	3.2

Note: Values within brackets represent standard error for n = 2. The significance between total protein and lysozyme activity, and between wash, membrane recovery and process recovery was not investigated.

* represents partial significance according to protein source.

** represents total significance according to protein source.

Two different recovery estimates were investigated in this study. Recovery from the membrane reflects the success of the elution step in removing bound protein from the membrane surface. Process recovery gives the amount of protein in the elution stream compared to the initial protein concentration present in the feed. This second recovery estimate is the one commonly reported in literature. The recovery of bound ESEW proteins from the membrane surface showed that less than half of the total protein was present in the collected elution streams (48.0 %). In contrast, 75.7 % of lysozyme activity was recovered from the membrane. Thus, the weak cation-exchange membrane was effective in recovering bound lysozyme from ESEW, while minimizing the elution of other egg white proteins. The total protein process recovery for ESEW was also significantly lower than that of pure

lysozyme (23.1 % compared to 75.2 %, $p < 0.10$), while the lysozyme activity process recoveries were closer in value, yet still statistically significant (64.1 % for ESEW compared to 88.6 % for pure lysozyme, $p < 0.10$). However, the lysozyme activity process recovery from ESEW bound without pressure (64.1 %) was on the lower range of those reported by Chiu, by Avramescu, and by Fang [7,12,21]. In these works, process recovery between 51.1 % and 95 % was typically achieved for the separation of ethanol soluble egg white proteins with cation-exchange membrane materials [7,12,21].

4.4.5.3. Protein selectivity through SDS-PAGE

The selectivity of the separation of ESEW proteins was characterized through SDS-PAGE, shown in Figure 21. Figure 21a shows the feed solutions before and after sample loading. The crude egg white solution (Figure 21a, lane 2) contained six visible polypeptide bands identified as ovotransferrin, ovoglobulins G2 and G3, ovalbumin, ovomucoid, and lysozyme [19]. Ovotransferrin (OT), with a size of approximately 71 kDa, and ovoglobulin G2 and G3 (OG) with molecular weights of approximately 48 and 59 kDa, respectively [19] were not present in ESEW due to their removal through ethanol precipitation. The 44 kDa polypeptide band corresponding to ovalbumin (OA) had the highest intensity, and is known to be the most abundant egg white protein [19]. OA remained in ESEW following the ethanol precipitation procedure, albeit in a lower concentration. Ovomucoid (OM) with an approximate 29 kDa MW was also present ESEW; however, unlike the previously identified egg white proteins, the intensity of OM in ESEW increased. The intensity of the 14.3 kDa MW polypeptide band, representing lysozyme, was very faint in crude egg white, confirming its low concentration. Conversely, ESEW (Figure 21a, lanes 5 and 8) had the highest lysozyme band intensity. There was no apparent discrepancy in the polypeptide distribution and relative polypeptide band intensity when comparing the initial ESEW solutions to the ESEW retentate solution after the loading step.

The SDS-PAGE gel for the permeate collected during the loading step and the wash solution is shown in Figure 21b. While the relative intensity of the OA polypeptide band in the permeate collected during the loading step (lanes 5) was similar to the initial feed solution (Figure 21a, lane 5), the intensity of OM increased indicating that the negatively charged protein at pH 7.5 permeated through the membrane. As well, an OG band not observed in

the initial feed was present, suggesting a greater ovoglobulin concentration passing through the membrane during sample loading. The lysozyme polypeptide band was not visible confirming that lysozyme was bound to the membrane. The polypeptide band distribution of the wash solution for ESEW (Figure 21b, lane 8) provided a measure of the proteins loosely bound to the membrane. The polypeptide band distribution and intensity for the wash solution was similar to the initial feed solution (Figure 21a, lane 5), indicating that membrane saturation was achieved. Higher polypeptide band intensity was observed in the wash streams for AEW and ASEW compared to ESEW, confirming their respective total protein concentration (Table 15).

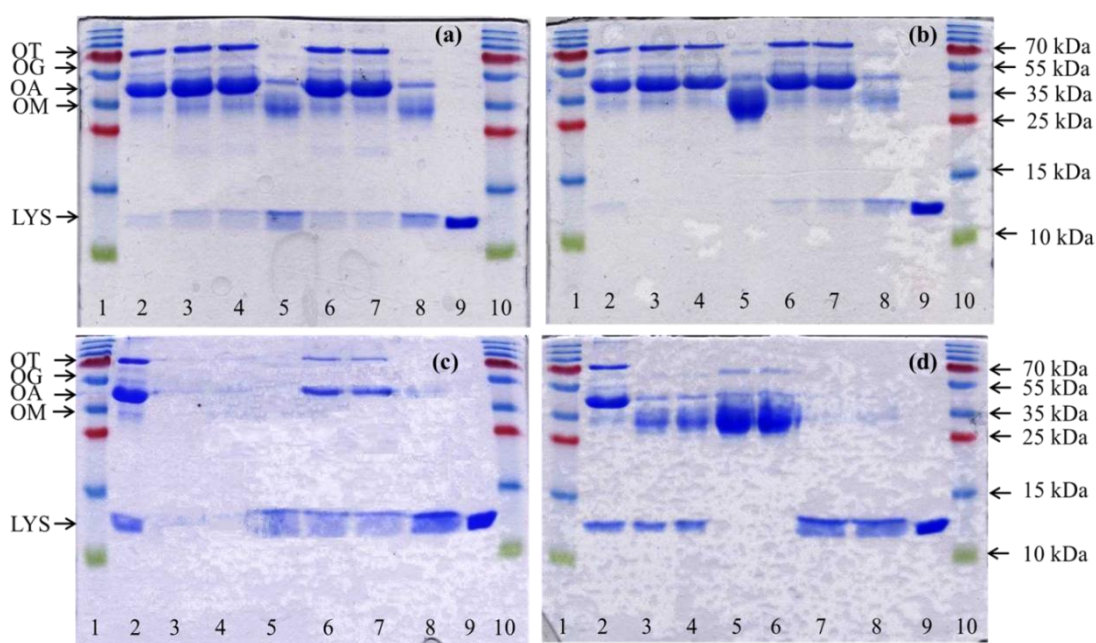


Figure 21. SDS-PAGE analysis on 15 % acrylamide gel, stained with Coomassie brilliant blue. For each gel, Lanes 1 and 10: protein ladder; Lane 2: 1.35 mg/ml total protein crude egg white solution; and Lane 9: 1.00 mg/ml pure lysozyme solution. Each well was loaded with 2.5 μ g of protein. (a) Initial egg white solutions and collected retentate after sample loading. Lanes 3, 4, and 5: initial binding solutions of AEW, ASEW, and ESEW, respectively; Lanes 6, 7, and 8: retentate solutions after sample loading of AEW, ASEW, and ESEW, respectively; (b) Collected permeate after sample loading and wash solutions. Lanes 3, 4, and 5: permeate collected after the loading step of AEW, ASEW, and ESEW, respectively; Lanes 6, 7, and 8: wash solutions of AEW, ASEW, and ESEW, respectively; (c) Collected retentate and permeate solutions after the elution step. Lanes 3, 4, and 5: retentate for AEW, ASEW, and ESEW, respectively; Lanes 6, 7, and 8: permeate for AEW, ASEW, and ESEW, respectively; (d) Comparison of initial egg white solutions, wash solutions, and collected permeate solutions after the elution step for ESEW bound at 0 kPa and at 14 kPa. Lanes 3 and 4: initial solutions of ESEW at 0 kPa and 14 kPa, respectively; Lanes 5 and 6: wash solutions of ESEW for loading at 0 kPa and 14 kPa, respectively; Lanes 7 and 8: elution permeate solutions of ESEW for loading at 0 kPa and 14 kPa, respectively.

Figure 21c displays the SDS-PAGE analysis of the retentate and permeate collected after the elution step. In the retentate of ESEW (lane 5), a lysozyme polypeptide band was detected, indicating the recovery of lysozyme from the membrane. The lysozyme polypeptide band had the highest intensity in the collected permeate for ESEW (lane 8), indicating high

lysozyme purity and lysozyme activity recovery from the membrane after elution. These observations reflected the membrane recovery results of Table 15, where high lysozyme activity was recovered from the membrane in ESEW.

4.4.5.4. Lysozyme purity measured by size-exclusion high-performance liquid chromatography (SEC-HPLC)

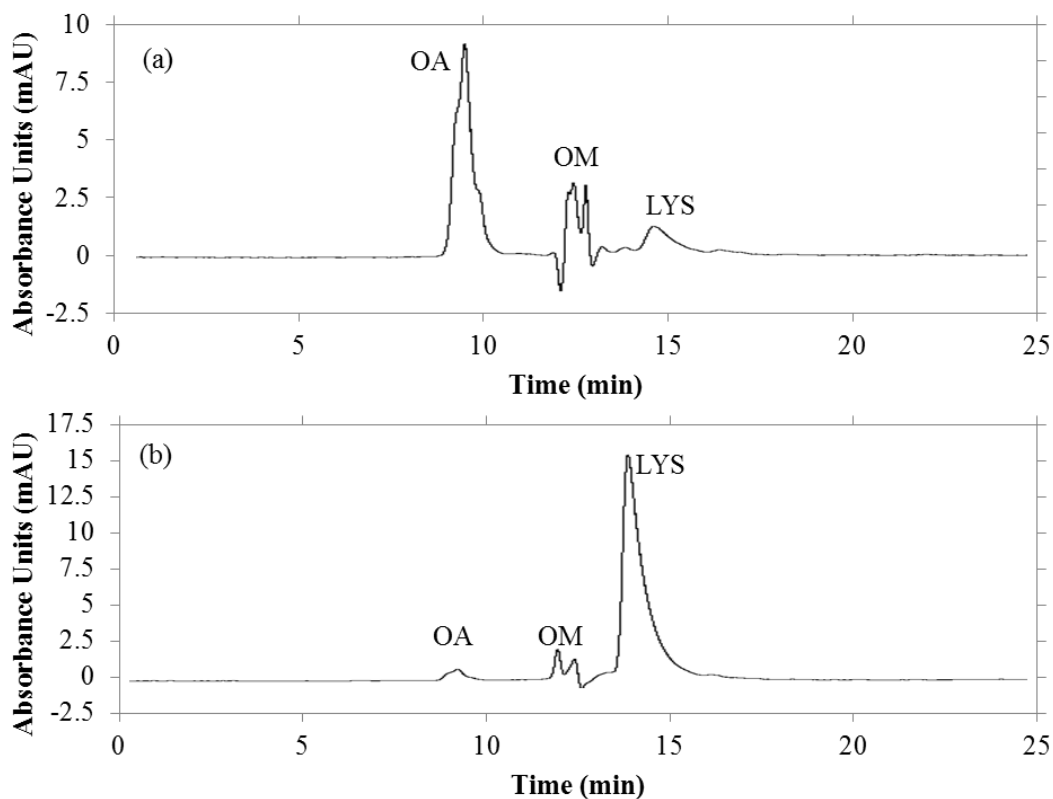


Figure 22. Typical SEC-HPLC chromatograms (a) ESEW feed, and (b) ESEW elution stream for binding at 0 kPa. Flow rate was 1.0 ml/min of a phosphate buffer, pH 7.0, detection by UV absorbance at 280 nm.

The purity of the lysozyme recovered during elution was assessed through SEC-HPLC by assigning molecular weight to major peaks (Appendix). Typical SE-HPLC chromatograms of the feed and elution samples for ESEW bound at 0 kPa are given in Figure 22. For the initial feed (Figure 22a), four peaks were identified. The first peak eluting at 9.5 minutes in the feed solution was identified as ovalbumin (OA), while the second and third peaks eluting at 12.5 minutes were ovomucoid (OM). The multiple peak formation was likely due to the formation of electrostatic complexes between lysozyme and ovomucoid [51,52], thereby increasing the overall molecular weight of the complex and the elution time through

the column. Peak 4 at 14.5 minutes was identified as lysozyme. For the elution sample (Figure 22b), one major peak identified as lysozyme was detected, with two minor peaks identified as OA and OM.

The purity of lysozyme collected during elution and estimated by equation 4-8, was 73.4 % for ESEW (Table 15). The lysozyme purity in the collected permeate following elution of ESEW was improved by nearly 6.5 times when compared to the initial feed solution and confirmed the polypeptide distribution detected by SDS-PAGE (Figure 21c, lane 8), where lysozyme was the most significant polypeptide band visible. The lysozyme purity demonstrated with the weak cation-exchange hydrogel membrane system was comparable to other flat-sheet cation-exchange materials [7,12,17]. Similar lysozyme purity was obtained by Chiu for ethanol-treated egg whites processed at 1 ml/min and 10 ml/min with a prepared strong cation-exchange membrane (78.9 % and 76.9 %) and a commercial unsupported cation-exchange membrane (60.4 % and 63.6 %) [7]. However, the initial lysozyme purity at the loading stage was considerably lower than in this study, so the lysozyme purification factors obtained by Chiu were considerably higher (31.6 and 25.4 for the prepared and commercial membrane, respectively) [7].

Successful lysozyme separation was achieved from ESEW using the weak cation-exchange membrane. Although the lysozyme activity process recovery (64.1 %) was slightly lower than those reported in other studies, high lysozyme selectivity and lysozyme purity was achieved. As well, a relatively low concentration of protein remained bound to the membrane, potentially allowing for subsequent separations with minimal cleaning necessary.

4.4.6. Dynamic separation of lysozyme from aqueous egg white solutions

Two aqueous egg white solutions were prepared through precipitation with 50 mM phosphate citrate, pH 4.8. Aqueous egg white (AEW) represented a diluted egg white solution with a lysozyme concentration similar to its naturally occurrence in egg white (3.5 %). In the second solution, 100 mM NaCl was added to the aqueous solution (ASEW) to promote the removal of egg white proteins, producing an intermediary lysozyme concentration solution between AEW and ESEW.

4.4.6.1. Membrane staining

Unlike the stained membranes following the elution of pure lysozyme and ESEW (Figure 20b and Figure 20c), a strong, uniform staining intensity was observed for the membrane surface in contact with the two aqueous egg white solutions (AEW and ASEW) (Figure 20e and Figure 20f, respectively). Assuming that Coomassie brilliant blue predominantly interacts with bound protein, the high staining intensity indicated a non-specific binding mechanism in addition to electrostatic interaction between proteins and the membrane surface. The higher staining intensity along the membrane surface suggested low protein recovery from the membrane; however, based on the mass balances around the dynamic binding process (Section 4.4.3) nearly all of the total protein bound to the membrane was recovered in the wash and elution streams. The discrepancy between estimates of bound protein and membrane staining intensity for AEW and ASEW may be associated with changes in protein-membrane interactions. Coomassie brilliant blue dye forms protein-dye complexes with basic amino acid residues (such as arginine and lysine) and hydrophobic interactions [61,63,79]. By increasing any of these two factors, the retention of dye on the membrane will be affected. The increased dye intensity could also reflect altered membrane chemistry, not the retention of bound protein on the membrane surface. The addition of NaCl to the binding solutions did not impact the distribution of bound protein retained on the surface, as the staining intensity for the AEW and ASEW membranes was similar.

4.4.6.2. Lysozyme membrane recovery and process recovery

For the two aqueous egg white solutions, AEW and ASEW, the wash solution had a higher total protein content of loosely bound proteins (63.0 % and 54.1 %, respectively) compared to ESEW (29.5 %, $p > 0.10$). However, similar to the ESEW wash solution, the lysozyme activity present in the wash solution was less than 12 % confirming that only negatively-charged proteins were present in the wash solution.

In the elution of aqueous egg white proteins, approximately 40 % of the bound total protein of AEW and ASEW were recovered from the membrane (Table 15), similar to the total protein membrane recovery for ESEW ($p > 0.10$). The lysozyme activity recovery from the membrane for the two aqueous egg white solutions was also approximately 40 %. Thus,

in the presence of a higher concentration of competitive proteins bound to the weak cation-exchange membrane, elution through electrostatic interaction manipulation was not as effective in selectively removing lysozyme. The total protein process recovery for AEW and ASEW was half of the total protein process recovery of ESEW. This confirms the total protein breakthrough curves for the two aqueous egg white solutions, as most of the total protein passed through the membrane (Figure 15). Since more protein was loosely bound to the membrane and was removed in the wash step, the lower total protein process recovery of aqueous egg white may be attributed to increased competitive binding to the membrane. As well, stained membrane images indicated the potential for a higher concentration of bound protein on the membrane surface after elution (Figure 20e and Figure 20f), although the mass balance around the dynamic binding process provided conflicting results (Table 14). While the addition of 100 mM NaCl during the egg white preparation process did not affect the total protein process recovery, the lysozyme activity process recovery was found to decrease as a result (57.1 % for AEW compared to 33.4 % for ASEW). NaCl addition in the binding step would have likely produced a greater charge shielding effect, as oppositely charged ions would surround the membrane and proteins and would reduce electrostatic attraction between the two surfaces [28,47]. As discussed, separation of egg white with cation-exchange membrane materials have reported lysozyme activity process recovery between 50 % to 95 % [7,12,21,35], so the separation of aqueous egg white using the weak cation-exchange membrane material was not as effective.

4.4.6.3. Protein selectivity through SDS-PAGE

Comparison of the aqueous egg white solutions (AEW and ASEW) to crude egg white shows that the dilution and precipitation process did not significantly alter the protein composition (Figure 21a). As well, throughout the dynamic separation process, the presence of NaCl in the binding solution did not change the polypeptide distribution or intensity of each collected stream. OT, OG, OA, and OM polypeptide bands were present in AEW and ASEW solutions (lanes 3 and 4) with similar intensities to crude egg white (lane 2), suggesting similar concentrations. The 14.3 kDa polypeptide band corresponding to lysozyme was also present in the aqueous egg white [19], with a slightly stronger intensity than in crude egg white. There was no apparent discrepancy in the polypeptide distribution

and relative polypeptide band intensity when comparing the initial feed solutions to the retentate sample collected after loading. Similarly, the polypeptide band intensity and distribution for the permeates collected after the sample loading step (Figure 21b, lanes 3 and 4) were similar to the respective AEW and ASEW feed solutions. Membrane saturation was likely achieved during the sample loading of AEW and ASEW, as the collected wash solutions (Figure 21b, lanes 6 and 7) showed that egg white proteins loosely bound to the membrane surface were in similar concentrations to their respective initial feed solutions. Higher polypeptide band intensity was observed in the wash streams for AEW and ASEW compared to ESEW, confirming their respective total protein concentration (Table 15). From the SDS-PAGE analysis of the retentate and permeate collected after the elution step (Figure 21c), negligible protein was visualized in the retentate samples for the two aqueous egg white preparations (lanes 3 and 4). In the permeate of AEW and ASEW (lanes 6 and 7), OT and OA polypeptide bands were observed in addition to the more desirable lysozyme polypeptide band. As a result, the lysozyme was not pure and an additional separation step would be required to increase its purity. These observations confirmed the notion that poorer lysozyme recovery was achieved with higher competitive binding. As reflected in the recovery results (Table 15), lower lysozyme activity was recovered from the membrane in AEW and ASEW compared to ESEW despite similar total protein recovery from the membrane.

4.4.6.4. Lysozyme purity measured by SEC-HPLC

The lysozyme purity of the collected permeate stream following elution (Table 15) showed the effectiveness of the dynamic separation process. For both aqueous egg white solutions, lysozyme comprised approximately 30 % of the elution permeate (28.8 % and 33.9 %, respectively). The similar lysozyme purities of the aqueous egg white solutions revealed that similar quantities of lysozyme were recovered from the two solutions. However, the lysozyme activity process recovery for ASEW was lower than that of AEW, indicating that the presence of salt deactivated some of the lysozyme. Thus an additional step may be required in the separation process in order to reactivate the recovered lysozyme. In comparison with other works, the lysozyme purity reported for aqueous egg white separation with cation-exchange membranes in a hollow-fibre configuration (95 %) [17]. While the recovered lysozyme purity was lower than that of ESEW (73.4 %) and reported elsewhere,

higher purification factors were achieved than ESEW due to the lower initial lysozyme purity. The similar purification factors of the two aqueous egg white solutions show that the addition of 100 mM NaCl during dilution did not promote protein precipitation, and so both aqueous egg white solutions contained similar initial lysozyme purities.

The dynamic separation of lysozyme from aqueous egg white was not as successful as the separation from ESEW. When solutions with a higher concentration of protein impurities was contacted with the weak cation-exchange membrane surface, the membrane quickly fouled with negatively-charged proteins, as seen from the membrane staining experiments. The increase in contaminant binding decreased the available binding sites for the more desirable lysozyme to interact with, reducing the lysozyme activity recovery from the membrane. It should be noted that a constant total protein concentration was recovered from the membrane during the elution step, regardless of the distribution of bound proteins across the membrane surface. Thus, lysozyme purity following elution was decreased for aqueous egg white proteins compared to ESEW. It is possible that much of the OA and OM present in the elution stream were loosely bound to the membrane yet not removed in the wash solution. Increasing the volume of wash solution collected may help to increase the end lysozyme purity following the binding of aqueous egg white.

4.4.7. Effect of pressure (Ethanol soluble egg white at 14 kPa)

The effect of increasing the feed-side pressure applied to the weak cation-exchange membrane during lysozyme separation was investigated. Due to the high lysozyme recovery and lysozyme purity in the elution stream, ESEW was loaded onto the membrane with a feed-side pressure of 14 kPa. The application of pressure increased the rate of permeation through the membrane, reducing processing times by a factor of 10.

4.4.7.1. Membrane staining

The staining of the membrane for binding with ESEW at 14 kPa (Figure 20d) revealed a strong, non-uniform staining intensity on the feed side which could be interpreted as protein clusters caused by aggregation. The application of pressure appeared to have caused protein aggregation during the protein binding process, possibly causing the protein to become embedded on the membrane surface. Similar to ESEW at 0 kPa (Figure 20c), approximately 37.25 % of the total bound protein remained on the membrane after the wash

and elution steps. Due to the presence of non-uniform staining and protein aggregates on the membrane surface for ESEW bound at 14 kPa would likely limit protein binding and total protein process recovery.

4.4.7.2. Lysozyme membrane recovery and process recovery

Despite the appearance of protein aggregates on the membrane surface, the amount of loosely bound proteins removed in the wash solution remained constant for ESEW bound at the two operational pressures (29.5 % at 0 kPa and 17.3 % at 14 kPa, $p > 0.10$). Likewise, the lysozyme activity recovered in the wash solution was low when binding at 14 kPa (6.8 %), indicating that only non-negative proteins were eluted during the wash step. Similar total protein recovery from the membrane was observed, regardless of pressure (48.0 % at 0 kPa and 46.3 % at 14 kPa, $p > 0.10$). In contrast, the lysozyme activity recovered from the membrane at 14 kPa (45.4 %) was reduced by 30 % compared to operation in the absence of pressure (75.7 %). The lower lysozyme activity recovery from the membrane may have resulted from lower processing times, as the membrane was in contact with the high salt elution buffer for a shorter time period at 14 kPa (6 minutes compared to 40 minutes). As well, lysozyme may have been lost through the formation of protein aggregates on the membrane surface (Figure 20d). Total protein process recovery was not influenced by the application of pressure, with approximately 25 % of initial protein present in the elution streams. Lysozyme activity process recovery was higher at 0 kPa (64.1 %) than at 14 kPa (51.7 %), but the difference was not statistically significant ($p > 0.10$). Similar observations were made by Chiu, as increasing the permeate flow rate by a factor of 10 decreased the lysozyme activity process recovery for two strong cation-exchange membrane materials [7]. As a result, while dynamic binding operation at 14 kPa greatly reduced the processing times, some deactivation of lysozyme was observed, which may limit the application of pressure for separations.

4.4.7.3. Protein selectivity through SDS-PAGE

Figure 21d presents the SDS-PAGE of the feed, wash, and permeate collected during the elution for ESEW at the two pressures. The feed solution (lanes 3 and 4) was similar to the ESEW feed previously identified (Figure 21a, lane 5). The polypeptide profile was similar for the wash solution obtained for operation at the two operating pressures

(Figure 21d, lanes 5 and 6), demonstrating no effect of pressure on the proteins loosely bound to the membrane. In the elution samples of ESEW (Figure 21d, lanes 7 and 8), the lysozyme polypeptide band had the highest intensity indicating increased purity in the elution stream. Faint OM and OA bands were visible in the elution streams of both pressures, with slightly higher intensity in the 14 kPa polypeptide bands. The similar band intensities at both pressures indicated that feed-side pressure did not significantly impact lysozyme selectivity during the separation process.

4.4.7.4. Lysozyme purity measured by SEC-HPLC

The purity of lysozyme in the collected permeate after elution was the same for operation at the two different pressures (73.4 %), confirming the polypeptide distribution detected by SDS-PAGE (Figure 21d, lanes 7 and 8), where lysozyme was the most significant polypeptide band visible. Similar results were obtained by Chiu, as higher permeate flow rates did not significantly change the lysozyme purity in the elution stream for strong cation-exchange membrane materials [7]. Due to the similar total protein process recoveries and recovered lysozyme purities for ESEW for the two different pressure operations, the decreased lysozyme activity process recovery may be a result of the protein aggregation observed on the membrane surface. Consequently, the similar lysozyme purities confirmed the notion that the application of pressure to the membrane had a deactivation effect on recovered lysozyme.

The application of 14 kPa pressure during the separation of ESEW was observed to be effective in rapidly producing a high lysozyme purity elution stream with a slightly decreased lysozyme activity process recovery in comparison to operation without applied pressure. The presence of protein aggregation on the surface following the separation process can limit the separation of lysozyme from egg white, as aggregates represent loss of protein and functionality. Therefore, the separation of ESEW in the absence of any applied pressure is likely more effective despite longer processing times. The use of pressure may still be investigated, for industrial applications, for the maximum amount of applied pressure prior to the appearance of protein aggregation.

4.5. Conclusion

In this study, the dynamic binding behaviour of lysozyme to a weak cation-exchange hydrogel membrane was investigated in a flow through system for binding and elution at pH 7.5 with no NaCl addition during binding. Very high dynamic binding capacity was observed for the membrane chromatography material at 10 % breakthrough from a 0.35 mg/ml pure lysozyme solution (167.3 mg lysozyme per ml membrane), significantly higher than the dynamic binding capacities of cation-exchange membrane systems reported in the literature. As well, while the dynamic binding capacity of other cation-exchange materials is often less than its static binding capacity, the dynamic binding capacity of the weak cation-exchange membrane was approximately 2.2 times its static binding capacity under similar conditions. Therefore, with some optimization the weak cation-exchange membrane may be well-suited for the dynamic separation of proteins due to the membrane's potential for very high binding capacities.

The feasibility of lysozyme separation from egg white with a high lysozyme process recovery and high lysozyme purity using the weak cation-exchange hydrogel membrane was demonstrated. Lysozyme recovery was evaluated and compared for three different egg white sources: ethanol soluble egg white (ESEW), aqueous egg white (AEW), and aqueous egg white with NaCl addition (ASEW). The highest lysozyme activity recovery from the membrane (75.7 %), process recovery (64.1 %), and lysozyme purity (73.4 %) in the elution stream was obtained with ESEW.

In comparison to ESEW, the separation of lysozyme from aqueous egg white (AEW and ASEW) was not as successful. Although similar lysozyme activity recovery from the membrane (40 %) and lysozyme purity in the elution (30 %) was achieved for the separation of aqueous egg white with (ASEW) and without (AEW) the addition of NaCl during pretreatment, these values were approximately 25 % and 45 % lower than the separation of ESEW with the weak cation-exchange membrane. The decrease in lysozyme separation for aqueous egg whites with the weak cation-exchange membrane was likely due to increased concentration of negatively-charged proteins in the feed solution. While negatively-charged proteins present in solution should not have interacted with the anionic membrane, membranes stained after the elution of bound aqueous egg whites showed a high concentration of protein retained on the membrane surface. Due to the excess protein retained

on the membrane surface, non-electrostatic binding, such as hydrophobic interactions, may have been a factor during the protein binding step and would limit lysozyme binding and recovery from the membrane. The presence of NaCl in the aqueous egg white (ASEW) was also shown to deactivate recovered lysozyme, as the lysozyme activity recovered by the separation process decreased by 25 % compared to AEW.

In general, the separation of egg whites with the weak cation-exchange membrane material was more effective with an initial ethanol pretreatment step, despite the additional processing time. With ESEW, only a single-pass separation was necessary for the production of a high purity lysozyme stream with high lysozyme activity process recovery. However, for the purification of a similar stream from aqueous egg whites, a multi-pass separation with the weak cation-exchange membrane would likely be necessary. As well, any further improvements to the recovery of lysozyme from aqueous egg whites would likely also lead to improved lysozyme recovery from ESEW. Consequently, as a result of the high concentration of protein impurities present in aqueous egg white, precipitation with ethanol remains necessary to produce a high lysozyme activity process recovery and lysozyme purity stream.

Significantly lower recovery of lysozyme activity from the membrane was achieved at 14 kPa (45.4 %) compared to 0 kPa, likely due to the formation of protein aggregates on the membrane surface after elution. Despite lower lysozyme recovery from the membrane at 14 kPa, the purity of lysozyme in the elution stream remained high (73.4 %). The application of pressure to the membrane allowed for the recovery of a high purity lysozyme product with an approximately 10-fold reduction in processing time with only a small reduction in lysozyme activity process recovery. However, as aggregations represent a loss of protein functionality and may present significant issues for pharmaceutical applications, operation at 14 kPa would not be recommended for separations where a high quality product was necessary. An alternative for the application of pressure may be to increase the feed-side pressure to a maximum where processing times may be minimized and protein aggregates are not formed.

The use of the weak cation-exchange membrane material may be extended beyond the simple lysozyme model investigated in this study to other protein mixtures. The separation of a small positively-charged protein was successfully demonstrated from a

mixture of proteins. This model system may be scaled up to the separation of a large protein, such as monoclonal antibodies, by manipulating binding pH such that the target protein possesses a net positive charge. Mixtures of several positively-charged proteins may also be investigated with the application of an elution gradient for improved protein selectivity. While the binding and elution of a pure lysozyme solution demonstrated high lysozyme activity recovery from the membrane and of the overall separation process, recovery decreased as the presence of negatively-charged proteins increased. Therefore, minimizing the concentration of these protein impurities in other mixtures should similarly improve selectivity for the target protein.

Future work should look at improving the lysozyme process recovery and purity. While higher dynamic binding capacity was observed in comparison to binding in static conditions, dynamic lysozyme activity process recovery was decreased suggesting that the elution of bound lysozyme from the membrane surface was not as effective. Consequently, improving the elution step during dynamic binding may eliminate the need for additional separation steps aimed at increasing lysozyme recovery and purity. Improving lysozyme recovery from the membrane may be accomplished through a number of methods, including altering the application of a pH gradient during the elution step, adjusting feed flow rates, and changing the retentate to permeate ratio. As well, since protein impurities and NaCl addition reduced lysozyme recovery from the membrane, they should be limited for the optimization of lysozyme recovery. Although the application of higher pressures may be advantageous for the production of a high purity lysozyme stream with minimal processing time, additional work is required to maximize the lysozyme activity process recovery without the formation of protein aggregates, thereby retaining protein functionality. Further investigations into the interactions between lysozyme and the membrane surface will aid in the understanding of hydrogel binding mechanisms, and would allow for the optimization of the lysozyme separation process and minimization of protein impurity binding.

5. Conclusions

In this work, the static and dynamic binding characteristics of a weak cation-exchange hydrogel membrane material were assessed through the separation of lysozyme from egg white. Among the conditions tested, the effect of pH and NaCl concentration in the binding and elution steps on protein binding, and total protein and lysozyme activity process recovery were determined. Optimum binding and elution conditions were determined based on high lysozyme process recovery and lysozyme purity results. Dynamic binding studies for different egg white solutions revealed the impacts of competitive binding, pressure, and membrane regeneration on lysozyme isolation and purification.

The pH of the binding solution during static incubation showed decreasing maximum protein binding to the membrane material when pH was increased from 4.5 to 7.5. Maximum protein binding capacity (82.6 mg/ml membrane) was observed at pH 4.5 and 0 mM NaCl for a 0.35 mg/ml pure lysozyme solution despite operation below the pK_a of the membrane hydrogel, the point at which the membrane carries no net surface charge. Therefore, at pH 4.5, positively-charged protein interacted with the neutral membrane surface, indicating a protein binding mechanism different from electrostatic interactions. Increasing pH of the binding solution increased the lysozyme activity of protein recovered off the membrane and process recovery at both NaCl concentrations. Two different binding and elution strategies were studied; binding and elution at constant pH, and binding at pH 4.5 and elution at variable pH. For binding and elution at constant pH, increasing the pH increased total protein and lysozyme activity recovery from the membrane for pure lysozyme aqueous solution and ethanol soluble egg whites (ESEW). High lysozyme activity recovery from the membrane was only observed when no NaCl was present for all pH conditions. By increasing the elution pH for binding at pH 4.5, increasing total protein and lysozyme activity recovery from the membrane was achieved for both lysozyme sources. The maximum lysozyme activity process recovery for ESEW (68.8 %) was obtained for elution at pH 7.5 and no NaCl addition during binding at pH 4.5.

The addition of NaCl (300 mM) to the binding solution during static incubation decreased protein binding to the membrane for both protein sources, as expected from

reduced electrostatic interactions. For example, the maximum binding capacity for the binding of pure lysozyme at pH 7.5 with no NaCl addition was 74.8 mg/ml membrane compared to 5.3 mg/ml membrane in the presence of 300 mM NaCl. As well, pH had a significant effect on maximum binding capacity when increasing the NaCl concentration of the binding solution. While similar maximum total protein binding was observed for all pH conditions when no NaCl was present, the maximum protein binding capacity decreased with increasing pH in the presence of 300 mM NaCl for both protein sources. Despite similar correlations observed between NaCl addition during binding and maximum total binding capacity for both protein sources, the presence of NaCl had a more significant influence on the binding of pure lysozyme due to its higher conductivity compared to ESEW. The addition of NaCl to the binding solution affected the recovery of lysozyme activity differently, depending on the binding and elution strategy. When binding and elution was performed at the same pH, the presence of NaCl in the binding solution demonstrated increasing inhibitory behaviour on lysozyme with increasing pH. Conversely, the addition of NaCl during binding promoted lysozyme elution at pH 6.0 and 7.5 for binding at pH 4.5 and varying elution pH.

Lysozyme selectivity, as characterized by SDS-PAGE, for ESEW static binding increased with increasing pH conditions, with elution streams at pH 7.5 showing the highest lysozyme polypeptide band intensity in SDS-PAGE for both binding and elution strategies. Ovomuroid was recovered from the membrane when binding at pH 4.5 with no NaCl addition, regardless of elution pH, indicating low lysozyme selectivity and confirming the existence of a non-specific binding interaction between other egg white proteins and the membrane under these conditions. When binding at pH 4.5 and variable elution pH, increasing elution pH increased lysozyme selectivity, but did not completely eliminate the elution of ovomuroid. When binding and elution were performed at constant pH 4.5, ovomuroid was not detected in the elution when binding with 300 mM NaCl.

Dynamic binding of lysozyme was evaluated for pure lysozyme solutions and egg white solutions at the conditions identified in the static binding study: pH 7.5 and no NaCl addition during binding. The feed concentration for pure lysozyme did not impact the maximum total protein binding to the membrane (approximately 200 mg protein). The dynamic binding capacity at 10 % breakthrough (167.3 mg total protein/ml membrane for 0.35 mg /ml pure lysozyme feed solution) was significantly higher than the maximum total

protein static binding capacity at the same conditions (74.8 mg/ml membrane at pH 7.5 and 0 mM NaCl), due to stronger, convective driving forces in the dynamic operation. The total protein process recovery for ESEW in the dynamic operation (23.1 % at pH 7.5 and 0 mM NaCl) and lysozyme activity process recovery (64.1 %) was indeed lower when compared to the static operation (36.9 % and 74.0 %, respectively), reflecting decreased recovery of lysozyme from the membrane. Therefore, improving the efficiency of the elution step during dynamic binding would likely increase lysozyme activity recovery of the dynamic separation process.

The dynamic separation of lysozyme from egg white was investigated for three egg white solutions: (1) ethanol soluble egg white (ESEW), (2) aqueous egg white (AEW), and (3) aqueous egg white with 100 mM NaCl (ASEW). Lysozyme purity in the elution and lysozyme activity recovered through the separation process were higher for ESEW (73.4 % and 64.1 %, respectively) compared to the two aqueous egg white solutions (28.8 % and 57.1 %, respectively for AEW). At pH 7.5, lysozyme should carry a net positive charge, while other egg white proteins should carry net negative charges based on the protein kP_a values. Thus, lysozyme should have been the only protein to bind to the negatively charged membrane. However, when the concentration of protein impurities increased, lysozyme selectivity and lysozyme purity in the elution stream decreased, indicating decreased lysozyme binding to the membrane. Interactions between the negatively-charged proteins and the membrane surface prevented lysozyme from binding to the membrane surface and confirmed a secondary, non-electrostatic protein-membrane binding mechanism. As improved lysozyme separation was demonstrated in the presence of lower protein impurity concentrations, ethanol treatment of egg white is necessary for separation when high lysozyme purity is desired.

The feed-side pressure during the separation of lysozyme from ESEW was adjusted at two pressures, 0 kPa and 14 kPa. Elution streams with similar lysozyme purity (73.4 %) regardless of the applied pressure suggesting that lysozyme was eluted from the membrane in a constant concentration despite differing processing times. Decreased lysozyme binding was observed when pressure was applied, as lysozyme activity recovery decreased from 75.7 % at 0 kPa to 45.4 % at 14 kPa despite similar total protein recovery from the membrane. A high lysozyme purity solution was achieved at a significant reduction in processing time with the

application of feed-side pressure; however, protein functionality was decreased due to the formation of protein aggregates on the membrane surface. Pressure application should be limited to prevent the aggregation formation, which reduced process efficiency and the quality of the end product.

Five cycles of membrane regeneration with 0.1 M NaOH did not impact protein binding to the membrane, as similar total protein and lysozyme activity was observed with increasing number of regeneration cycles. The potential reusability of the membrane to isolate low concentration protein mixtures was demonstrated.

Overall, a high purity lysozyme stream was successfully separated from egg white treated with 60 % (v/v) ethanol using a weak cation-exchange membrane material in a dynamic cross-flow set-up. While the lysozyme activity recovered through the separation process was lower than those captured with other cation-exchange membrane materials in literature, the potential for high lysozyme activity recovery was demonstrated using a pure lysozyme model system. Improving the efficiency of the dynamic elution step, will help to increase lysozyme recovery from the membrane and maximize the high lysozyme dynamic binding capacity. As well, ethanol precipitation was demonstrated as a necessary procedure for the recovery of a large quantity of lysozyme with high lysozyme purity, as increased protein impurity concentrations were observed to limit the binding of lysozyme to the membrane surface. The lysozyme model may be further expanded to the separation of large target proteins or the binding of several different proteins. By manipulating the pH of the binding step, proteins with a pK_a above the membrane pI (4.7) may be imparted with a positive-charge, allowing for electrostatic binding interactions with the weak cation-exchange membrane. The bound target protein may then be eluted through the application of a pH gradient or the addition of NaCl. Similarly, several different positively-charged proteins may be eluted from the membrane surface by increasing the pH of the elution buffer from pH 4.5 to 7.5.

Based on the findings of this study, the following work is recommended:

1. Improve the dynamic set-up by incorporating on-line UV-vis spectrophotometry analysis and conductivity measurements. These improvements would allow for more accurate determination of breakthrough and elution curves, would simplify the protein separation

process, and would allow for improved control over flow rates and pressures within the system.

2. Investigate non-specific protein binding to the membrane. Characterization of the protein binding mechanism would allow for further improvements for protein binding and selectivity, as well as potential applications of the membrane material. Examination of the hydrophobicity of the membrane material, as well as the quantification of lysozyme binding at pH above its pI (10.7) is proposed. Imaging and microscopy techniques of the membrane after binding may help to further understand protein binding mechanisms and the effects on the hydrogel layer. Investigation on the non-electrostatic binding mechanism may also allow for the potential application of the weak cation-exchange membrane as part of a multi-step orthogonal separation process using a single material.
3. Examine the effects of successive separations using egg white solutions. The presence of protein on the membrane surface after elution visualized through membrane staining should be quantified and imaged to determine surface coverage after elution. A cleaning step with 2 M NaCl could be implemented to remove unbound protein, allowing a single membrane material to be used for multiple separations.
4. Improve lysozyme purity and purification factor in the elution stream. Although lysozyme purity is on par with similar membrane chromatography system in other works for ESEW, the lysozyme purity from aqueous egg white was significantly lower. The potential for high lysozyme binding in a dynamic set-up may be improved by reducing competitive binding to the membrane surface. Varying feed flow rates or the permeate to retentate ratio may be investigated to improve purity and increase lysozyme activity recovery from the membrane during the elution step.
5. Optimize the lysozyme separation process in terms of binding pH, salt concentration, elution pH, and applied pressure. The application of pH gradients or salt gradients may improve protein selectivity and may be useful in the production of different protein streams. The manipulation of pH and salt conditions may also aid in the production of a multi-step separation process solely using the membrane material. The effect of applied pressure on the binding and elution process may also be determined in terms of reduced processing time for optimization of lysozyme separation as an industrial application.

References

- [1] U. Gottschalk. Bioseparation in Antibody Manufacturing: The Good, The Bad and The Ugly. *Biotechnology Progress*, 24 (2008) 496.
- [2] C. Boi, S. Dimartino, and G.C. Sarti. Performance of a new Protein A affinity membrane for the primary recovery of antibodies. *Biotechnology Progress*, 24 (2008) 640.
- [3] A.A. Shukla, B. Hubbard, T. Tressel, S. Guhan, and D. Low. Downstream processing of monoclonal antibodies – Application of platform approaches. *Journal of Chromatography B*, 848 (2007) 28.
- [4] R. Ghosh. Protein separation using membrane chromatography: opportunities and challenges. *Journal of Chromatography A*, 952 (2002) 13.
- [5] C. Boi. Membrane adsorbers as purification tools for monoclonal antibody purification. *Journal of Chromatography B*, 848 (2007) 19.
- [6] J. Wang, R. Faber, and M. Ulbricht. Influence of pore structure and architecture of photo-grafted functional layers on separation performance of cellulose-based macroporous membrane adsorbers. *Journal of Chromatography A*, 1216 (2009) 6490.
- [7] H. Chiu, C. Lin, and S. Suen. Isolation of lysozyme from hen egg albumen using glass fiber-based cation-exchange membranes. *Journal of Membrane Science*, 290 (2007) 259.
- [8] G. Bayramoğlu, G. Ekici, N. Beşirli, and M. Yakup Arica. Preparation of ion-exchange beads based on poly(methacrylic acid) brush grafted chitosan beads: Isolation of lysozyme from egg white in batch system. *Colloids and Surfaces A: Physicochemical and Engineering Aspects*, 310 (2007) 86.
- [9] F. Dimer, M. Petzold, and J. Hubbach. Effects of ionic strength and mobile phase pH on the binding orientation of lysozyme on different ion-exchange adsorbents. *Journal of Chromatography A*, 1194 (2008) 11.
- [10] M.C. Stone, Y. Tao, and G. Carta. Protein adsorption and transport in agarose and dextran-grafted agarose media for ion-exchange chromatography: Effect of ionic strength and protein characteristics. *Journal of Chromatography A*, 1216 (2009) 4465.
- [11] S.R. Wickramasinghe, J.O. Carlson, C. Teske, J. Hubbuch, and M. Ulbricht. Characterizing solute binding to macroporous ion exchange membrane adsorbers using confocal laser scanning microscopy. *Journal of Membrane Science*, 281 (2006) 609.

- [12] M.-E. Avramescu, Z. Borneman, and M. Wessling. Particle-loaded hollow-fiber membrane adsorbers for lysozyme separation. *Journal of Membrane Science*, 322 (2008) 306.
- [13] R. Huang, L.K. Kostanski, C.D.M. Filipe, and R. Ghosh. Environment-responsive hydrogel-based ultrafiltration membranes for protein bioseparation. *Journal of Membrane Science*, 336 (2009) 42.
- [14] R. Ghosh. Purification of lysozyme by microporous PVDF membrane-based chromatographic process. *Biochemical Engineering Journal*, 14 (2003) 109.
- [15] R. Ghosh, Z.F. Cui. Purification of Lysozyme Using Ultrafiltration. *Biotechnology and Bioengineering*, 68 (1999) 191.
- [16] E. Ruckenstein, X. Zeng. Macroporous Chitin Affinity Membranes for Lysozyme Separation. *Biotechnology and Bioengineering*, 56 (1997) 610.
- [17] A.M. Ventura, H.M. Fernandez Lahore, E.E. Smolko, and M. Grasselli. High-speed protein purification by adsorptive cation-exchange hollow-fiber cartridges. *Journal of Membrane Science*, 321 (2008) 350.
- [18] F. Ming, J. Howell, F. Acosta, and J. Hubble. Study on Separation of Conalbumin and Lysozyme from High Concentration Fresh Egg White at High Flow Rates by a Novel Ion-Exchanger. *Biotechnology and Bioengineering*, 42 (1993) 1086.
- [19] Y. Mine, M. Yang, Chapter 29. Functional Properties of Egg Components in Food Systems, in I. Guerrero-Legarreta (Ed.), *Handbook of Poultry Science and Technology*, Volume 1: Primary Processing, Hoboken, New Jersey, John Wiley and Sons Inc., 2010, pp. 592.
- [20] M.A. Hashim, K.H. Chu, and P.S. Tsan. Effects of Ionic Strength and pH on the Adsorption Equilibria of Lysozyme on Ion Exchangers. *Journal of Chemical Technology and Biotechnology*, 62 (1995) 253.
- [21] J. Fang, H. Chiu, J. Wu, and S. Suen. Preparation of polysulfone-based cation-exchange membranes and their application in protein separation with a plate-and-frame module. *Reactive & Functional Polymers*, 59 (2004) 171.
- [22] C. Charcosset. Membrane processes in biotechnology: An overview. *Biotechnology Advances*, 24 (2006) 482.
- [23] D. Low, R. O'Leary, and N.S. Pujar. Future of antibody purification. *Journal of Chromatography B*, 848 (2007) 48.
- [24] H. Schlüter, J. Jankowski, Chapter 11: Displacement Chromatography, in M. Kastner (Ed.), *Protein Liquid Chromatography*, Amsterdam, Elsevier Science BV, 2000, pp. 505-526.

- [25] A. Jungbauer, C. Machold, 16. Chromatography of proteins, in E. Heftmann (Ed.), *Chromatography: Applications*, New York, Elsevier Science Publishers Inc., 2004, pp. 669-728.
- [26] S.M. Cramer, V. Natarajan, *Chromatography, Ion Exchange*, in M.C. Flickinger and S.W. Drew (Ed.), *Encyclopedia of Bioprocess Technology – Fermentation, Biocatalysis, and Bioseparation*, Volumes 1-5, John Wiley & Sons, 1999, pp. 612-627.
- [27] F.G. Helfferich, 1. Elementary Principles, in Anonymous, *Ion Exchange*, New York, McGraw-Hill, 1999, pp. 5-9.
- [28] Y. Liang, N. Hilal, P. Langston, and V. Starov. Interaction forces between colloidal particles in liquid: theory and experiment. *Advances in Colloid and Interface Science*, 134-135 (2007) 151.
- [29] A.L. Lehninger, D.L. Nelson, and M.M. Cox, Chapter 3 – Amino Acids, Peptides, and Proteins, in Anonymous, *Lehninger Principles of Biochemistry*, Gordonville, VA., W. H. Freeman, 2004, pp. 75-115.
- [30] A.R. Da Costa, A.G. Fane, and D.E. Wiley. Spacer characterization and pressure drop modeling in spacer-filled channels for ultrafiltration. *Journal of Membrane Science*, 87 (1994) 79.
- [31] S.A. Camperi, A.A. Navarro del Cañizo, F.J. Wolman, E.E. Smolko, O. Cascone, and M. Grasselli. Protein Adsorption onto Tentacle Cation-Exchange Hollow-Fiber Membranes. *Biotechnology Progress*, 15 (1999) 500.
- [32] R. Ghosh, Z.F. Cui. Protein purification by ultrafiltration with pre-treated membrane. *Journal of Membrane Science*, 167 (2000) 47.
- [33] M. Grasselli, S.A. Camperi, A.A. Navarro del Cañizo, and O. Cascone. Direct lysozyme separation from egg white by dye membrane affinity chromatography. *Journal of the Science of Food and Agriculture*, 79 (1999) 333.
- [34] D.A. Omana, J. Wang, and J. Wu. Co-extraction of egg white proteins using ion-exchange chromatography from ovomucin-removed egg whites. *Journal of Chromatography B*, 878 (2010) 1771.
- [35] C. Jiang, M. Wang, W. Chang, and H. Chang. Isolation of Lysozyme from Hen Egg Albumen by Alcohol-Insoluble Cross-Linked Pea Pod Solid Ion-Exchange Chromatography. *Journal of Food Science*, 66 (2001) 1089.
- [36] E. Komkova, *Principles of Ion-Exchange Chromatography for Buffer Optimization*, Natrix Separations Inc., Burlington, ON, TN1001 rev.0610 2010.

- [37] F.G. Helfferich, 2. Structure and Properties of Ion-Exchangers, in Anonymous , Ion Exchange, New York, McGraw-Hill, 1995, pp. 10-25.
- [38] Natrix Separations Inc., Lab Scale Product Catalogue, Natrix Separations Inc., Burlington 2010.
- [39] A. Nussinovitch, 2. Bead Formation, Strengthening, and Modification, in Anonymous , Polymer Macro- and Micro-Gel Beads: Fundamentals and Applications, New York, Springer, 2010, pp. 27-52.
- [40] S. Gemili, E.S. Umdu, N. Yaprak, F.I. Ustok, F.Y.G. Yener, C. Mecitoglu Gucbilmez, et al. Partial purification of hen egg white lysozyme by ethanol precipitation method and determination of the thermal stability of its lyophilized form. Turkish Journal of Agriculture and Forestry, 31 (2007) 125.
- [41] S.A. Iqbal, Y. Mido, 2. Protein in Man's Diet, in Anonymous , Food Chemistry, New Delhi, India, Discovery Publishing House, 2005, pp. 34-39.
- [42] C. Guérin-Dubiard, M. Pasco, A. Hietanen, A. Quiros del Bosque, F. Nau, and T. Croguennec. Hen egg white fractionation by ion-exchange chromatography. Journal of Chromatography A, 1090 (2005) 58.
- [43] K. Sasahara, K. Nitta. Effect of Ethanol on Folding of Hen Egg-White Lysozyme Under Acidic Condition. Proteins: Structure, Function, and Bioinformatics, 63 (2006) 135.
- [44] F.E. Cunningham, V.A. Proctor, and S.J. Goetsch. Egg-white lysozyme as a food preservative: an overview. World's Poultry Science Journal, 47 (1991) 141.
- [45] A.L. Lehninger, D.L. Nelson, and M.M. Cox, Chapter 4 – Three-Dimensional Structure of Proteins, in Anonymous , Lehninger Principles of Biochemistry, Gordonville, VA., W. H. Freeman, 2004, pp. 116-156.
- [46] P. Sassi, G. Onori, A. Giugliarelli, M. Paolantoni, S. Cinelli, and A. Morresi. Conformational changes in the unfolding process of lysozyme in water and ethanol/water solutions. Journal of Molecular Liquids, 159 (2011) 112.
- [47] D.E. Kuehner, J. Engmann, F. Fergg, M. Wernick, H.W. Blanch, and J.M. Prausnitz. Lysozyme Net Charge and Ion Binding in Concentrated Aqueous Electrolyte Solutions Journal of Physical Chemistry B, 103 (1999) 1368.
- [48] S.B. Howard, P.J. Twigg, J.K. Baird, and E.J. Meehan. The solubility of hen egg-white lysozyme. Journal of Crystal Growth, 90 (1988) 94.
- [49] A. Deshpande, S. Nimsadkar, and S.C. Mande. Effect of alcohols on protein hydration: crystallographic analysis of hen egg-white lysozyme in the presence of alcohols. Acta Crystallographica, Section D, Biological Crystallography, 61 (2005) 1005.

- [50] S. Damodaran, K. Anand, and L. Razumovsky. Competitive Adsorption of Egg White Proteins at the Air-Water Interface: Direct Evidence for Electrostatic Complex Formation between Lysozyme and Other Egg Proteins at the Interface. *Journal of Agricultural and Food Chemistry*, 46 (1998) 872.
- [51] T. Matsuda, K. Watanabe, and Y. Sato. Interaction between ovomucoid and lysozyme. *Journal of Food Science*, 47 (1982) 637.
- [52] S. De Boeck, J. Stockx. Mode of Interaction between Lysozyme and the Other Proteins of the Hen's Egg Vitelline Membrane. *International Journal of Biochemistry*, 18 (1986) 623.
- [53] A. Kumar, I. Yu.Galaev, and B. Mattiasson, Precipitation of Proteins: Nonspecific and Specific, in R. Hatti-Kaul and B. Mattiasson (Ed.), *Isolation and Purification of Proteins*, New York, Marcel Dekker, 2003, pp. 209-255.
- [54] R.K. Scopes, Chapter 4: Separation by Precipitation, in Anonymous, *Protein Purification: Principles and Practice*, New York, Springer-Verlag, 1994, pp. 71-101.
- [55] W. Wang, N. Li, and S. Speaker, 4. External Factors Affecting Protein Aggregation, in W. Wang and C.J. Roberts (Ed.), *Aggregation of Therapeutic Proteins*, Hoboken, NJ, John Wiley and Sons, 2010, pp. 119-204.
- [56] E.L.V. Harris, 6.6 Purification and concentration by precipitation, in S. Roe (Ed.), *Protein Purification Techniques: A Practical Approach*, Oxford, Oxford University Press, 2001, pp. 132-142.
- [57] S. Tanaka, Y. Oda, M. Ataka, K. Onuma, S. Fujiwara, and Y. Yonezawa. Denaturation and Aggregation of Hen Egg Lysozyme in Aqueous Ethanol Solution Studied by Dynamic Light Scattering. *Biopolymers*, 59 (2001) 370.
- [58] C.M. Stoscheck, [6] Quantitation of Protein, in M.P. Deutscher (Ed.), *Methods in Enzymology*, Academic Press, 1990, pp. 50-68.
- [59] B.J.S.C. Olson, J. Markwell, Assays for Determination of Protein Concentration, in Anonymous, *Current Protocols in Pharmacology*, John Wiley and Sons Inc., 2007, pp. A.3.4.1-A.3.4.29.
- [60] M. Altikatoglu, M. Celebi. Enhanced Stability and Decolorization of Coomassie Brilliant Blue R-250 by Dextran Aldehyde-modified Horseradish Peroxidase. *Artificial Cell, Blood Substitutes, and Biotechnology*, 39 (2011) 185.
- [61] S.J. Compton, C.G. Jones. Mechanism of Dye Response and Interference in the Bradford Protein Assay. *Analytical Biochemistry*, 151 (1985) 369.
- [62] T. Zor, Z. Selinger. Linearization of the Bradford Protein Assay Increases Its Sensitivity: Theoretical and Experimental Studies. *Analytical Biochemistry*, 236 (1996) 302.

- [63] M.M. Bradford. A rapid and sensitive method for the quantitation of microgram quantities of protein utilizing the principle of protein-dye binding. *Analytical Biochemistry*, 72 (1976) 248.
- [64] Q. Shi, G. Jackowski, One-dimensional polyacrylamide gel electrophoresis, in B.D. Hames (Ed.), *Gel Electrophoresis of Proteins: A Practical Approach*, New York, Oxford University Press Inc., 1998, pp. 1-50.
- [65] U.K. Laemmli. Cleavage of Structural Proteins during the Assembly of the Head of Bacteriophage T4. *Nature*, 227 (1970) 680.
- [66] A.K. Banga, Structure and Analysis of Therapeutic Peptides and Proteins, in Anonymous, *Therapeutic Peptides and Proteins: Formulation, Processing, and Delivery Systems*, Boca Raton, FL, CRC Press, 2006, pp. 33-66.
- [67] Y.V. Kazakevich, R. LoBrutto, Size-Exclusion Chromatography, in Y.V. Kazakevich and R. LoBrutto (Ed.), *HPLC for Pharmaceutical Scientists*, Hoboken, NJ, John Wiley and Sons Inc., 2007, pp. 263-279.
- [68] R. Zhang, M. Tang, A. Bowyer, R. Eienthal, and J. Hubble. A novel pH- and ionic-strength-sensitive carboxy methyl dextran hydrogel. *Biomaterials*, 26 (2005) 4677.
- [69] M.M. Rohani, A.L. Zydney. Effect of surface charge distribution on protein transport through semipermeable ultrafiltration membranes. *Journal of Membrane Science*, 337 (2009) 324.
- [70] R. Helal, M.F. Melzig. Determination of lysozyme activity by a fluorescence technique in comparison with the classical turbidity assay. *Pharmazie*, 63 (2008) 415.
- [71] M.R.J. Salton. Cell wall of *Micrococcus lysodeikticus* as the substrate of lysozyme. *Nature*, 170 (1952) 746.
- [72] D.C. Montgomery, Simple Comparative Experiments, in Anonymous, *Design and Analysis of Experiments*, Hoboken, NJ., USA, John Wiley & Sons Inc., 2005, pp. 23-59.
- [73] S. Tanabe, S. Tesaki, and M. Watanabe. Producing a Low Ovomuroid Egg White Preparation by Precipitation with Aqueous Ethanol. *Bioscience, Biotechnology, and Biochemistry*, 64 (2000) 2005.
- [74] A.H. Mohd Yusof, M. Ulbricht. Polypropylene-based membrane adsorbers via photo-initiated graft copolymerization: Optimizing separation performance by preparation conditions. *Journal of Membrane Science*, 311 (2008) 294.
- [75] H.B. Jensen, K. Kleppe. Effect of Ionic Strength, pH, Amines and Divalent Cations on the Lytic Activity of T4 Lysozyme. *European Journal of Biochemistry*, 28 (1972) 116.

[76] R. Ghosh, S.S. Silva, and Z. Cui. Lysozyme separation by hollow-fibre ultrafiltration. *Biochemical Engineering Journal*, 6 (2000) 19.

[77] B.H. Chiang, C.K. Su, G.J. Tsai, and G.T. Tsao. Egg White Lysozyme Purification by Ultrafiltration and Affinity Chromatography. *Journal of Food Science*, 58 (1993) 303.

[78] Z. Zhou, Y. Yang, and J. Zhang. Ion-exchange-membrane-based enzyme micro-reactor coupled online with liquid chromatography-mass spectrometry for protein analysis. *Analytical and Bioanalytical Chemistry*, 403 (2012) 239.

[79] C.D. Georgiou, K. Grintzalis, G. Zervoudakis, and I. Papapostolou. Mechanism of Coomassie brilliant blue G-250 binding to proteins: a hydrophobic assay for nanogram quantities of proteins. *Analytical and Bioanalytical Chemistry*, 391 (2008) 391.

Appendix

Derivation of Initial Protein Binding Rate

The static binding capacity of protein to the membrane was defined by equation 3-1.

$$q = \frac{q_{\max}t}{K + t}$$

The initial protein binding rate may be determined through the derivation of equation 3-1, taken at time $t = 0$.

$$\frac{dq}{dt} = \frac{q_{\max}(K + t) - q_{\max}t(1)}{(K + t)^2}$$

$$\frac{dq}{dt} = \frac{q_{\max}K + q_{\max}t - q_{\max}t}{(K + t)^2}$$

$$\frac{dq}{dt} = \frac{q_{\max}K}{(K + t)^2}$$

$$\left. \frac{dq}{dt} \right|_{t=0} = \frac{q_{\max}K}{(K + (0))^2}$$

$$\left. \frac{dq}{dt} \right|_{t=0} = \frac{q_{\max}K}{K^2}$$

$$\left. \frac{dq}{dt} \right|_{t=0} = \frac{q_{\max}}{K}$$

UV Absorbance Calibration

A sample calibration curve relating lysozyme concentration to the UV absorbance at 280 nm through the sample is given in Figure 23.

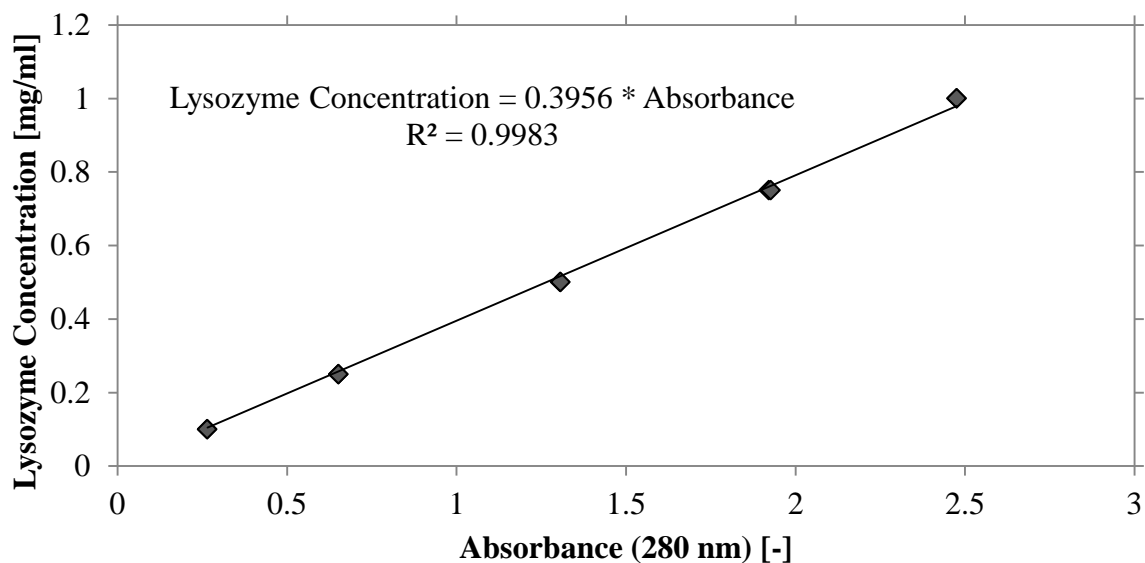


Figure 23. Calibration curve for UV absorbance at 280 nm. Lysozyme standards over the range of 0.1 mg/ml to 1.0 mg/ml was used to determine absorbance.

Lysozyme Activity

Lysozyme activity was determined through a turbidimetric assay at 450 nm and 37 °C using lysozyme activity standards with activities ranging from 10 U/ml to 120 U/ml, where 1 U is a unit of activity defined as a decrease in absorbance of 0.001 based on the conditions above. The calibration curve depicting the change in absorbance over time for each of the standards is shown in Figure 24. Figure 25 shows the determination of the linear slopes of the calibration curve.

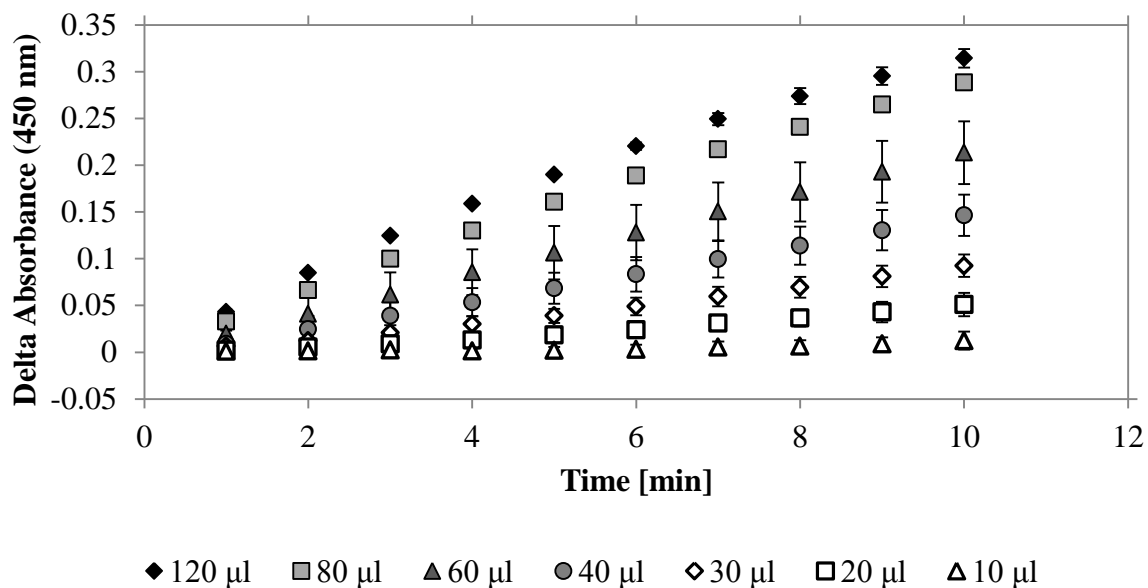


Figure 24. Sample lysozyme calibration curve for the turbidimetric assay showing the change in absorbance at 450 nm over time for the prepared lysozyme standards.

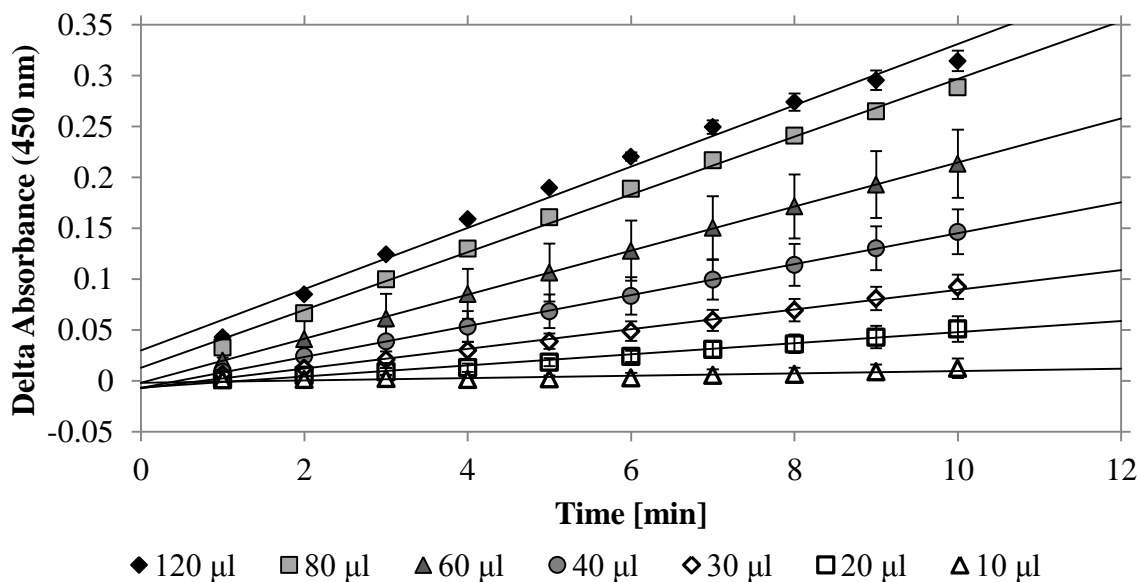


Figure 25. Linearization of the lysozyme standard calibration curve presented in Figure 24 demonstrating the change in absorbance at 450 nm over time.

The slopes of each lysozyme standard were related to the actual activity based on the definition of a unit of activity. Figure 26 shows the relationship between the actual activity determined by the slope and the known activity standards. The slope of this line determines the corrected lysozyme activity. Figure 27 relates the change in absorbance over time for each known lysozyme standard to the corrected activity value.

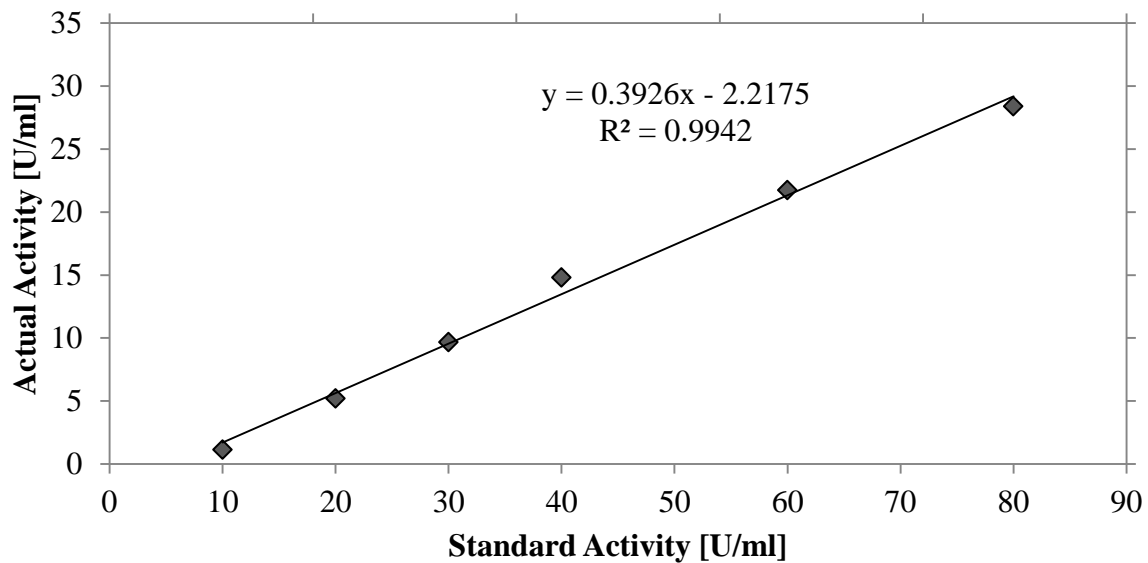


Figure 26. Calibration curve relating the activities of the prepared lysozyme standards to the actual lysozyme activity based on the change in absorbance at 450 nm over time.

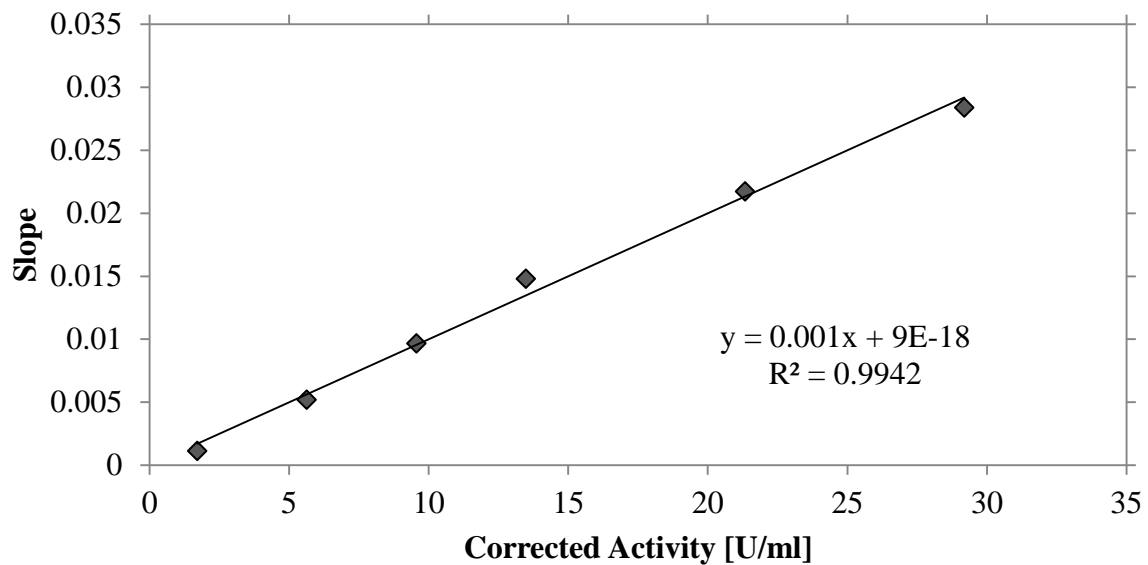


Figure 27. Calibration curve relating the slope for the change in absorbance at 450 nm over time to the corrected lysozyme activity.

SDS-PAGE Calibration

A sample calibration curve for molecular weight identification through SDS-PAGE is shown in Figure 28. The migration distance through the gel was correlated to the known molecular weights of the undisclosed polypeptide bands in the protein ladder standard.

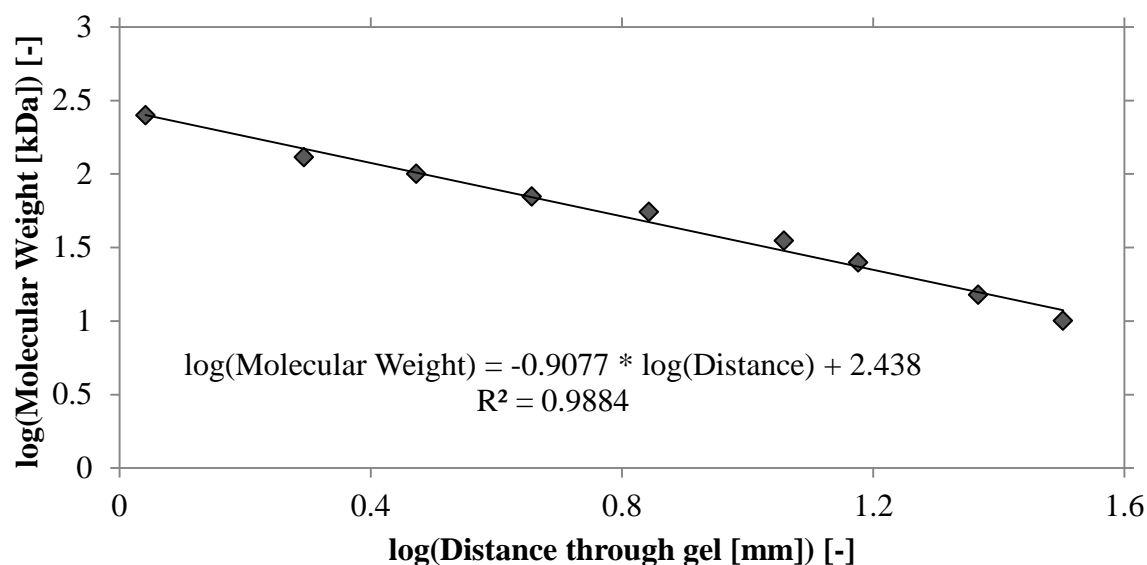


Figure 28. SDS-PAGE calibration curve relating the molecular weight of a sample and the distance migrated through a 15 % acylamide-bis resolving gel.

HPLC Calibration

Sample calibration curves for SEC-HPLC are presented in Figure 29 for component identification through retention times and Figure 30 for lysozyme quantification. Table 16 presents the retention times of three known protein samples through the SEC-HPLC column: BSA, lipase, and lysozyme.

Table 16. Comparison of protein elution times after injection into SEC-HPLC at 1.0 ml/min

Protein	Molecular Weight (kDa)	Retention Time (min)
BSA	66.5	9.50 (0.01)
Lipase	35	10.59 (0.06)
Lysozyme	14.3	14.17 (0.08)

*Values in brackets represent standard error, n = 15

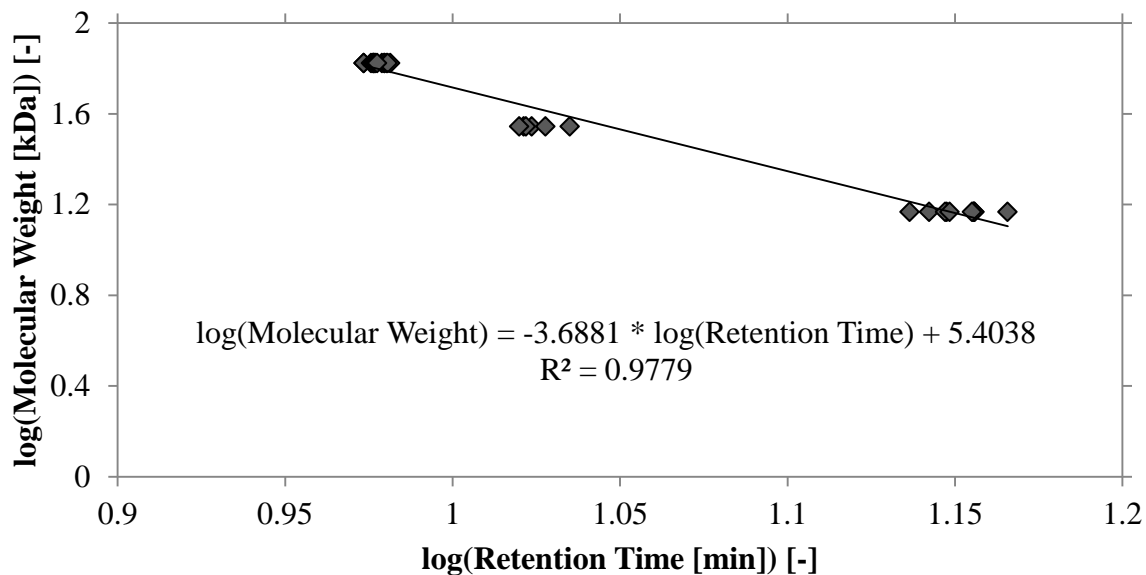


Figure 29. SEC-HPLC calibration curve relating component retention time to molecular weight for peak identification. BSA, lipase, and lysozyme were used as model proteins. Flow rate = 1.0 ml/min

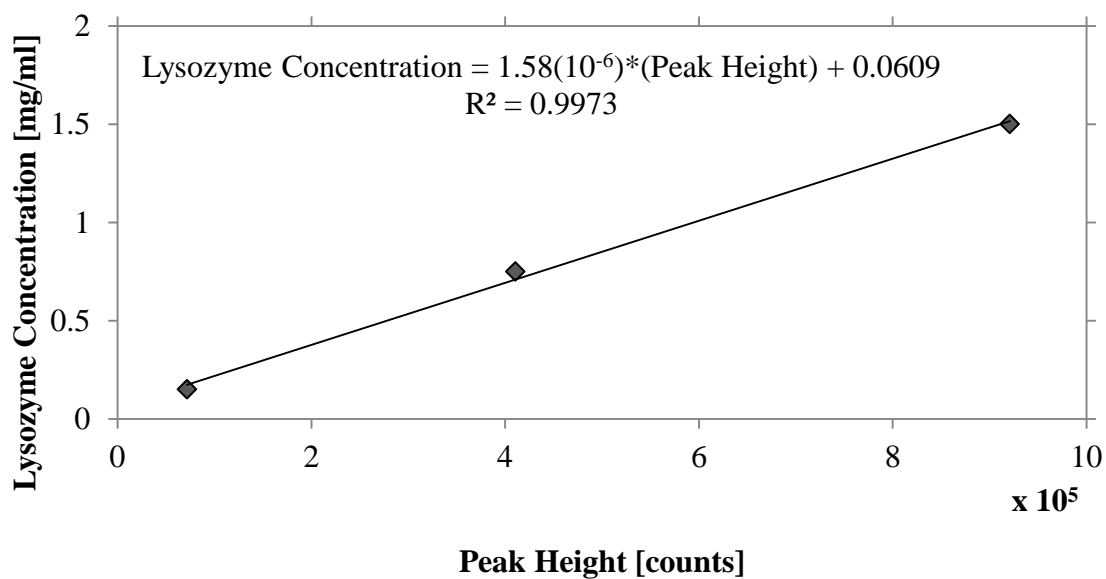


Figure 30. Lysozyme calibration curve through the SEC-HPLC system for protein quantitation. Lysozyme concentrations ranging from 0.15 mg/ml to 1.50 mg/ml were tested.

Ethanol Precipitation and the Effect of Storage Temperature

Bradford analysis

Total protein concentration was measured using the Bradford method adapted from Bradford [63]. Bio-Rad Protein Assay reagent containing Coomassie brilliant blue R250 was diluted to 20 % (v/v) with ultrapure (Type 1, > 18 M Ω · cm at 25 °C) water and passed through a Whatman #1 filter (Whatman, now part of GE Healthcare, Waukesha, WI, USA). A bovine serum albumin calibration curve was prepared in the range of 0.05 g/l to 0.5 g/l. Samples were diluted into the same range. Ten microliters of each sample were transferred into a 96 well microplate in triplicate. The reaction was started with the addition of 200 μ l of diluted Bradford reagent. The microplate was incubated in a dark location for 15 minutes and the absorption was measured at room temperature with a Synergy 4 plate reader at 595 nm.

Total solids analysis

Approximately 10 g egg white samples were weighed in an aluminum dish and placed in a 100 °C oven overnight. After allowing the humidity of the sample to stabilize in a dessicator, the samples were re-weighed and a mass balance was performed. Samples of crude egg white, the solution after incubation with ethanol, precipitated protein, and ESEW were taken for analysis.

Ethanol Precipitation Comparison

The effect of ethanol precipitation on the removal of both total egg white solids and lysozyme activity is shown in Table 17. Approximately 94 % of the total solids content and 89 % of the total protein content was removed through ethanol precipitation ($p < 0.10$). Conversely the activity of lysozyme in solution remained constant at approximately 21000 U/ml after precipitation with ethanol. The storage temperature did not affect protein removal, as the decrease in total protein was 89 % after storage at room temperature and at -20 °C ($p < 0.10$). In contrast, the lysozyme activity was affected by storage temperature. When stored at room temperature for two weeks, the lysozyme activity of the ESEW solution decreased by 12.3 %, but only by 5.0 % when stored at -20 °C. Thus, samples were stored at -20 °C for subsequent analysis.

Table 17. Total solids content, total protein, and lysozyme activity of crude egg white and ESEW

Property	Storage Temperature [°C]	Crude Egg White	ESEW
Total Solids [% w/w]		12.53 (0.25)	0.80 (0.03)
Total Protein [mg/ml]	22	16.62 (1.53)	1.77 (0.07)
	-20	21.47 (0.84)	2.22 (0.30)
Lysozyme Activity [U/ml]	22	21 861	19 177
	-20	22 473	21 350

*Values in brackets represent standard deviation with n = 3.

**Total protein concentration determined by Bradford analysis.

Dynamic lysozyme separation volumes

Table 18. Breakdown of the individual stream volumes during the dynamic separation of lysozyme from egg white

Separation	Loading				Wash	Elution		
	Initial volume (ml)	Permeate volume collected (ml)	Residual Feed solution volume (ml)	Volume lost to system (ml)	Wash solution volume (ml)	Permeate volume collected (ml)	Residual Elution solution volume (ml)	Volume lost to system (ml)
ESEW – 0 kPa Trial 1	430	203	186	41	9	204	32	64
ESEW – 0 kPa Trial 2	415	210	190	15	6	202	52	46
ESEW – 14 kPa Trial 1	320	208	108	4	12	203	29	68
ESEW – 14 kPa Trial 2	255	200	31	24	11	198	37	65
AEW Trial 1	400	202	154	44	10	206	8	86
AEW Trial 2	450	210	205	35	10	198	39	63
ASEW Trial 1	465	206	226	33	11	202	20	78
ASEW Trial 2	430	202	176	52	10	198	40	62
Pure lysozyme	246	207	16	23	11	201	23	76

Lysozyme Activity Breakthrough Curves for Egg White Separation

Breakthrough curves for lysozyme activity during the sample loading stage of the egg white separation process are shown in Figure 31. There was no significant effect of pressure (Figure 31a) or NaCl addition during precipitation (Figure 31b) throughout the loading step.

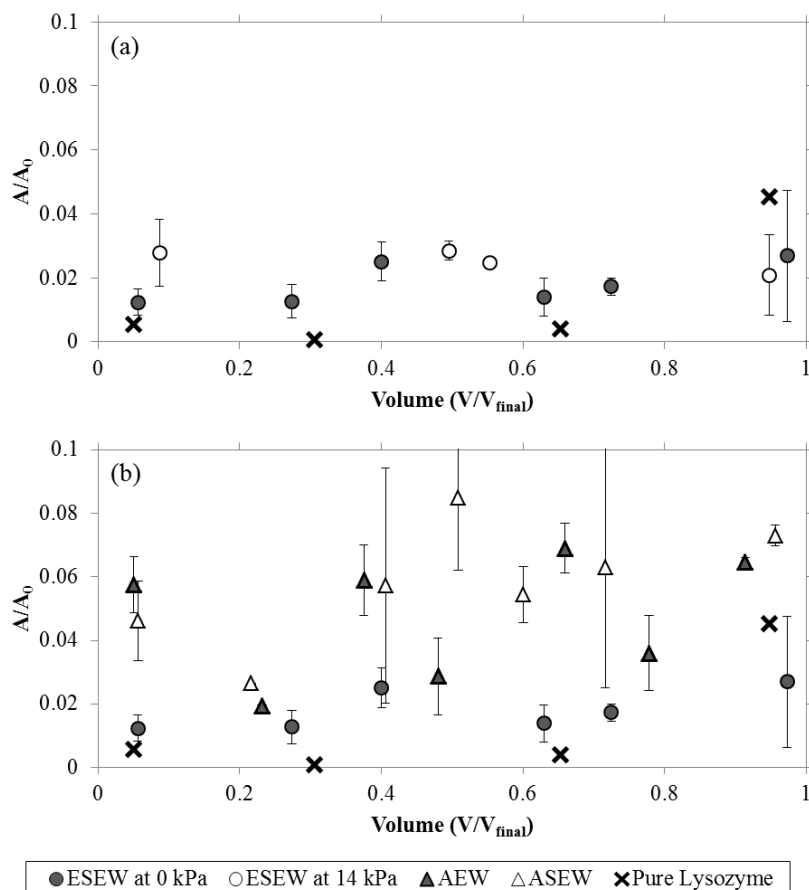


Figure 31. Lysozyme activity breakthrough curves for (a) ESEW at two different pressures and (b) aqueous egg white solutions (with and without NaCl) at pH 7.5 using Natrix Weak C membranes. Feed flow rate was 160 ml/min. Lysozyme activity (A) was normalized based on the initial lysozyme activity (A_0). Volume (V) was normalized based on the final permeate volume (V_{final}). Error bars represent standard error for $n = 2$.

Mass and Activity Balances

Protein mass and lysozyme activity balances are shown in Table 19, Table 20, Table 21, Table 22, Table 23, and Table 25. For all balances, Ret represent the retentate stream, Per represents the permeate stream, and Purge represents the retentate volume collected when switching feeds during the wash step. For total protein balances, R Sample and P Sample

represent the protein removed from the retentate and permeate, respectively, for further analysis.

Membrane Regeneration Mass Balances

Table 19. Protein mass balance for experiments testing the effect of membrane regeneration membrane recovery and protein recovery. For all trials, the first digit signifies the membrane sample number and the second show the number of regeneration cycles (X-X). Feed solution was 0.35 mg/ml pure lysozyme at pH 7.5. Feed flow rate was 160 ml/min

Trial	Step	Sample	Total Protein Concentration (mg/ml)	Volume (ml)	Mass of Protein (mg)	Feed* (%)
1-1	Feed		0.35	200	69.21	100.00
	Loading	Ret	0.31	22	6.76	9.77
		R Sample			2.92	4.22
		Per	0.01	142	1.33	1.92
		P Sampled			0.06	0.09
	Elution	Ret	0.01	31	0.36	0.52
		R Sampled			0.06	0.09
		Per	0.28	160	44.12	63.75
		P Sampled			0.86	1.24
	Regeneration Cycle 1-1 Protein Loss					12.73
1-2	Feed		0.35	200	69.45	100.00
	Loading	Ret	0.28	31	9.56	13.77
		R Sampled			1.68	2.42
		Per	0.01	134	0.94	1.35
		P Sampled			0.04	0.06
	Elution	Ret	0.01	38	0.50	0.72
		R Sampled			0.06	0.09
		Per	0.27	150	40.66	58.55
		P Sampled			0.08	0.12
	Regeneration Cycle 1-2 Protein Loss					15.92
1-3	Feed		0.35	200	69.06	100.00
	Loading	Ret	0.29	18	5.27	7.63
		R Sampled			2.08	3.01
		Per	0.01	142	1.33	1.93
		P Sampled			0.06	0.09
	Wash	Per	0.21	64	13.80	19.98
	Elution	Ret	0.01	16	0.14	0.20
		R Sampled			0.03	0.04
		Per	0.25	170	42.89	62.11
		P Sampled			1.82	2.64
Regeneration Cycle 1-3 Protein Loss					1.64	2.37
1-4	Feed		0.35	200	69.06	100.00
	Loading	Ret	0.29	24.5	7.05	10.21
		R Sampled			2.07	3.00
		Per	0.00	137	0.59	0.85

Trial	Step	Sample	Total Protein Concentration (mg/ml)	Volume (ml)	Mass of Protein (mg)	Feed* (%)
		P Sampled			0.03	0.04
	Wash	Per	0.22	66	14.20	20.56
	Elution	Ret	0.01	27	0.39	0.56
		R Sampled			0.05	0.07
		Per	0.25	166	41.69	60.37
		P Sampled			1.99	2.88
	Regeneration Cycle 1-4 Protein Loss					1.01
1-5	Feed		0.35	200	69.83	100.00
	Loading	Ret	0.28	17	4.83	6.92
		R Sampled			2.35	3.37
		Per	0.01	148	1.50	2.15
		P Sampled			0.08	0.11
	Wash	Per	0.21	64	13.35	19.12
	Elution	Ret	0.01	16	0.22	0.32
		R Sampled			0.07	0.10
		Per	0.27	164	43.88	62.84
		P Sampled			2.40	3.44
Regeneration Cycle 1-5 Protein Loss					1.14	1.63
2-1	Feed		0.35	200	69.45	100.00
	Loading	Ret	0.32	22	7.10	10.22
		R Sampled			0.99	1.43
		Per	0.01	167	2.09	3.01
		P Sampled			0.03	0.04
	Wash	Per	0.24	64	15.40	22.17
	Elution	Ret	0.02	27	0.52	0.75
		R Sampled			0.03	0.04
		Per	0.25	164	40.61	58.47
		P Sampled			1.42	2.04
Regeneration Cycle 2-1 Protein Loss					1.27	1.83
3-1	Feed		0.35	200	69.68	100.00
	Loading	Ret	0.32	17	5.45	7.82
		R Sampled			0.99	1.42
		Per	0.01	170	2.46	3.53
		P Sampled			0.04	0.06
	Wash	Per	0.24	63.5	15.13	21.71
	Elution	Ret	0.03	33	0.90	1.29
		R Sampled			0.04	0.06
		Per	0.27	156	41.62	59.73
		P Sampled			1.43	2.05
Regeneration Cycle 3-1 Protein Loss					1.62	2.33

* Feed (%) = Mass of Protein in Stream / Mass of Protein in Feed * 100%

Membrane Regeneration Activity Balances

Table 20. Lysozyme activity balance for experiments testing the effect of membrane regeneration membrane recovery and protein recovery. For all trials, the first digit signifies the membrane sample number and the second show the number of regeneration cycles (X-X). Feed solution was 0.35 mg/ml pure lysozyme at pH 7.5. Feed flow rate was 160 ml/min

Trial	Step	Sample	Lysozyme Activity (U/ml)	Volume (ml)	Total Activity (U)	Feed* (%)
1-1	Feed		1325 ± 395	200	264985 ± 78960	100.00
	Loading	Ret	1225 ± 119	22	26960 ± 2625	10.17
		Per	8.9 ± 11.2	142	1262 ± 1588	0.48
	Elution	Ret	4.6 ± 1.6	31	143 ± 51	0.05
		Per	1073 ± 218	160	171733 ± 34860	64.81
	Regeneration Cycle 1-1 Activity Loss					64886
1-2	Feed		1345 ± 283	200	268985 ± 56547	100.00
	Loading	Ret	1049 ± 268	31	37752 ± 9636	14.04
		Per	8.1 ± 12	134	1090 ± 1542	0.41
	Elution	Ret	5.2 ± 0.6	38	196 ± 23	0.07
		Per	1251 ± 459	150	187609 ± 68820	69.75
	Regeneration Cycle 1-2 Activity Loss					42337
1-3	Feed		1568 ± 265	200	313682 ± 52947	100.00
	Loading	Ret	1155 ± 365	18	20790 ± 6561	6.63
		Per	7.8 ± 11	142	1103 ± 1560	0.35
	Wash	Per	985 ± 388	64	63052 ± 24816	20.10
	Elution	Ret	2.7 ± 2.7	16	43 ± 43	0.01
		Per	968 ± 135	170	180754 ± 0	57.62
Regeneration Cycle 1-3 Activity Loss					47940	15.28
1-4	Feed		1346 ± 389	200	269152 ± 77739	100.00
	Loading	Ret	1180 ± 190	24.5	28906 ± 4651	10.74
		Per	11 ± 14	137	1461 ± 1906	0.54
	Wash	Per	889 ± 285	66	58695 ± 18833	21.81
	Elution	Ret	7.9 ± 1.1	27	213 ± 29	0.08
		Per	1219 ± 443	166	202302 ± 73563	75.16
Regeneration Cycle 1-4 Activity Loss					-22425	-8.33
1-5	Feed		1328 ± 300	200	265606 ± 59911	100.00
	Loading	Ret	1092 ± 377	17	18558 ± 6402	6.99
		Per	7.7 ± 11	148	1140 ± 1612	0.43
	Wash	Per	894 ± 312	64	57187 ± 19945	21.53
	Elution	Ret	9.8 ± 0.21	16	158 ± 3.4	0.06
		Per	1488 ± 798	164	151516 ± 0	57.05
Regeneration Cycle 1-5 Activity Loss					37048	13.95
2-1	Feed		1629 ± 71	200	325803 ± 14206	100.00
	Loading	Ret	1346 ± 74	22	29616 ± 1621	9.09
		Per	20 ± 2.2	167	3390 ± 375	1.04
	Wash	Per	1089 ± 130	64	69722 ± 8323	21.40
	Elution	Ret	24 ± 9.0	27	660 ± 244	0.20
		Per	935 ± 77	164	153293 ± 12619	47.05
Regeneration Cycle 2-1 Activity Loss					69123	21.22

Trial	Step	Sample	Lysozyme Activity (U/ml)	Volume (ml)	Total Activity (U)	Feed* (%)
3-1	Feed		1605 ± 32	200	32100 ± 6343	100.00
	Loading	Ret	1620 ± 319	17	27534 ± 5418	8.58
		Per	24 ± 2.2	170	4099 ± 370	1.28
	Wash	Per	776 ± 192	63.5	49247 ± 12197	15.34
	Elution	Ret	25 ± 8.3	33	819 ± 274	0.26
		Per	1045 ± 211	156	163044 ± 32852	50.79
Regeneration Cycle 3-1 Activity Loss					76257	23.76

* Feed (%) = Total Activity in Stream / Total Activity in Feed * 100%

**Values shown with standard deviation, n = 2

Breakthrough Study Mass Balance

Table 21. Protein mass balances for breakthrough curves of different pure lysozyme feed concentrations at pH 7.5. Feed flow rate was 160 ml/min

Trial	Step	Stream	Total Protein Concentration (mg/ml)	Volume (ml)	Mass of Protein (mg)	Feed* (%)
0.35 mg/ml LYS	Feed		0.35	1100	383.60	100
	Loading	Ret	0.36	20	7.25	1.89
		R Sampled			2.10	0.55
		Per	0.07	1040	69.87	18.21
		P Sampled			0.92	0.24
	Wash	Purge	0.29	68	19.50	5.08
	Elution	Ret	0.02	30	0.73	0.19
		Per	1.17	162	189.83	49.49
		P Sampled			2.70	0.70
	0.35 mg/ml Lysozyme Protein Loss					93.40
1.00 mg/ml LYS	Feed		0.94	500	472.03	100
	Loading	Ret	0.97	24.5	23.80	5.04
		R Sampled			8.52	1.80
		Per	0.18	423	77.82	16.49
		P Sampled			4.33	0.92
	Wash	Ret	0.11	48	5.34	1.13
		Purge	0.09	65	5.64	1.19
	Elution	Ret	0.81	62	50.15	0.72
		Per	1.08	228	246.68	52.26
		P Sampled			8.56	1.81
1.00 mg/ml Lysozyme Protein Loss					41.19	18.64
5.00 mg/ml LYS	Feed		0.23	298.9	2311.09	100
	Loading	Ret	0.22	305	1317.57	57.01
		R Sampled			0.34	0.01
		Per	0.17	180	299.50	12.96
		P Sampled			1.63	0.07
	Wash	Ret	0.15	79	23.08	1.00
Purge		0.99	66	260.88	11.29	

Trial	Step	Stream	Total Protein Concentration (mg/ml)	Volume (ml)	Mass of Protein (mg)	Feed* (%)
	Elution	Ret	0.06	128	7.15	0.31
		Per	0.20	166	324.19	14.03
		P Sampled			0.32	0.01
	5.00 mg/ml Lysozyme Protein Loss				76.75	3.31

* Feed (%) = Mass of Protein in Stream / Mass of Protein in Feed * 100%

Dynamic Separation Mass Balances

Table 22. Protein mass balances for the dynamic separation of lysozyme for egg white. Feed solution was 1.35 mg/ml at pH 7.5 for all egg white solutions. Feed flow rate was 160 ml/min

Trial	Step	Stream	Total Protein Concentration (mg/ml)	Volume (ml)	Mass of Protein (mg)	Feed* (%)
LYS	Feed		1.31	246	322.84	100.00
	Loading	Ret	1.25	16	21.00	6.50
		R Sampled			3.12	0.97
		Per	0.03	207	7.11	2.20
		P Sampled			0.09	0.03
	Wash	Ret	0.11	31	3.42	1.06
		Purge	1.11	53	58.79	18.21
		Per	0.04	11	0.47	0.15
	Elution	Ret	0.19	23	4.28	1.33
		Per	0.99	201	199.73	61.87
		P Sampled			20.78	6.44
	Pure Lysozyme Protein Loss					4.00
ESEW (0 kPa) 1	Feed		0.35	430	600.60	100.00
	Loading	Ret	1.69	186	259.79	43.26
		R Sampled			4.28	0.71
		Per	0.47	203	95.46	15.90
		P Sampled			4.15	0.69
	Wash	Ret	0.22	68	15.30	2.55
		Purge	1.43	69	98.42	16.39
	Elution	Ret	0.10	32	3.27	0.54
		Per	0.29	204	58.33	9.71
		P Sampled			5.21	0.87
ESEW (0 kPa) 1 Protein Loss					56.39	9.38
ESEW (0 kPa) 2	Feed		1.45	415	601.05	100.00
	Loading	Ret	1.82	190	275.18	45.78
		R Sampled			9.80	1.63
		Per	0.20	210	84.48	14.06
		P Sampled			5.11	0.85
	Wash	Ret	0.33	33	10.83	1.80
Purge		1.14	70.5	80.63	13.41	

Trial	Step	Stream	Total Protein Concentration (mg/ml)	Volume (ml)	Mass of Protein (mg)	Feed* (%)
	Elution	Per	0.09	6	0.51	0.08
		Ret	0.08	52	3.94	0.66
		Per	0.35	202	71.64	11.91
		P Sampled			7.73	1.29
	ESEW (0 kPa) 2 Protein Loss					51.27
ESEW (14kPa) 1	Feed		1.42	320	454.33	100.00
	Loading	Ret	1.48	108	153.34	33.75
		R Sampled			2.31	0.51
		Per	0.40	208	83.52	18.38
		P Sampled			1.85	0.41
	Wash	Ret	0.12	30	3.46	0.76
		Purge	1.16	58	67.06	14.76
		Per	0.36	12	4.35	0.96
	Elution	Ret	0.10	29	2.81	0.62
		Per	0.36	203	73.58	16.20
		P Sampled			3.21	0.71
ESEW (14 kPa) 1 Protein Loss					58.79	12.94
ESEW (14kPa) 2	Feed		1.29	255	329.48	100.00
	Loading	Ret	1.23	31	40.05	12.16
		R Sampled			2.31	0.70
		Per	0.37	200	74.37	22.57
		P Sampled			1.85	0.56
	Wash	Ret	0.16	27	4.28	1.27
		Purged	1.21	52.5	63.73	19.34
		Per	0.35	11	4.0	1.21
	Elution	Ret	0.06	37	2.36	0.72
		Per	0.33	202	67.22	20.40
		P Sampled			3.21	0.97
ESEW (14 kPa) 2 Protein Loss					66.23	20.10
AEW 1	Feed		1.40	400	559.32	100.00
	Loading	Ret	1.43	154	215.34	38.50
		R Sampled			8.90	1.59
		Per	0.90	202	182.41	32.61
		P Sampled			15.55	2.78
	Wash	Ret	0.13	65	8.20	1.47
		Purge	1.32	69	91.41	16.34
	Elution	Ret	0.08	8	0.62	0.11
		Per	0.16	206	32.51	5.81
		P Sampled			1.97	0.35
AEW 1 Protein Loss					2.41	0.44
AEW 2	Feed		1.43	450	645.41	100.00
	Loading	Ret	1.76	205	294.02	45.56
		R Sampled			14.30	2.22
		Per	0.85	200	169.67	26.29

Trial	Step	Stream	Total Protein Concentration (mg/ml)	Volume (ml)	Mass of Protein (mg)	Feed* (%)
		P Sampled			17.32	2.68
	Wash	Ret	0.21	49	10.33	1.60
		Purge	1.94	50	96.87	15.00
		Per	0.23	10	9.11	1.41
	Elution	Ret	0.05	39	2.06	0.32
		Per	0.20	198	39.29	6.09
		P Sampled			2.12	0.33
AEW 2 Protein Loss					-9.68	-1.50
ASEW 1	Feed		1.23	465	571.75	100.00
	Loading	Ret	0.32	226	277.88	48.60
		R Sampled			9.15	1.60
		Per	0.18	206	146.12	25.56
		P Sampled			13.43	2.35
	Wash	Ret	0.12	70	8.20	1.43
		Purge	1.22	63	76.87	13.44
	Elution	Ret	0.08	20	1.66	0.29
		Per	0.15	202	29.53	5.16
		P Sampled			4.22	0.74
ASEW 1 Protein Loss					4.69	0.83
ASEW 2	Feed		1.31	430	561.63	100.00
	Loading	Ret	1.48	176	229.88	40.93
		R Sampled			12.87	2.29
		Per	0.78	202	157.17	27.98
		P Sampled			14.06	2.50
	Wash	Ret	0.16	45	7.14	1.27
		Purge	1.57	54	84.89	15.11
		Per	0.82	10	8.19	1.46
	Elution	Ret	0.05	40	1.83	0.33
		Per	0.19	198	37.12	6.61
Per Sampled				2.36	0.42	
ASEW 2 Protein Loss					91.26	1.10

* Feed (%) = Mass of Protein in Stream / Mass of Protein in Feed * 100%

Dynamic Separation Activity Balance

Table 23. Lysozyme activity balances for the dynamic separation of lysozyme for egg white. Feed solution was 1.35 mg/ml at pH 7.5 for all egg white solutions. Feed flow rate was 160 ml/min

Trial	Step	Sample	Lysozyme Activity (U/ml)	Volume (ml)	Total Activity (U)	Feed* (%)
LYS	Feed		5089 ± 997	246	1425309	100.00
	Loading	Ret	4397 ± 750	16	61868	4.34
		Per	69 ± 0.7	207	14300 ± 148	1.00
	Wash	Ret	336 ± 65	31	10422 ± 2005	0.73

Trial	Step	Sample	Lysozyme Activity (U/ml)	Volume (ml)	Total Activity (U)	Feed* (%)
		Purge	4052 ± 891	53	214775 ± 47243	15.07
		Per	54 ± 5.8	11	597 ± 64	0.04
	Elution	Ret	539 ± 75	23	12401 ± 1725	0.87
		Per	5951 ± 3454	201	1196163 ± 694190	83.92
	Pure Lysozyme Activity Loss					-85216
ESEW (0 kPa) 1	Feed		1676 ± 125	430	720719 ± 53624	100.00
	Loading	Ret	1859.09 ± 106	186	345791 ± 19657	47.98
		Per	3.9	153	439.6 ± 216	0.06
	Wash	Ret	127 ± 0.5	68	8603 ± 31	1.19
		Purge	1125 ± 192	69	77654.7 ± 16573	10.77
	Elution	Ret	265 ± 3.0	33	8474 ± 96	1.18
		Per	1081 ± 29	204	220518 ± 5892	30.6
ESEW (0 kPa) 1 Activity Loss					59239	8.22
ESEW (0 kPa) 2	Feed		1247 ± 165	415	517467 ± 68507	100.00
	Loading	Ret	1331 ± 95	190	252938 ± 17985	48.88
		Per	33 ± 8.8	210	6957 ± 1854	1.34
	Wash	Ret	97 ± 17	33	3199 ± 576	0.62
		Purge	712 ± 127	61	43407 ± 7718	8.39
		Per	6.6 ± 0.3	6	39 ± 1.6	0.01
	Elution	Ret	94 ± 30	52	4889 ± 1546	0.94
Per		856 ± 30	202	172898 ± 6148	33.41	
ESEW (0 kPa) 2 Activity Loss					33140	6.40
ESEW (14kPa) 1	Feed		1357 ± 129	320	434212 ± 41184	100.00
	Loading	Ret	1148.5 ± 96	108	124036 ± 10385	28.57
		Per	50 ± 4.3	208	10346.4 ± 896	2.38
	Wash	Ret	74 ± 0.7	30	2221 ± 20	0.51
		Purge	918 ± 43	58	53237 ± 2471	12.26
		Per	1.6 ± 0.8	12	20 ± 10	0.005
	Elution	Ret	98 ± 11	29	2836 ± 312	0.65
Per		832 ± 33	203	168938 ± 6688	38.91	
ESEW (14 kPa) 1 Activity Loss					72578	16.71
ESEW (14kPa) 2	Feed		1435 ± 37	255	365948 ± 9311	100.00
	Loading	Ret	1240 ± 6.4	31	38434 ± 200	10.50
		Per	51 ± 5.3	200	10127 ± 1056	2.77
	Wash	R	181 ± 23	27	4894 ± 610	1.34
		Purge	1139 ± 119	52.5	59783 ± 6223	16.34
		Per	2.9 ± 0.1	11	32 ± 0.6	0.01
	Elution	Ret	129 ± 1.5	37	4776 ± 54	1.31
Per		755 ± 16	202	152574 ± 3207	41.69	
ESEW (14 kPa) 2 Activity Loss					155110.3	26.05
AEW 1	Feed		750 ± 10	400	300022 ± 3871	100.00
	Loading	Ret	818 ± 114	154	125981 ± 17608	41.99
		Per	61 ± 10	202	12249 ± 2121	4.08
	Wash	Ret	71 ± 6.7	65	4627 ± 438	1.54
Purge		638 ± 43	69	44007 ± 2979	14.67	

Trial	Step	Sample	Lysozyme Activity (U/ml)	Volume (ml)	Total Activity (U)	Feed* (%)
	Elution	Ret	149 ± 9.0	8	484 ± 155	0.40
		Per	484 ± 155	206	99660.3 ± 31861	33.22
	AEW 1 Activity Loss				13014	4.10
AEW 2	Feed		667 ± 32	450	300145 ± 14572	100.00
	Loading	Ret	667 ± 32	205	136733 ± 6638	45.56
		Per	20 ± 1.2	200	4030 ± 241	1.34
	Wash	Ret	68 ± 1.3	49	3343 ± 64	1.11
		Purge	460 ± 166	50	23019 ± 8287	7.67
		Per	1.0 ± 0.2	10	10 ± 2.4	0.00
	Elution	Ret	70 ± 5.8	39	2747 ± 228	0.92
		Per	451 ± 87	198	89265 ± 17323	29.74
AEW 2 Activity Loss				40999	13.66	
ASEW 1	Feed		774 ± 65	465	359744 ± 30127	100.00
	Loading	Ret	751 ± 45	226	169745 ± 10171	47.19
		Per	31 ± 7.6	206	6331 ± 1573	1.76
	Wash	Ret	164 ± 22	70	11498 ± 1537	3.20
		Purge	628 ± 19	63	39561 ± 1225	11.00
	Elution	Ret	162 ± 11	20	3229.3 ± 215	0.90
		Per	239 ± 0.9	202	48174 ± 173	13.39
ASEW 1 Activity Loss				81206	22.56	
ASEW 2	Feed		600 ± 76	430	257883 ± 32561.6	100
	Loading	Ret	353 ± 97	176	62096 ± 17038.4	24.08
		Per	23	202	4745	1.84
	Wash	Ret	50 ± 15	45	2242 ± 663	0.87
		Purge	446 ± 117	54	24079 ± 6300	9.33
		Per	11 ± 1.8	10	106 ± 18	0.04
	Elution	Ret	53 ± 1	40	2125.5 ± 42	0.82
		Per	382 ± 45	198	75669 ± 8922	29.34
ASEW 2 Activity Loss				86820	33.67	

*Feed (%) = Total Activity of Sample / Total Activity of Feed

**Values shown with standard deviation, n = 2

Precipitation Mass Balance

Table 24. Total solids balances around the egg white precipitation process

Sample	Total Solids (mg)	Total Solids Removed by Precipitation (%)
ESEW 1 Precipitate	9.33	72.4
ESEW 1 Supernatant	3.74	
ESEW 1 Solids Removed		
ESEW 2 Precipitate	8.26	67.4
ESEW 2 Supernatant	3.66	
ESEW 2 Solids Removed		
ESEW 3 Precipitate	23.60	69.2
ESEW 3 Supernatant	10.48	
ESEW 3 Solids Removed		
AEW Precipitate	0.47	1.5
AEW Supernatant	30.11	
AEW Solids Removed		
ASEW Precipitate	0.74	3.0
ASEW Supernatant	23.56	
ASEW Solids Removed		

*Total Solids Removed by Precipitation (%) = Total Solids in Precipitate / Total Solids

Permeate Flow Rates

The mass of permeate collected during the loading step and elution step of the dynamic separation comparison tests were measured. The permeate flow rates are presented in Figure 32 for the loading step and in Figure 33 in the elution step. All trials were compared to a 1.35 mg/ml pure lysozyme aqueous solution.

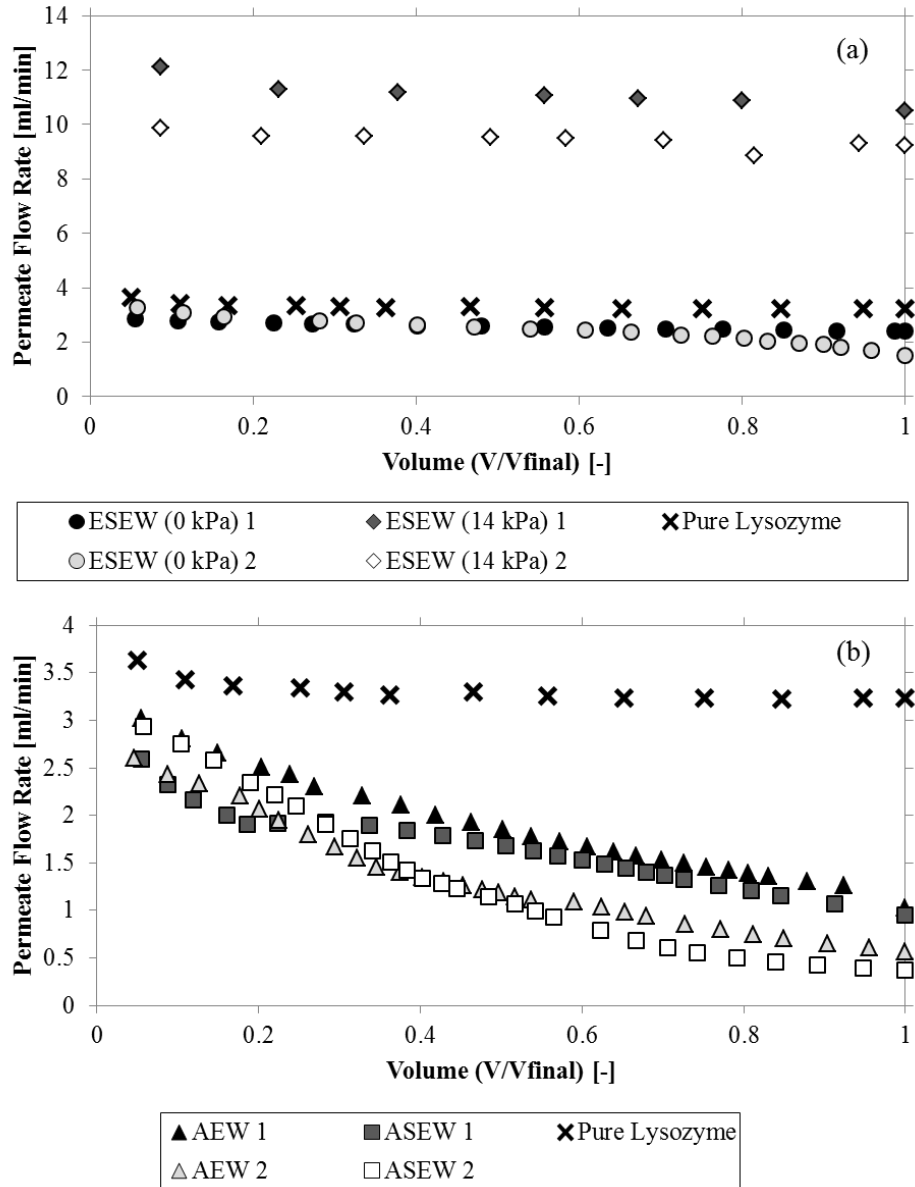


Figure 32. Rate of permeate collection for each trial of dynamic separation of egg white during the loading step. (a) Comparison of ESEW at 0 kPa and ESEW at 14 kPa; (b) comparison of the aqueous egg whites (AEW and ASEW). All trials were compared to pure lysozyme at 1.35 mg/ml (x). Feed flow rate was 160 ml/min for all trials. Permeate volume (V) is presented as a ration to the total permeate volume (V_{final}).

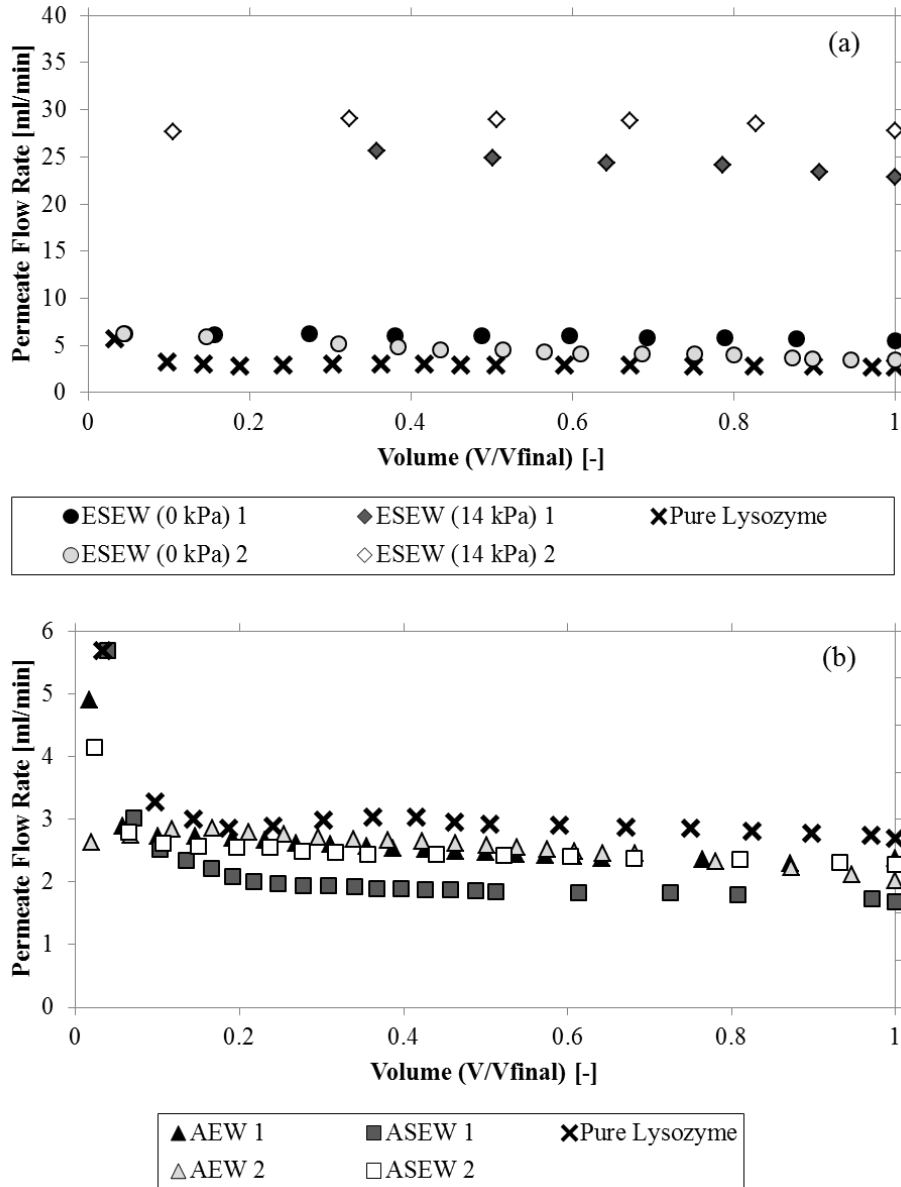


Figure 33. Rate of permeate collection for each trial of dynamic separation of egg white during the elution step. (a) Comparison of ESEW at 0 kPa and ESEW at 14 kPa; (b) comparison of the aqueous egg whites (AEW and ASEW). All trials were compared to pure lysozyme at 1.35 mg/ml (x). Feed flow rate was 160 ml/min for all trials. Permeate volume (V) is presented as a ratio to the total permeate volume (V_{final}).

Sample Calculations

Static binding capacity estimation

Static binding capacity was estimated for pure lysozyme at pH 7.5 and no NaCl addition after 48 hours of membrane incubation, trial 2. From the data collected during membrane incubation, the static binding capacity may be determined by equation 3-1, where C_0 represents initial total protein concentration (mg/ml), C_f final total protein concentration (mg/ml), V_{solution} the volume of binding solution (10 ml), and V_{membrane} the volume of membrane material (0.0626 ml)

$$q = (C_0 - C_f) * \frac{V_{\text{solution}}}{V_{\text{membrane}}}$$

At time $t = 2880$ minutes, $C_0 = 0.369$ mg/ml and $C_f = 0.041$ mg/ml. Therefore:

$$q = \left(0.369 \frac{\text{mg}}{\text{ml}} - 0.041 \frac{\text{mg}}{\text{ml}} \right) * \frac{10 \text{ ml solution}}{0.0626 \text{ ml membrane}} = 52.4 \frac{\text{mg}}{\text{ml membrane}}$$

Static membrane recovery and process recovery

The static membrane recovery and process recovery was estimated for membrane incubation with ESEW at pH 7.5 and no salt addition and constant pH from binding and elution (trial 2) according to equation 3-6 and equation 3-7, respectively.

$$\text{Recovery}_{\text{Membrane, P}} (\%) = \frac{C_{\text{eluted}} V_{\text{eluted}}}{C_{\text{initial}} V_{\text{initial}} - C_{\text{final}} V_{\text{final}}} * 100 \%$$

$$\text{Recovery}_{\text{Process, P}} (\%) = \frac{C_{\text{eluted}} V_{\text{eluted}}}{C_{\text{initial}} V_{\text{initial}}} * 100 \%$$

After 48 hour incubation, $C_{\text{eluted}} = 0.089$ mg/ml, $V_{\text{eluted}} = 15$ ml, $C_{\text{initial}} = 0.368$ mg/ml, $V_{\text{initial}} = 10$ ml, $C_{\text{final}} = 0.232$ mg/ml, $V_{\text{final}} = 10$ ml. Therefore:

$$\text{Recovery}_{\text{Membrane, P}} (\%) = \frac{\left(\frac{0.089 \text{ mg}}{\text{ml}} * 15 \text{ ml} \right)}{\left(\frac{0.368 \text{ mg}}{\text{ml}} * 10 \text{ ml} \right) - \left(\frac{0.232 \text{ mg}}{\text{ml}} * 10 \text{ ml} \right)} * 100 \%$$

$$\text{Recovery}_{\text{Membrane, P}} (\%) = 98.2 \%$$

$$\text{Recovery}_{\text{Membrane, P}} (\%) = \frac{\left(\frac{0.089\text{mg}}{\text{ml}} * 15\text{ml}\right)}{\left(\frac{0.368\text{mg}}{\text{ml}} * 10\text{ml}\right)} * 100 \%$$

$$\text{Recovery}_{\text{Membrane, P}} (\%) = 36.3 \%$$

Dynamic binding capacity estimation

Dynamic binding capacity was estimated for 0.35 mg/ml pure lysozyme solution at pH 7.5 according to 10 % breakthrough of total protein by equation 4-1, where C_0 is the initial total protein concentration (mg/ml), $V_{10\% \text{ BT}}$ is the volume at which 10 % breakthrough occurs (ml), V_{DV} is the dead volume of the system (0 ml), and V_{membrane} is the active membrane volume (1.176 ml membrane)

$$Q(\text{DBC}_{10\%}) = \frac{C_0 * (V_{10\% \text{ BT}} - V_{\text{DV}})}{V_{\text{membrane}}}$$

As off-line measurements were recorded, the volume at which 10 % breakthrough occurred was estimated using the slope between breakthrough concentration and permeate volume, where V_1 is the total permeate volume collected at time 1 (ml), V_2 total permeate volume collected at time 2 (ml), C_1 total protein concentration of the permeate collected at time 1 (mg/ml), C_2 total protein concentration of the permeate collected at time 2 (mg/ml), and $C_{10\%}$ 10 % of the initial total protein concentration (0.03484 mg/ml)

$$V_{10\% \text{ BT}} = \left(\frac{V_2 - V_1}{C_2 - C_1}\right) (C_{10\%} - C_1) + V_1$$

At time t_1 , $V_1 = 564.61$ ml and $C_1 = 0.03476$ mg/ml, while at time t_2 , $V_2 = 580.01$ ml and $C_2 = 0.03984$ mg/ml. Therefore:

$$V_{10\% \text{ BT}} = \left(\frac{580.01\text{ml} - 564.61\text{ml}}{\frac{0.03984\text{mg}}{\text{ml}} - \frac{0.03476\text{mg}}{\text{ml}}}\right) \left(\frac{0.03484\text{mg}}{\text{ml}} - \frac{0.03476\text{mg}}{\text{ml}}\right) + 564.61\text{ml}$$

$$V_{10\% \text{ BT}} = 564.85\text{ml}$$

Therefore, we can solve for dynamic binding capacity, when $C_0 = 0.348$ mg/ml and $V_{\text{membrane}} = 1.176$ ml membrane:

$$Q(\text{DBC}_{10\%}) = \frac{0.348\text{mg}}{\text{ml}} * (564.85\text{ml} - 0\text{ml}) = \frac{167.3\text{mg}}{\text{ml membrane}}$$

Dynamic membrane recovery and process recovery

The total protein present in the wash, membrane recovery, and process recovery of the dynamic separation of ESEW at 0 kPa, trial 2 was estimated according to equation 4-2, equation 4-3, and equation 4-4, respectively. The following data shows the total protein concentration and volumes for each stream used in the calculation of membrane and process recovery.

Table 25. Process stream total protein and volume data for the separation of ESEW at 0 kPa, trial 2

Stream	Total Protein Concentration (mg/ml)	Volume (ml)
Initial Solution	1.45	415
Loading Retentate (LR)	1.45	190
Loading Permeate (LP)	0.40	210
Wash Retentate (WR)	0.33	33
Wash Permeate (WP)	0.09	6
Wash Purge (Purge)	1.27	61
Elution Retentate (ER)	0.08	52
Elution Permeate (EP)	0.35	202

Therefore, the following calculations may be made:

$$\text{Washed}_P (\%) = \frac{C_{WR}V_{WR} + C_{WP}V_{WP} + (C_{Purge}V_{Purge} - C_{LR}V_{Lost})}{C_{initial}V_{initial} - C_{LR}V_{LR} - C_{LP}V_{LP} - C_{LR}V_{Lost}} * 100\% = 29.6\%$$

$$\text{Recovery}_{\text{Membrane, P}} (\%) = \frac{C_{ER}V_{ER} + C_{EP}V_{EP}}{C_{initial}V_{initial} - C_{LR}V_{LR} - C_{LP}V_{LP} - C_{LR}V_{Lost}} * 100\% = 48.8\%$$

$$\text{Recovery}_{\text{Process, P}} (\%) = \frac{C_{ER}V_{ER} + C_{EP}V_{EP}}{C_{initial}V_{initial} - C_{LR}V_{LR}} * 100\% = 22.9\%$$

Time-Dependent static binding curve data

Table 26. Static binding concentrations, membrane volumes, and static binding capacities according to binding pH and NaCl concentration for the time-dependent static binding curves in Figure 9

Time (min)	Solution Conc (mg/ml)	Membrane Mass (g)	Membrane Volume (ml)	Static Binding Capacity (q)
Pure Lysozyme, pH 4.5, 0 mM NaCl - Trial 1				
0	0.379	0.0000	0.0000	0.0
0	0.380	0.0000	0.0000	0.0
60	0.336	0.0264	0.0667	6.5
60	0.336	0.0264	0.0667	6.5
130	0.364	0.0252	0.0667	2.2
130	0.363	0.0252	0.0667	2.4
180	0.296	0.0287	0.0667	12.5
180	0.296	0.0287	0.0667	12.5
240	0.301	0.0233	0.0584	13.4
240	0.301	0.0233	0.0584	13.4
300	0.297	0.0222	0.0584	14.0
300	0.297	0.0222	0.0584	14.0
360	0.279	0.0240	0.0584	17.2
360	0.279	0.0240	0.0584	17.2
1320	0.106	0.0232	0.0584	46.8
1320	0.105	0.0232	0.0584	46.9
1380	0.138	0.0248	0.0626	38.6
1380	0.138	0.0248	0.0626	38.5
1440	0.138	0.0264	0.0626	38.5
1440	0.138	0.0264	0.0626	38.5
2760	0.054	0.0235	0.0578	56.2
2760	0.053	0.0235	0.0578	56.4
2820	0.044	0.0237	0.0584	57.5
2820	0.043	0.0237	0.0584	57.5
2880	0.042	0.0234	0.0578	58.3
2880	0.041	0.0234	0.0578	58.4
Pure Lysozyme, pH 4.5, 0 mM NaCl - Trial 2				
0	0.384	0.0000	0.0000	0.0
0	0.385	0.0000	0.0000	0.0
60	0.340	0.0260	0.0626	7.1

Time (min)	Solution Conc (mg/ml)	Membrane Mass (g)	Membrane Volume (ml)	Static Binding Capacity (q)
60	0.340	0.0260	0.0626	7.1
120	0.328	0.0212	0.0506	11.2
120	0.328	0.0212	0.0506	11.2
180	0.300	0.0231	0.0584	14.5
180	0.299	0.0231	0.0584	14.6
250	0.296	0.0246	0.0584	15.2
250	0.296	0.0246	0.0584	15.2
300	0.289	0.0242	0.0584	16.4
300	0.290	0.0242	0.0584	16.2
360	0.263	0.0252	0.0584	20.8
360	0.262	0.0252	0.0584	21.0
1320	0.155	0.0222	0.0542	42.2
1320	0.156	0.0222	0.0542	42.2
1380	0.107	0.0254	0.0667	41.6
1380	0.107	0.0254	0.0667	41.6
1440	0.134	0.0246	0.0584	42.9
1440	0.134	0.0246	0.0584	42.8
2760	0.089	0.0202	0.0506	58.4
2760	0.089	0.0202	0.0506	58.3
2820	0.056	0.0242	0.0584	56.2
2820	0.055	0.0242	0.0584	56.5
2880	0.037	0.0234	0.0584	59.6
2880	0.036	0.0234	0.0584	59.6
Ethanol Soluble Egg White, pH 4.5, 0 mM NaCl - Trial 1				
0	0.394	0.0000	0.0000	0.0
0	0.395	0.0000	0.0000	0.0
60	0.365	0.0253	0.0584	5.0
60	0.366	0.0253	0.0584	5.0
120	0.341	0.0251	0.0563	9.6
120	0.342	0.0251	0.0563	9.3
180	0.343	0.0233	0.0563	9.3
180	0.341	0.0233	0.0563	9.5
240	0.330	0.0271	0.0565	11.5
240	0.330	0.0271	0.0565	11.4

Time (min)	Solution Conc (mg/ml)	Membrane Mass (g)	Membrane Volume (ml)	Static Binding Capacity (q)
300	0.325	0.0256	0.0542	12.9
300	0.325	0.0256	0.0542	12.8
360	0.318	0.0254	0.0545	14.1
360	0.319	0.0254	0.0545	13.9
1320	0.246	0.0273	0.0506	29.4
1320	0.246	0.0273	0.0506	29.3
1380	0.221	0.0278	0.0623	27.9
1380	0.221	0.0278	0.0623	27.9
1440	0.228	0.0221	0.0584	28.5
1440	0.229	0.0221	0.0584	28.4
2760	0.177	0.0277	0.0545	40.0
2760	0.177	0.0277	0.0545	39.9
2820	0.179	0.0256	0.0545	39.6
2820	0.180	0.0256	0.0545	39.4
2880	0.182	0.0280	0.0545	39.1
2880	0.183	0.0280	0.0545	38.9
Ethanol Soluble Egg White, pH 4.5, 0 mM NaCl - Trial 2				
0	0.384	0.0000	0.0000	0.0
0	0.386	0.0000	0.0000	0.0
60	0.360	0.0239	0.0584	4.3
60	0.359	0.0239	0.0584	4.4
130	0.354	0.0215	0.0506	6.1
130	0.354	0.0215	0.0506	6.1
180	0.336	0.0256	0.0626	7.8
180	0.337	0.0256	0.0626	7.7
240	0.333	0.0222	0.0584	8.9
240	0.333	0.0222	0.0584	8.9
300	0.332	0.0222	0.0545	9.7
300	0.331	0.0222	0.0545	9.9
360	0.313	0.0236	0.0584	12.3
360	0.314	0.0236	0.0584	12.2
1320	0.223	0.0221	0.0584	27.8
1320	0.223	0.0221	0.0584	27.8
1380	0.231	0.0248	0.0584	26.4

Time (min)	Solution Conc (mg/ml)	Membrane Mass (g)	Membrane Volume (ml)	Static Binding Capacity (q)
1380	0.230	0.0248	0.0584	26.5
1440	0.236	0.0267	0.0626	23.8
1440	0.236	0.0267	0.0626	23.8
2770	0.192	0.0230	0.0545	35.4
2770	0.192	0.0230	0.0545	35.4
2820	0.192	0.0232	0.0545	35.4
2820	0.193	0.0232	0.0545	35.3
2880	0.183	0.0258	0.0626	32.3
2880	0.183	0.0258	0.0626	32.3
Pure Lysozyme, pH 4.5, 300 mM NaCl - Trial 1				
0	0.392	0.0000	0.0000	0.0
0	0.393	0.0000	0.0000	0.0
60	0.347	0.0259	0.0623	7.3
60	0.347	0.0259	0.0623	7.3
130	0.327	0.0287	0.0667	9.8
130	0.327	0.0287	0.0667	9.8
180	0.310	0.0268	0.0626	13.2
180	0.311	0.0268	0.0626	13.1
240	0.309	0.0257	0.0626	13.4
240	0.309	0.0257	0.0626	13.4
300	0.262	0.0256	0.0626	20.9
300	0.262	0.0256	0.0626	20.8
360	0.207	0.0240	0.0584	31.8
360	0.207	0.0240	0.0584	31.7
1320	0.103	0.0256	0.0626	46.3
1320	0.103	0.0256	0.0626	46.3
1380	0.116	0.0241	0.0626	44.1
1380	0.117	0.0241	0.0626	44.0
1440	0.096	0.0253	0.0623	47.5
1440	0.096	0.0253	0.0623	47.5
2760	0.027	0.0234	0.0623	58.8
2760	0.027	0.0234	0.0623	58.6
2820	0.055	0.0219	0.0506	66.6
2820	0.057	0.0219	0.0506	66.4

Time (min)	Solution Conc (mg/ml)	Membrane Mass (g)	Membrane Volume (ml)	Static Binding Capacity (q)
2880	0.027	0.0252	0.0667	54.8
2880	0.026	0.0252	0.0667	54.9
Pure Lysozyme, pH 4.5, 300 mM NaCl - Trial 2				
0	0.373	0.0000	0.0000	0.0
0	0.372	0.0000	0.0000	0.0
60	0.334	0.0240	0.0584	6.6
60	0.333	0.0240	0.0584	6.7
120	0.311	0.0260	0.0578	10.6
120	0.312	0.0260	0.0578	10.5
180	0.215	0.0256	0.0626	25.2
180	0.215	0.0256	0.0626	25.2
250	0.269	0.0233	0.0584	17.8
250	0.269	0.0233	0.0584	17.7
300	0.263	0.0261	0.0667	16.4
300	0.263	0.0261	0.0667	16.4
360	0.253	0.0235	0.0584	20.5
360	0.254	0.0235	0.0584	20.2
1320	0.129	0.0232	0.0545	44.7
1320	0.129	0.0232	0.0545	44.6
1380	0.134	0.0230	0.0545	43.7
1380	0.134	0.0230	0.0545	43.7
1440	0.119	0.0218	0.0542	46.8
1440	0.119	0.0218	0.0542	46.8
2760	0.056	0.0236	0.0584	54.1
2760	0.056	0.0236	0.0584	54.1
2820	0.043	0.0235	0.0584	56.5
2820	0.044	0.0235	0.0584	56.2
2880	0.074	0.0206	0.0470	63.5
2880	0.074	0.0206	0.0470	63.5
Ethanol Soluble Egg White, pH 4.5, 300 mM NaCl - Trial 1				
0	0.389	0.0000	0.0000	0.0
0	0.389	0.0000	0.0000	0.0
60	0.369	0.0248	0.0626	3.2
60	0.368	0.0248	0.0626	3.3

Time (min)	Solution Conc (mg/ml)	Membrane Mass (g)	Membrane Volume (ml)	Static Binding Capacity (q)
140	0.365	0.0242	0.0626	3.9
140	0.366	0.0242	0.0626	3.7
180	0.362	0.0256	0.0584	4.6
180	0.362	0.0256	0.0584	4.5
240	0.361	0.0259	0.0626	4.6
240	0.362	0.0259	0.0626	4.4
300	0.352	0.0240	0.0545	6.7
300	0.351	0.0240	0.0545	7.0
360	0.333	0.0290	0.0712	7.9
360	0.333	0.0290	0.0712	7.8
1330	0.260	0.0251	0.0626	20.6
1330	0.261	0.0251	0.0626	20.5
1380	0.259	0.0279	0.0667	19.4
1380	0.259	0.0279	0.0667	19.5
1440	0.257	0.0245	0.0623	21.3
1440	0.257	0.0245	0.0623	21.3
2760	0.228	0.0265	0.0667	24.1
2760	0.229	0.0265	0.0667	24.0
2820	0.227	0.0265	0.0626	26.0
2820	0.227	0.0265	0.0626	25.9
2880	0.226	0.0279	0.0667	24.4
2880	0.225	0.0279	0.0667	24.6
Ethanol Soluble Egg White, pH 4.5, 300 mM NaCl - Trial 2				
0	0.385	0.0000	0.0000	0.0
0	0.385	0.0000	0.0000	0.0
75	0.365	0.0241	0.0584	3.4
75	0.366	0.0241	0.0584	3.2
120	0.359	0.0260	0.0623	4.2
120	0.359	0.0260	0.0623	4.2
180	0.352	0.0260	0.0623	5.4
180	0.353	0.0260	0.0623	5.2
240	0.346	0.0222	0.0584	6.7
240	0.347	0.0222	0.0584	6.5
300	0.344	0.0255	0.0584	7.1

Time (min)	Solution Conc (mg/ml)	Membrane Mass (g)	Membrane Volume (ml)	Static Binding Capacity (q)
300	0.344	0.0255	0.0584	7.0
360	0.338	0.0242	0.0584	8.1
360	0.339	0.0242	0.0584	7.9
1320	0.275	0.0225	0.0545	20.2
1320	0.275	0.0225	0.0545	20.2
1380	0.259	0.0242	0.0584	21.6
1380	0.261	0.0242	0.0584	21.3
1440	0.271	0.0234	0.0542	21.0
1440	0.271	0.0234	0.0542	21.0
2760	0.227	0.0262	0.0584	27.1
2760	0.228	0.0262	0.0584	26.9
2820	0.220	0.0264	0.0623	26.4
2820	0.220	0.0264	0.0623	26.4
2880	0.227	0.0241	0.0542	29.1
2880	0.226	0.0241	0.0542	29.3
Pure Lysozyme, pH 6.0, 0 mM NaCl - Trial 1				
0	0.387	0.0000	0.0000	0.0
0	0.387	0.0000	0.0000	0.0
70	0.338	0.0241	0.0626	7.8
70	0.338	0.0241	0.0626	7.8
120	0.325	0.0266	0.0626	9.8
120	0.325	0.0266	0.0626	9.8
180	0.303	0.0253	0.0626	13.3
180	0.303	0.0253	0.0626	13.4
240	0.278	0.0255	0.0623	17.4
240	0.278	0.0255	0.0623	17.4
300	0.280	0.0202	0.0506	21.1
300	0.281	0.0202	0.0506	20.9
360	0.264	0.0221	0.0545	22.4
360	0.264	0.0221	0.0545	22.4
1320	0.105	0.0270	0.0626	45.0
1320	0.106	0.0270	0.0626	44.9
1380	0.089	0.0225	0.0584	50.9
1380	0.089	0.0225	0.0584	51.0

Time (min)	Solution Conc (mg/ml)	Membrane Mass (g)	Membrane Volume (ml)	Static Binding Capacity (q)
1440	0.089	0.0227	0.0584	51.0
1440	0.088	0.0227	0.0584	51.1
2770	0.066	0.0233	0.0545	58.8
2770	0.066	0.0233	0.0545	58.8
2820	0.046	0.0254	0.0626	54.4
2820	0.046	0.0254	0.0626	54.4
2880	0.037	0.0234	0.0584	59.9
2880	0.036	0.0234	0.0584	60.0
Pure Lysozyme, pH 6.0, 0 mM NaCl - Trial 2				
0	0.365	0.0000	0.0000	0.0
0	0.366	0.0000	0.0000	0.0
60	0.331	0.0260	0.0545	6.4
60	0.331	0.0260	0.0545	6.3
120	0.320	0.0215	0.0545	8.5
120	0.318	0.0215	0.0545	8.7
180	0.302	0.0274	0.0623	10.2
180	0.301	0.0274	0.0623	10.4
240	0.285	0.0238	0.0545	14.8
240	0.283	0.0238	0.0545	15.1
300	0.254	0.0256	0.0626	17.8
300	0.255	0.0256	0.0626	17.6
360	0.222	0.0208	0.0542	26.5
360	0.223	0.0208	0.0542	26.4
1335	0.113	0.0254	0.0542	46.6
1335	0.114	0.0254	0.0542	46.5
1390	0.113	0.0234	0.0506	49.9
1390	0.113	0.0234	0.0506	49.9
1440	0.090	0.0238	0.0545	50.6
1440	0.090	0.0238	0.0545	50.5
2760	0.036	0.0226	0.0506	65.1
2760	0.036	0.0226	0.0506	65.1
2820	0.045	0.0228	0.0506	63.4
2820	0.045	0.0228	0.0506	63.4
2880	0.028	0.0253	0.0584	57.9

Time (min)	Solution Conc (mg/ml)	Membrane Mass (g)	Membrane Volume (ml)	Static Binding Capacity (q)
2880	0.028	0.0253	0.0584	57.8
Ethanol Soluble Egg White, pH 6.0, 0 mM NaCl - Trial 1				
0	0.380	0.0000	0.0000	0.0
0	0.382	0.0000	0.0000	0.0
60	0.367	0.0253	0.0626	2.3
60	0.367	0.0253	0.0626	2.2
120	0.351	0.0251	0.0626	4.9
120	0.351	0.0251	0.0626	4.8
180	0.343	0.0233	0.0584	6.5
180	0.344	0.0233	0.0584	6.3
240	0.343	0.0271	0.0712	5.3
240	0.344	0.0271	0.0712	5.2
300	0.336	0.0256	0.0578	7.8
300	0.337	0.0256	0.0578	7.7
360	0.331	0.0254	0.0667	7.5
360	0.330	0.0254	0.0667	7.7
1320	0.247	0.0273	0.0712	18.9
1320	0.247	0.0273	0.0712	18.9
1380	0.256	0.0278	0.0690	18.2
1380	0.255	0.0278	0.0690	18.3
1440	0.258	0.0221	0.0545	22.6
1440	0.259	0.0221	0.0545	22.5
2760	0.220	0.0277	0.0647	24.9
2760	0.221	0.0277	0.0647	24.7
2820	0.238	0.0256	0.0667	21.4
2820	0.238	0.0256	0.0667	21.5
2880	0.208	0.0280	0.0667	25.9
2880	0.209	0.0280	0.0667	25.7
Ethanol Soluble Egg White, pH 6.0, 0 mM NaCl - Trial 2				
0	0.379	0.0000	0.0000	0.0
0	0.380	0.0000	0.0000	0.0
60	0.366	0.0252	0.0626	2.2
60	0.366	0.0252	0.0626	2.1
120	0.354	0.0246	0.0584	4.4

Time (min)	Solution Conc (mg/ml)	Membrane Mass (g)	Membrane Volume (ml)	Static Binding Capacity (q)
120	0.353	0.0246	0.0584	4.4
180	0.351	0.0196	0.0506	5.6
180	0.351	0.0196	0.0506	5.6
240	0.341	0.0240	0.0584	6.5
240	0.343	0.0240	0.0584	6.3
300	0.330	0.0237	0.0542	9.1
300	0.329	0.0237	0.0542	9.3
360	0.332	0.0244	0.0584	8.1
360	0.334	0.0244	0.0584	7.9
1320	0.264	0.0237	0.0542	21.2
1320	0.264	0.0237	0.0542	21.2
1380	0.259	0.0237	0.0584	20.6
1380	0.260	0.0237	0.0584	20.5
1440	0.279	0.0258	0.0545	18.4
1440	0.279	0.0258	0.0545	18.5
2760	0.230	0.0228	0.0542	27.5
2760	0.232	0.0228	0.0542	27.2
2820	0.220	0.0221	0.0584	27.4
2820	0.221	0.0221	0.0584	27.1
2880	0.241	0.0248	0.0542	25.5
2880	0.241	0.0248	0.0542	25.6
Pure Lysozyme, pH 6.0, 300 mM NaCl - Trial 1				
0	0.380	0.0000	0.0000	0.0
0	0.380	0.0000	0.0000	0.0
70	0.353	0.0257	0.0626	4.4
70	0.354	0.0257	0.0626	4.2
120	0.340	0.0226	0.0584	7.0
120	0.341	0.0226	0.0584	6.8
180	0.326	0.0235	0.0584	9.4
180	0.325	0.0235	0.0584	9.5
240	0.318	0.0253	0.0584	10.8
240	0.318	0.0253	0.0584	10.6
300	0.309	0.0242	0.0626	11.4
300	0.308	0.0242	0.0626	11.5

Time (min)	Solution Conc (mg/ml)	Membrane Mass (g)	Membrane Volume (ml)	Static Binding Capacity (q)
360	0.303	0.0228	0.0542	14.2
360	0.303	0.0228	0.0542	14.3
1320	0.229	0.0251	0.0623	24.3
1320	0.229	0.0251	0.0623	24.3
1380	0.192	0.0255	0.0584	32.3
1380	0.193	0.0255	0.0584	32.2
1440	0.212	0.0231	0.0545	30.8
1440	0.212	0.0231	0.0545	30.8
2770	0.202	0.0216	0.0506	35.3
2770	0.202	0.0216	0.0506	35.2
2820	0.204	0.0203	0.0506	34.9
2820	0.204	0.0203	0.0506	34.9
2880	0.198	0.0274	0.0667	27.3
2880	0.198	0.0274	0.0667	27.4
Pure Lysozyme, pH 6.0, 300 mM NaCl - Trial 2				
0	0.367	0.0000	0.0000	0.0
0	0.367	0.0000	0.0000	0.0
60	0.334	0.0257	0.0545	6.1
60	0.334	0.0257	0.0545	6.1
120	0.316	0.0284	0.0626	8.1
120	0.316	0.0284	0.0626	8.1
180	0.322	0.0265	0.0542	8.3
180	0.320	0.0265	0.0542	8.6
240	0.286	0.0211	0.0506	16.1
240	0.286	0.0211	0.0506	16.0
300	0.305	0.0239	0.0542	11.5
300	0.304	0.0239	0.0542	11.6
360	0.289	0.0279	0.0626	12.4
360	0.290	0.0279	0.0626	12.3
1335	0.232	0.0236	0.0506	26.6
1335	0.232	0.0236	0.0506	26.7
1390	0.229	0.0235	0.0506	27.3
1390	0.229	0.0235	0.0506	27.2
1440	0.231	0.0249	0.0542	25.1

Time (min)	Solution Conc (mg/ml)	Membrane Mass (g)	Membrane Volume (ml)	Static Binding Capacity (q)
1440	0.231	0.0249	0.0542	25.0
2760	0.214	0.0214	0.0506	30.1
2760	0.216	0.0214	0.0506	29.9
2820	0.196	0.0273	0.0584	29.3
2820	0.196	0.0273	0.0584	29.2
2880	0.205	0.0236	0.0545	29.6
2880	0.207	0.0236	0.0545	29.4
Ethanol Soluble Egg White, pH 6.0, 300 mM NaCl - Trial 1				
0	0.389	0.0000	0.0000	0.0
0	0.389	0.0000	0.0000	0.0
60	0.374	0.0284	0.0667	2.3
60	0.375	0.0284	0.0667	2.2
120	0.375	0.0285	0.0662	2.2
120	0.375	0.0285	0.0662	2.2
180	0.368	0.0260	0.0626	3.4
180	0.369	0.0260	0.0626	3.3
240	0.362	0.0250	0.0626	4.4
240	0.360	0.0250	0.0626	4.7
300	0.357	0.0263	0.0667	4.9
300	0.357	0.0263	0.0667	4.9
360	0.348	0.0316	0.0667	6.1
360	0.350	0.0316	0.0667	5.9
1290	0.293	0.0262	0.0623	15.4
1290	0.293	0.0262	0.0623	15.4
1380	0.286	0.0271	0.0626	16.4
1380	0.287	0.0271	0.0626	16.3
1440	0.290	0.0271	0.0626	15.9
1440	0.291	0.0271	0.0626	15.8
2730	0.264	0.0280	0.0667	18.8
2730	0.264	0.0280	0.0667	18.8
2820	0.253	0.0251	0.0626	21.8
2820	0.254	0.0251	0.0626	21.6
2880	0.255	0.0259	0.0626	21.5
2880	0.253	0.0259	0.0626	21.7

Time (min)	Solution Conc (mg/ml)	Membrane Mass (g)	Membrane Volume (ml)	Static Binding Capacity (q)
Ethanol Soluble Egg White, pH 6.0, 300 mM NaCl - Trial 2				
0	0.384	0.0000	0.0000	0.0
0	0.384	0.0000	0.0000	0.0
60	0.373	0.0215	0.0545	2.1
60	0.373	0.0215	0.0545	2.0
120	0.368	0.0222	0.0542	2.9
120	0.368	0.0222	0.0542	3.0
180	0.364	0.0234	0.0545	3.7
180	0.364	0.0234	0.0545	3.7
240	0.346	0.0245	0.0623	6.1
240	0.346	0.0245	0.0623	6.0
300	0.350	0.0247	0.0623	5.5
300	0.350	0.0247	0.0623	5.5
360	0.336	0.0242	0.0578	8.3
360	0.337	0.0242	0.0578	8.0
1320	0.279	0.0227	0.0545	19.2
1320	0.281	0.0227	0.0545	18.9
1380	0.293	0.0217	0.0506	18.1
1380	0.292	0.0217	0.0506	18.1
1440	0.285	0.0220	0.0542	18.2
1440	0.285	0.0220	0.0542	18.2
2760	0.257	0.0231	0.0542	23.3
2760	0.257	0.0231	0.0542	23.4
2820	0.254	0.0211	0.0506	25.6
2820	0.255	0.0211	0.0506	25.5
2880	0.248	0.0252	0.0578	23.4
2880	0.249	0.0252	0.0578	23.3
Pure Lysozyme, pH 7.5, 0 mM NaCl - Trial 1				
0	0.369	0.0000	0.0000	0.0
0	0.370	0.0000	0.0000	0.0
60	0.341	0.0244	0.0623	4.6
60	0.340	0.0244	0.0623	4.7
130	0.316	0.0224	0.0506	10.5
130	0.317	0.0224	0.0506	10.3

Time (min)	Solution Conc (mg/ml)	Membrane Mass (g)	Membrane Volume (ml)	Static Binding Capacity (q)
180	0.289	0.0299	0.0667	12.0
180	0.290	0.0299	0.0667	11.9
240	0.300	0.0221	0.0542	12.8
240	0.301	0.0221	0.0542	12.6
300	0.264	0.0248	0.0626	16.8
300	0.265	0.0248	0.0626	16.7
360	0.264	0.0218	0.0545	19.4
360	0.263	0.0218	0.0545	19.5
1320	0.130	0.0241	0.0578	41.4
1320	0.129	0.0241	0.0578	41.5
1380	0.101	0.0221	0.0545	49.3
1380	0.102	0.0221	0.0545	49.0
1440	0.096	0.0232	0.0584	46.8
1440	0.096	0.0232	0.0584	46.7
2760	0.040	0.0251	0.0584	56.3
2760	0.041	0.0251	0.0584	56.3
2820	0.080	0.0200	0.0470	61.6
2820	0.079	0.0200	0.0470	61.7
2880	0.042	0.0268	0.0626	52.3
2880	0.041	0.0268	0.0626	52.5
Pure Lysozyme, pH 7.5, 0 mM NaCl - Trial 2				
0	0.368	0.0000	0.0000	0.0
0	0.369	0.0000	0.0000	0.0
60	0.337	0.0240	0.0626	5.0
60	0.337	0.0240	0.0626	5.1
120	0.314	0.0244	0.0584	9.3
120	0.315	0.0244	0.0584	9.2
180	0.295	0.0212	0.0545	13.5
180	0.296	0.0212	0.0545	13.4
240	0.287	0.0245	0.0545	15.0
240	0.287	0.0245	0.0545	14.9
300	0.239	0.0230	0.0578	22.3
300	0.239	0.0230	0.0578	22.3
360	0.255	0.0251	0.0584	19.4

Time (min)	Solution Conc (mg/ml)	Membrane Mass (g)	Membrane Volume (ml)	Static Binding Capacity (q)
360	0.255	0.0251	0.0584	19.5
1320	0.116	0.0224	0.0545	46.3
1320	0.118	0.0224	0.0545	46.0
1380	0.089	0.0245	0.0584	47.8
1380	0.089	0.0245	0.0584	47.8
1450	0.129	0.0214	0.0545	44.0
1450	0.129	0.0214	0.0545	44.0
2775	0.027	0.0258	0.0626	54.5
2775	0.027	0.0258	0.0626	54.5
2830	0.042	0.0276	0.0626	52.2
2830	0.043	0.0276	0.0626	52.1
2880	0.048	0.0213	0.0542	59.0
2880	0.047	0.0213	0.0542	59.3
Ethanol Soluble Egg White, pH 7.5, 0 mM NaCl - Trial 1				
0	0.382	0.0000	0.0000	0.0
0	0.383	0.0000	0.0000	0.0
60	0.375	0.0219	0.0506	1.5
60	0.375	0.0219	0.0506	1.4
120	0.370	0.0230	0.0584	2.1
120	0.371	0.0230	0.0584	1.9
180	0.363	0.0262	0.0626	3.1
180	0.363	0.0262	0.0626	3.1
240	0.356	0.0199	0.0470	5.7
240	0.356	0.0199	0.0470	5.6
300	0.342	0.0256	0.0605	6.7
300	0.342	0.0256	0.0605	6.7
360	0.345	0.0237	0.0563	6.6
360	0.345	0.0237	0.0563	6.6
1320	0.265	0.0195	0.0545	21.5
1320	0.265	0.0195	0.0545	21.5
1380	0.262	0.0274	0.0667	18.1
1380	0.262	0.0274	0.0667	18.0
1440	0.268	0.0231	0.0545	20.9
1440	0.269	0.0231	0.0545	20.8

Time (min)	Solution Conc (mg/ml)	Membrane Mass (g)	Membrane Volume (ml)	Static Binding Capacity (q)
2760	0.240	0.0305	0.0667	21.4
2760	0.240	0.0305	0.0667	21.4
2820	0.228	0.0250	0.0585	26.4
2820	0.230	0.0250	0.0585	26.1
2880	0.247	0.0265	0.0626	21.6
2880	0.247	0.0265	0.0626	21.6
Ethanol Soluble Egg White, pH 7.5, 0 mM NaCl - Trial 2				
0	0.368	0.0000	0.0000	0.0
0	0.369	0.0000	0.0000	0.0
60	0.359	0.0215	0.0506	1.9
60	0.359	0.0215	0.0506	1.8
120	0.349	0.0207	0.0506	3.9
120	0.349	0.0207	0.0506	3.8
180	0.343	0.0234	0.0545	4.7
180	0.343	0.0234	0.0545	4.6
240	0.336	0.0236	0.0584	5.5
240	0.337	0.0236	0.0584	5.4
300	0.326	0.0254	0.0584	7.2
300	0.326	0.0254	0.0584	7.2
360	0.289	0.0238	0.0626	12.6
360	0.291	0.0238	0.0626	12.4
1330	0.257	0.0251	0.0623	17.8
1330	0.259	0.0251	0.0623	17.5
1380	0.257	0.0254	0.0623	17.8
1380	0.257	0.0254	0.0623	17.8
1440	0.247	0.0269	0.0667	18.2
1440	0.248	0.0269	0.0667	18.0
2775	0.230	0.0217	0.0470	29.3
2775	0.234	0.0217	0.0470	28.7
2820	0.228	0.0245	0.0626	22.4
2820	0.228	0.0245	0.0626	22.5
2880	0.232	0.0267	0.0667	20.4
2880	0.232	0.0267	0.0667	20.5
Pure Lysozyme, pH 7.5, 300 mM NaCl - Trial 1				

Time (min)	Solution Conc (mg/ml)	Membrane Mass (g)	Membrane Volume (ml)	Static Binding Capacity (q)
0	0.378	0.0000	0.0000	0.0
0	0.377	0.0000	0.0000	0.0
60	0.366	0.0214	0.0506	2.2
60	0.366	0.0214	0.0506	2.3
130	0.363	0.0269	0.0584	2.5
130	0.364	0.0269	0.0584	2.4
180	0.358	0.0221	0.0542	3.6
180	0.359	0.0221	0.0542	3.5
240	0.356	0.0225	0.0545	3.9
240	0.357	0.0225	0.0545	3.7
300	0.352	0.0268	0.0626	4.1
300	0.353	0.0268	0.0626	4.0
360	0.355	0.0226	0.0545	4.2
360	0.355	0.0226	0.0545	4.2
1320	0.347	0.0242	0.0584	5.2
1320	0.347	0.0242	0.0584	5.3
1380	0.344	0.0244	0.0584	5.7
1380	0.346	0.0244	0.0584	5.5
1440	0.349	0.0240	0.0584	4.9
1440	0.349	0.0240	0.0584	4.9
2760	0.351	0.0230	0.0545	4.9
2760	0.352	0.0230	0.0545	4.7
2820	0.346	0.0275	0.0626	5.0
2820	0.346	0.0275	0.0626	5.1
2880	0.344	0.0283	0.0667	5.0
2880	0.344	0.0283	0.0667	5.0
Pure Lysozyme, pH 7.5, 300 mM NaCl - Trial 2				
0	0.384	0.0000	0.0000	0.0
0	0.383	0.0000	0.0000	0.0
60	0.368	0.0237	0.0623	2.4
60	0.367	0.0237	0.0623	2.6
120	0.362	0.0246	0.0626	3.4
120	0.362	0.0246	0.0626	3.4
180	0.359	0.0233	0.0584	4.1

Time (min)	Solution Conc (mg/ml)	Membrane Mass (g)	Membrane Volume (ml)	Static Binding Capacity (q)
180	0.360	0.0233	0.0584	3.9
240	0.359	0.0229	0.0584	4.2
240	0.359	0.0229	0.0584	4.1
300	0.357	0.0263	0.0584	4.5
300	0.357	0.0263	0.0584	4.5
360	0.353	0.0289	0.0626	4.9
360	0.353	0.0289	0.0626	4.9
1320	0.358	0.0266	0.0626	4.0
1320	0.358	0.0266	0.0626	4.1
1380	0.355	0.0259	0.0584	4.7
1380	0.355	0.0259	0.0584	4.7
1450	0.356	0.0246	0.0584	4.6
1450	0.357	0.0246	0.0584	4.4
2775	0.346	0.0277	0.0626	5.9
2775	0.346	0.0277	0.0626	5.9
2830	0.353	0.0210	0.0542	5.5
2830	0.354	0.0210	0.0542	5.3
2880	0.349	0.0284	0.0667	5.1
2880	0.348	0.0284	0.0667	5.2
Ethanol Soluble Egg White, pH 7.5, 300 mM NaCl - Trial 1				
0	0.391	0.0000	0.0000	0.0
0	0.391	0.0000	0.0000	0.0
60	0.369	0.0262	0.0626	3.5
60	0.369	0.0262	0.0626	3.5
120	0.370	0.0289	0.0626	3.4
120	0.370	0.0289	0.0626	3.4
180	0.366	0.0255	0.0584	4.4
180	0.364	0.0255	0.0584	4.6
240	0.363	0.0227	0.0542	5.2
240	0.364	0.0227	0.0542	5.1
300	0.364	0.0245	0.0584	4.7
300	0.362	0.0245	0.0584	4.9
360	0.361	0.0215	0.0506	5.9
360	0.363	0.0215	0.0506	5.6

Time (min)	Solution Conc (mg/ml)	Membrane Mass (g)	Membrane Volume (ml)	Static Binding Capacity (q)
1320	0.337	0.0222	0.0542	10.0
1320	0.339	0.0222	0.0542	9.7
1380	0.337	0.0221	0.0545	10.0
1380	0.337	0.0221	0.0545	9.9
1440	0.337	0.0258	0.0626	8.6
1440	0.337	0.0258	0.0626	8.6
2760	0.326	0.0214	0.0563	11.5
2760	0.325	0.0214	0.0563	11.8
2820	0.329	0.0222	0.0560	11.0
2820	0.329	0.0222	0.0560	11.1
2880	0.321	0.0269	0.0626	11.2
2880	0.321	0.0269	0.0626	11.1
Ethanol Soluble Egg White, pH 7.5, 300 mM NaCl - Trial 2				
0	0.369	0.0000	0.0000	0.0
0	0.370	0.0000	0.0000	0.0
60	0.361	0.0228	0.0506	1.7
60	0.361	0.0228	0.0506	1.6
120	0.357	0.0247	0.0584	2.1
120	0.358	0.0247	0.0584	2.0
180	0.353	0.0249	0.0584	2.9
180	0.353	0.0249	0.0584	2.9
240	0.350	0.0189	0.0470	4.2
240	0.350	0.0189	0.0470	4.2
300	0.347	0.0267	0.0623	3.6
300	0.347	0.0267	0.0623	3.6
360	0.344	0.0245	0.0545	4.6
360	0.346	0.0245	0.0545	4.3
1330	0.318	0.0264	0.0623	8.3
1330	0.318	0.0264	0.0623	8.3
1380	0.326	0.0218	0.0506	8.6
1380	0.327	0.0218	0.0506	8.4
1440	0.317	0.0257	0.0626	8.4
1440	0.318	0.0257	0.0626	8.2
2775	0.317	0.0255	0.0584	9.0

Time (min)	Solution Conc (mg/ml)	Membrane Mass (g)	Membrane Volume (ml)	Static Binding Capacity (q)
2775	0.317	0.0255	0.0584	9.0
2820	0.315	0.0254	0.0626	8.7
2820	0.315	0.0254	0.0626	8.7
2880	0.320	0.0256	0.0626	7.9
2880	0.320	0.0256	0.0626	7.9